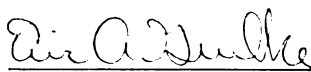This is to certify that the

dissertation entitled

The Peroxidases of Phanerochaete Chrysosporium:
Culture Modelling and Application

presented by

Frederick Carl Michel Jr.

has been accepted towards fulfillment
of the requirements for

_____Ph.D._____ degree in _Chem. Engr._

_____
Major professor

Date __2/24/92_____

PLACE IN RETURN BOX to remove this checkout from your record.
TO AVOID FINES return on or before date due.

DATE DUE	DATE DUE	DATE DUE

MSU Is An Affirmative Action/Equal Opportunity Institution

c:\circ\datedue.pm3-p.1

THE PEROXIDASES OF *PHANEROCHAETE CHRYSOSPORIUM*:
CULTURE MODELLING AND APPLICATION

by

Frederick Carl Michel Jr.

A DISSERTATION

Submitted to Michigan State University

in partial fulfillment of the requirements for the degree of

DOCTOR OF PHILOSOPHY

Department of Chemical Engineering

1991

ABSTRACT

THE PEROXIDASES OF *PHANEROCHAETE CHRYSOSPORIUM*:
CULTURE MODELLING and APPLICATION

By:

Frederick Carl Michel Jr.

Many industrially significant microbial products are produced during secondary metabolism by fungal pellets. The white-rot basidiomycete *Phanerochaete chrysosporium* produces extra-cellular lignin peroxidases (LIP) and manganese peroxidases (MNP) which have been implicated in the degradation of lignin and many aromatic xenobiotics during secondary metabolism. A novel unstructured kinetic model for mycelial pellet cultures of *P. chrysosporium* is presented which describes the culture dry weight, respiration, glucose consumption, nutrient nitrogen uptake, pellet size and oxygen effectiveness factor during the lag, primary growth, secondary metabolic, and death phases. Intrinsic Michaelis-Menten kinetic parameters for respiration were determined (Vmax= 0.76 ± 0.1 g/m^3 pellet/s, Km= 0.5 ± 0.3 g/m^3) by measuring oxygen concentration profiles using oxygen microelectrodes and were confirmed by measuring the rates of oxygen depletion and carbon dioxide evolution. The model shows good agreement with experimental data from cultures with initial glucose concentrations of 5,000, 10,000, 11,000 and 15,000 g/m^3 and initial nutrient nitrogen concentrations of 2, 39 and 117 g/m^3. Model simulations for air-flushed, high nitrogen and large pellet cultures, in which the production of LIPs and MNPs is greatly reduced, show that in these cases the oxygen effectiveness factor is significantly less than one.

The role of LIPs and MNPs in decolorizing industrial and synthetic paper mill bleach plant effluents (BPE) containing soluble chlorolignin is studied by controlling the levels of production of LIP and MNP using manganese, nutrient nitrogen and mutant

strains. Negligible BPE decolorization is exhibited by cultures which produce no LIPs or MNPs. *lip* mutant cultures of *P. chrysosporium*, and wild-type cultures grown with 100 ppm manganese, produce MNPs but not LIPs but show significant decolorization activity. Also, high rates of BPE decolorization are seen in 3 day old cultures which exhibit a relatively high level of MNP activity but little or no LIP activity. In cultures with 0 ppm Mn(II), high levels of LIPs but low levels of MNPs are produced and the rate and extent of BPE decolorization is relatively low. These results indicate that MNPs play a relatively more important role than LIPs in BPE decolorization by *P. chrysosporium*.

To Emily

ACKNOWLEDGEMENTS

Table of Contents

Chapter V:... 51

Model for submerged, peroxidase producing, mycelial pellet cultures of *P. chrysosporium*

List of Figures

Notation

Symbol	Definition	Unit
Bi	Biot number	(-)
C	Oxygen concentration	g/m^3
Cb	Uniform bulk solute concentration	g/m^3
Ci	Oxygen concentration in pellet	g/m^3
Cg	Gas phase oxygen concentration	g/m^3
Cl	Liquid phase oxygen concentration	g/m^3
Cs	Oxygen concentration at pellet surface	g/m^3
Csat	Oxygen equilibrium concentration in media	g/m^3
C.U.	Pt-Co Color Units	(-)
D	Diffusivity of oxygen in water	m^2/s
De	Effective diffusivity of oxygen in pellets	m^2/s
Dslab	Overall diffusivity in cell and gel matrix	m^2/s
E_O	Effectiveness factor for zero order kinetics	(-)
E_1	Effectiveness factor for first order kinetics	(-)
E	Effectiveness factor for oxygen	(-)
$E_{M.M.}$	Effectiveness factor for M.M. order kinetics	(-)
fpg	Glucose metabolism factor	g/g
fr	Glucose metabolism factor	g/g
fx	Glucose metabolism factor	g/g
G	Glucose concentration	g/m^3
H	Henry's law constant	(-)
i	Index value for numerical method	(-)
k	apparent rate constant for decolorization	dy^{-1}
kl	Mass transfer coefficient for oxygen	m/s
Km	Kinetic coefficient for oxygen	g/m^3
Ks	Kinetic coefficient for glucose	g/m^3
l	Gel matrix plate (or slab) thickness	m
M_{inf}	Total solute diffused into slab at infinite time	g/m^3
M_t	Total solute diffused into slab at time t	g/m^3
MW	Molecular weight	g/mol
n	Number of steps in numerical method	(-)
N	Ammonium concentration	g/m^3
P	Pressure	atm
pG	Polysaccharide concentration	g/m^3
Q	Ratio of total pellet volume to plate volume	m^3/m^3
q_n	Non-zero roots of equation in section 3.11	(-)

QO_2	Specific oxygen uptake rate	s^{-1}
QO_{2max}	Maximum specific oxygen uptake rate	s^{-1}
R	Ideal gas law constant	m^3 atm/mol/K
R	Characteristic pellet radius	m
r	Distance from pellet center	m
RCO_2	Bulk rate of carbon dioxide production	$g/m^3/s$
rO_2	Rate of respiration by pellets	$g/m^3/s$
RO_2	Bulk rate of oxygen consumption	$g/m^3/s$
Rg	Bulk rate of glucose uptake	$g/m^3/s$
Rn	Bulk rate of ammonium uptake	$g/m^3/s$
Rpg	Bulk rate of polysaccharide synthesis	$g/m^3/s$
Rx	Bulk rate of biomass production	$g/m^3/s$
T	Temperature	K
t_{lag}	Length of the lag phase	s
v	Reaction rate equation for oxygen	$g/m^3/s$
V_{hs}	Head space volume	m^3
V_l	Liquid phase volume	m^3
$Vmax$	Rate constant for oxygen	$g/m^3/s$
V_{pel}	Characteristic pellet volume	m^3
x	Distance from the plate interface	m
X	Biomass concentration (cell dry weight)	g/m^3
X_f	Final biomass concentration	g/m^3
Y_{CO_2/O_2}	CO2 produced per oxygen consumed	g/g
Y_{g/O_2}	Glucose used per oxygen consumed	g/g
$Y_{g/x}$	Growth yield coefficient for glucose	g/g
$Y_{n/x}$	Growth yield coefficient for nitrogen	g/g

Greek Symbols

α	Liquid volume divided by plate (or slab) volume	m^3/m^3
ϕ	First order modulus	(-)
Φ	Observed mass transfer modulus	(-)
η	Pellet number	m^3
μ_e	Effective growth rate constant	s^{-1}
μ_{max}	Growth rate constant	s^{-1}
ρ	Pellet density (dry weight/pellet volume)	g/m^3

CHAPTER I

INTRODUCTION

This study had two primary objectives reflecting the dual interests of the author. The first was to develop a simple unstructured kinetic model to describe growth, respiration, substrate utilization and mass transfer in submerged batch cultures of the white-rot fungus *Phanerochaete chrysosporium* which describes the life-cycle phases of primary growth, secondary metabolism and death. One aim of the culture modelling was to examine the effect of oxygen limitations on the production of the extracellular lignin peroxidases (LIP) and manganese peroxidases (MNP) which are produced during secondary metabolism and are primary components of the lignin degrading system of this organism. The second objective was to apply the lignin degrading enzymes to the treatment of paper mill bleach plant effluents (BPE) which contain toxic chlorolignin components and study the roles of LIP and MNP in BPE degradation.

The ligninolytic white-rot fungi such as *Phanerochaete chrysosporium* are the primary degraders of lignin in the environment. This organism is one of very few organisms which can mineralize lignin completely to carbon dioxide (Kirk *et al.*, 1978). In addition, *P. chrysosporium* can degrade a wide range of xenobiotic chemicals (Bumpus *et al.*, 1985) which are structurally similar to lignin such as DDT (Bumpus and Aust, 1987), dioxins (Eaton, 1984; Hammel *et al.*, 1986), chlorinated phenols (Lamar *et al.*, 1990; Lin and Wang, 1990, Lackner *et al.*, 1991) and poly-aromatic hydrocarbons (Hammel *et al.*, 1986). This ability is due to the non-specific nature of the lignin degrading system. *P. chrysosporium* produces two families of extracellular glycosylated heme proteins, designated lignin peroxidases (LIPs) and manganese peroxidases (MNPs), along with an H_2O_2-generating system as the major components of its ligninolytic system (Dass and Reddy, 1990; Gold *et al.*, 1989; Kirk and Farrel, 1987). This system is

1

expressed only during secondary metabolism and is triggered by carbon, nitrogen or sulfur limitation (Jefferies *et al.*, 1981). Both LIPs and MNPs are families of isozymes. They are heme glycoproteins which contain a single high spin ferric protoheme IX. The LIPs catalyze the non-specific one-electron oxidation of non phenolic aromatic substrates, including the C_α-C_β bond of lignin model compounds, yielding a multiplicity of final products (Kirk and Farrel, 1987). MNPs, on the other hand, oxidize Mn(II) to Mn(III), a highly reactive compound which oxidizes phenolic substrates (Gold *et al.*, 1989, Paszczynski *et al.*, 1985, Kuwahara *et al.*, 1984). These enzymes are thought to be directly involved in the mineralization of lignin by the white-rot fungi (Kirk and Farrel, 1987, Kuwahara *et al.*, 1984,).

In submerged agitated cultures, *P. chrysosporium* grows in the form of spherical aggregates known as mycelial pellets (Burkholder and Sinnott, 1945). Studies have shown that oxygen mass transfer limitations can influence the growth kinetics of mycelial pellets (Pirt, 1966; Metz and Kossen, 1977) and lead to oxygen starvation at the pellet center (Schugerl *et al.*, 1983). An important engineering concept developed in these studies was the oxygen effectiveness factor, defined as the observed rate of oxygen utilization divided by the rate expected without mass transfer limitations. Interestingly, the production of LIPs and MNPs by *P. chrysosporium* has been shown to be greatly affected by the level of oxygen in the culture (Barlev and Kirk, 1981; Dosoretz *et al.*,1990a; Dosoretz and Grethlein, 1991) and by mycelial pellet size (Michel *et al.*, 1990). However an analysis of mass transfer limitations in these cultures has not been reported. One objective of this study was to determine the kinetics of oxygen mass transfer and respiration in pellet cultures of *P. chrysosporium* and to examine the effect of oxygen limitations on the production of the LIPs and MNPs.

Although genes encoding LIP and MNP isozymes have been cloned and sequenced (Zhang *et al.*, 1991, de Boer et. al., 1987; Tien and Tu, 1987; Naidu and Reddy, 1990), introduction of these genes into simple, fast growing microorganisms like *Escherichia*

coli and *Saccharomyces cerevisiae* has not resulted in the production of active LIPs or MNPs. These organisms cannot glycosylate the LIPs or MNPs and may not have been able to fold the peroxidases properly or incorporate heme into the active site.

In order to produce active LIPs and MNPs for biotechnological applications, bioreactor systems employing the white-rot fungi are necessary. For any bioreactor design and scale-up, culture respiration, substrate utilization, biomass production and product expression are interelated and are key design considerations. Previous models of mycelial pellet culture growth and respiration largely consider only the primary (or exponential) growth phase of *Aspergillus* or *Penicillium* species, assume zero-order kinetics for respiration and are tested against only one or two initial substrate conditions. In practice, many industrially significant products are secondary metabolites produced after a limiting nutrient is exhausted. In addition Michaelis-Menten kinetics more accurately describes the kinetics of microbial respiration. A central aim of this study was to develop a simple unstructured kinetic model, which describes the growth, respiration, substrate utilization and mass transfer in mycelial pellet cultures of *P. chrysosporium* during the lag, primary growth, secondary metabolic and death phases.

In the paper industry, processes which chemically liberate residual lignin from wood pulp require chlorine bleaching and result in approximately 3 billion gallons of toxic and intensely colored waste effluents annually (EPA report #600/8-80-042a). The primary contributor to the color and toxicity of these streams is the bleach plant effluent (BPE) which contains high molecular weight, modified and chlorinated lignin and its degradation products (Boominathan and Reddy, 1991; Campbell, 1983; Huynh *et al.*, 1985; Paice and Jurasek, 1984). This material is not readily degraded by conventional bacterial water treatment processes (Boominathan and Reddy, 1991; Ericksson and Kolar, 1985; Forney, 1978) and typically enters receiving waters untreated. Cultures of the white-rot fungi *P. chrysosporium* and *Coriolus* (*Trametes*) *versicolor* are able to decolorize, dechlorinate and reduce the molecular weight of the chlorolignin component

of BPE. Although it has been assumed that the peroxidases of *P. chrysosporium* play a role in the biodegradation of paper mill bleach plant effluents, the actual contribution of these enzymes has never been documented (Eaton *et al.*, 1983; Messner *et al.*, 1990; Paice and Jurasek, 1984). A primary objective of this study was to determine the roles of LIPs and MNPs in the degradation of BPE by *P. chrysosporium*.

CHAPTER II

LITERATURE REVIEW

2.1 Mycelial pellet culture modelling

Filamentous fungi, like the lignin degrading basidiomycete *P. chrysosporium*, commonly grow in the form of spherical mycelial pellets in agitated submerged cultures (Metz and Kossen,1977; Whitaker and Long, 1973). This form of growth offers key advantages in the large-scale manufacture of microbial products. Compared to filamentous or single cell cultures, mycelial pellet cultures have lower media viscosities, greater cell densities and require simple product separation techniques. In effect, the organism is immobilized but free of the problems associated with artificial immobilization matrices. Industrial scale processes utilizing mycelial pellets include the production of citric acid using *Aspergillus* species (Sodeck *et al.*,1981), the production of antibiotics using *Penicillium* species (Whitaker and Long, 1973) the continuous hydrolysis of raffinose in beet molasses using *Mortierella vinacea* (Kobayashi and Suzuki, 1972) and the production of mushroom flavorings (Litchfield, 1977). Van Suijdam *et al.* (1982), have described the main influences on the growth of mycelial pellets (Figure 2.1). These include the pellet size and density, the biomass concentration, the limiting substrate concentration, the dissolved oxygen concentration and the oxygen effectiveness factor.

The growth of *P. chrysosporium* in the form of mycelial pellets has long been known (Burkholder and Sinnot, 1945), but Jager *et al.*, (1985) were the first to produce lignin and manganese peroxidases using mycelial pellet cultures of this fungus. Michel *et al.* (1990) studied the characteristics of pellet cultures of *P. chrysosporium* and found that the formation of mycelial pellets from a homogenized mycelial inocula was complete within 8 hours after inoculation, and that the number of pellets formed and the characteristic pellet size were functions of the rate of agitation. They showed that LIP
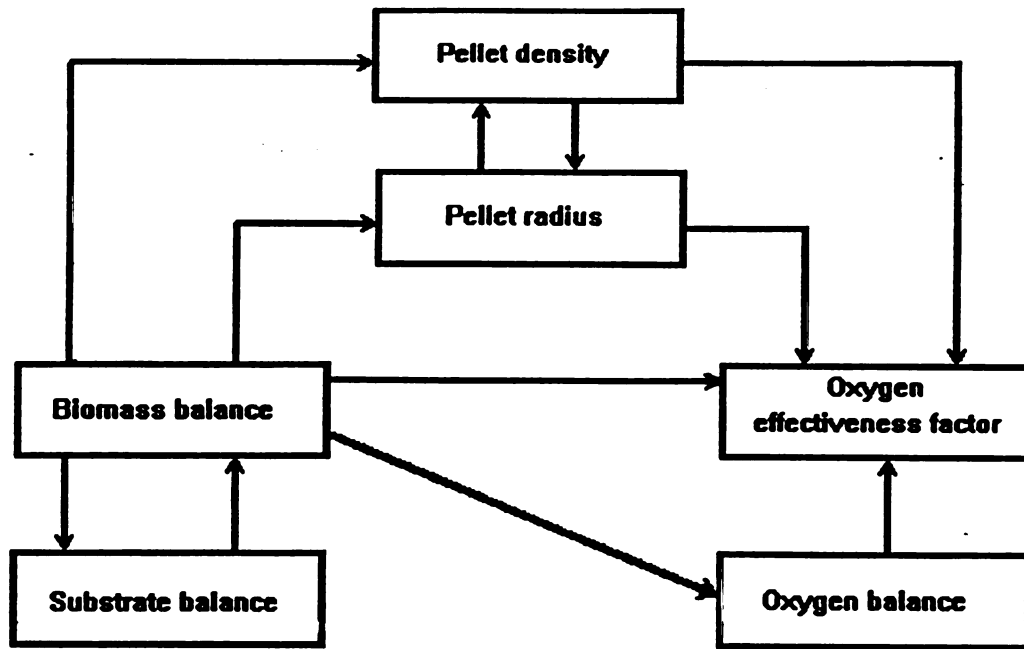
Figure 2.1   Influences on mycelial pellet cultures from van Suijdam *et al.*, (1982).

production was inhibited in cultures with both large pellets (diam.=6.6 mm) formed at low agitation rates, and small pellets (diam.=1.3 mm) formed at high agitation rates (Table 2.1).

Table 2.1 Effect of the rate of agitation on mycelial pellet size and the production of lignin peroxidase (LIP) by nitrogen-limited cultures of *P. chrysosporium* (from Michel *et al.*, 1990).

RPM (min^{-1})	Characteristic Pellet Diameter (mm)	LIP (U/l)
100	6.63 ± 1.06	0
150	1.83 ± 0.32	341 ± 73
200	1.29 ± 0.21	376 ± 33
250	1.27 ± 0.23	62 ± 100

Liebeskind *et al.* (1990) showed that for mycelial pellets of *P. chrysosporium* up to 5 mm in diameter, the pellet volume fraction (and hence pellet density) was constant.

Oxygen mass transfer limitations in mycelial pellets

Oxygen mass transfer limitations within mycelial pellets can influence mycelial pellet growth kinetics and could explain the low levels of LIP produced by large pellets of *P. chrysosporium*. Pirt (1966) was one of the first scientists to describe "cube root" growth kinetics for mycelial pellets of *Penicillium chrysogenum*. The cube-root growth model assumes that growth occurs only in an outer zone of the pellet due to intra-pellet oxygen limitations. Phillips (1966) calculated the critical diameter for growing mycelial pellets of *Penicillium*, where oxygen depletion first occurs at the pellet center by assuming zero order kinetics for respiration. Yoshida *et al.* (1968), developed a model

for oxygen consumption in pellets of *Lentinus edodes* using Michaelis-Menten kinetics. They used an eddy diffusion term that was larger than the value of oxygen diffusivity in water and reported that the specific oxygen consumption rate was a function of the depth within the pellet. Kobayashi *et al.* (1973) solved the differential equation describing oxygen transfer by molecular diffusion in pellets of *Aspergillus niger* using Michaelis-Menten kinetics and two other cases of respiratory activity. They used an approximate solution for effectiveness factors in immobilized enzyme systems developed by Moo-Young and Kobayashi (1972). In one case they assumed that mycelia can adapt to a particular oxygen concentration by changing their maximum rate of oxygen consumption (Vmax). Van-Suijdam *et al.* (1982) developed an unstructured growth model for mycelial pellets of *P. chrysogenum* in a bubble column. This model considered biomass growth, substrate depletion, respiration and pellet density. It incorporated functions for mass transfer processes in both the pellet and in the bulk liquid and assumed zero order kinetics for respiration. An empirical relationship for the gas-liquid mass transfer coefficient (kla) was obtained which showed that the resistance to oxygen mass transfer from the gas to liquid phase was negligible for pellet volume fractions less than 40%.

Wittler *et al.* (1986) investigated mechanisms of oxygen transfer for individual mycelial pellets of *P. chrysogenum*. They used an oxygen microprobe to determine the oxygen concentration profile within and immediately outside of mycelial pellets under a variety of different hydrodynamic and aeration conditions. Their results indicated that the mass transfer of oxygen into mycelial pellets may occur by means of eddy diffusion, molecular diffusion and convection. While the pellets used by Wittler *et al.* (1986) were probably in secondary metabolism, the media used for oxygen profile measurements were different than the growth media due to calcium and ammonium ion interference with the microprobe. Also, no attempt was made to correlate the respiration in individual pellets to bulk culture behavior. A summary of previous models of mycelial pellet growth and respiration is presented in Table 2.2.

Table 2.2. Summary of studies of mycelial pellet growth and respiration.

Reference	Organism	Oxygen Kinetics	Growth Phase
Yano *et al.*, 1961	*A. niger*	zero-order	primary
Philips, 1966	*P. chrysogenum*	zero-order	primary
Pirt, 1966	*P. chrysogenum*	cube-root	primary
Yoshida *et al.*, 1967	*Letinus edodes*	zero-order	primary
Trinci, 1970	*A. nidulans*		logarithmic
Moo-Young *et al.*, 1972	(enzymes)	Michaelis-Menten	
Kobayashi *et al.*, 1973	*A. niger*	M.M.; adaptive	primary
van Suijdam *et al.*, 1982	*P. chrysogenum*	zero-order	primary and death
Wittler *et al.*, 1986	*P. chrysogenum*	zero-order	data

Evident from this summary of previous studies is that only the primary or exponential growth phase is considered and secondary metabolism is largely ignored. In practice, many important products are secondary metabolites expressed after a limiting nutrient has been exhausted and primary growth has ended. Therefore an understanding of the physiological state of the organism during this period is important. Also apparent is that models for the growth and respiration of cultures of the white-rot fungus *P. chrysosporium* have not been developed. Furthermore, in general, the kinetics of respiration is assumed to be zero-order when in fact Michaelis-Menten kinetics more accurately describes respiration by microorganisms in submerged culture conditions. This is done for reasons of mathematic simplicity. The oxygen effectiveness factor for zero-order kinetics is easily calculated (see for example Phillips, 1966) while calculation of the effectiveness factor for Michaelis-Menten kinetics requires a trial and error iterative technique (see Moo-Young and Kobayashi, 1972). Metz and Kossen (1977) summarized

some other problems associated with early studies of oxygen mass transfer and respiration in mycelial pellets. In brief, they are that external mass transfer resistances have not been considered, that oxygen measurements have been done under improper conditions (e.g. not using the growth media) and that unusual kinetic parameter values have been used (e.g. unrealistic Km and diffusivity values).

One way of studying oxygen transfer and respiration by mycelial pellets is through the use of oxygen microelectrodes. Revsbech *et al.* (1983) have reviewed the use of micro-electrodes in microbial ecology. These improved Clark micro-electrodes feature a small tip diameter of 2 μm- 5 μm and allow the measurement of oxygen profiles in whole tissues, cell cultures and microbial films without interference by calcium or ammonium ions (as described by Wittler *et al.* 1986). In this study these devices were used to directly measure oxygen concentration gradients within and immediately outside of mycelial pellets of *P. chrysosporium*. This allowed an accurate determination of kinetic coefficients for respiration and permitted the study of respiration and oxygen mass transfer under conditions essentially the same as culture conditions.

Although many studies have addressed oxygen limitations in mycelial pellets, few have demonstrated the effect of oxygen starvation on product expression. Kobayashi and Suzuki (1972) showed that in pellet cultures of *Mortierella vinacea* which produce α-galactosidase, the specific enzyme activity decreased in pellets whose diameter was greater than 0.25 mm. They concluded that in the larger pellets the transfer of oxygen limited enzyme production. Morrin and Ward (1989), showed that altering the fungal morphology from filamentous to pelleted growth in the production of fumaric acid by *Rhizopus arrhizus*, leads to a three-fold decrease in fumaric acid production. Dosoretz *et al.* (1990a) showed that submerged mycelial pellet cultures of *P. chrysosporium*, flushed daily with air, yield no lignin peroxidase and two thirds less manganese peroxidase as compared to cultures flushed daily with oxygen (Figure 2.2). Thus evidence indicates that oxygen transfer limitations in mycelial pellets can limit product expression.
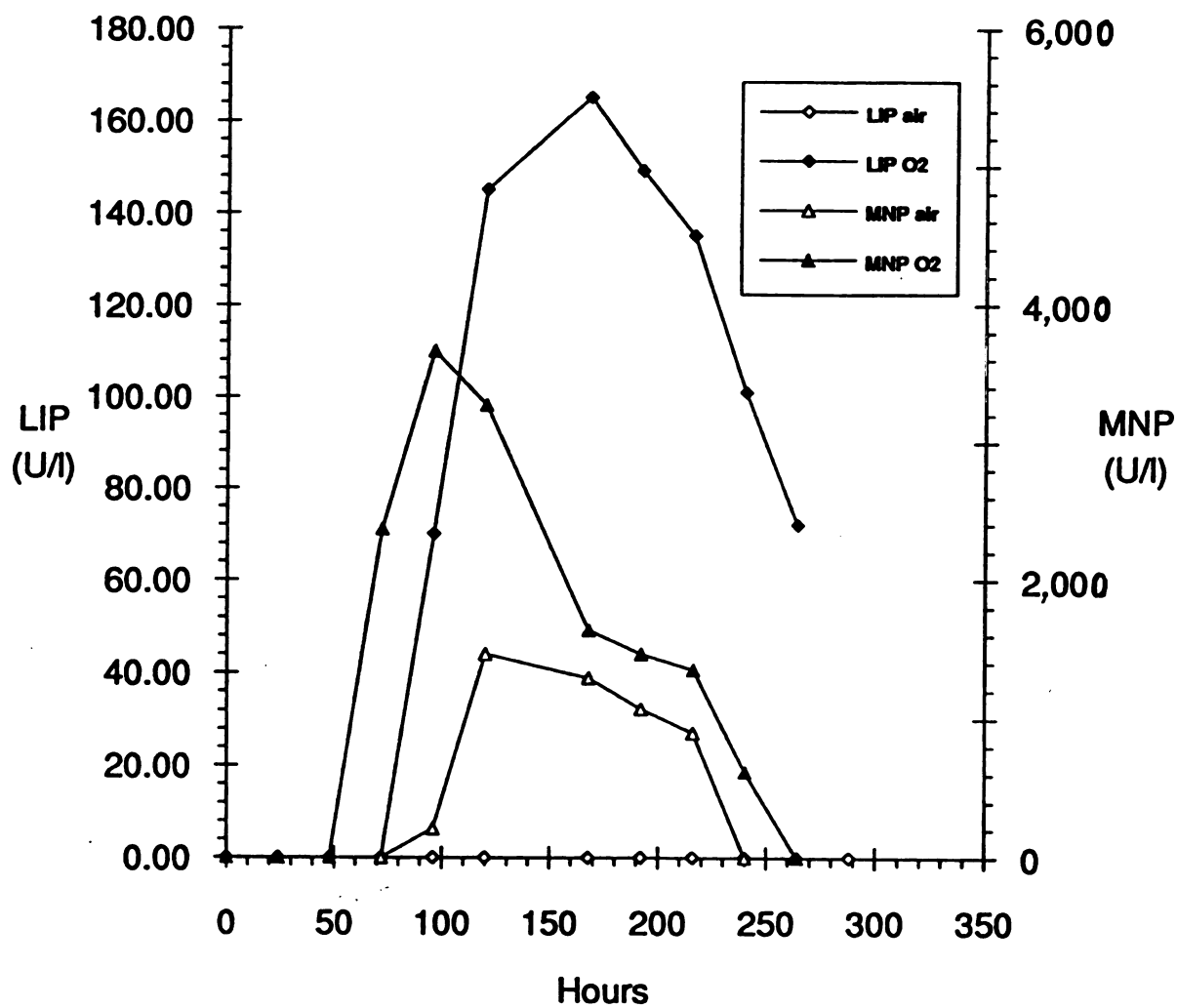
Figure 2.2 Lignin peroxidase (LIP) and manganese peroxidase (MNP) activities in air-flushed and oxygen flushed cultures from Dosoretz *et al.*, (1990). Cultures were grown in nitrogen limited conditions.

A primary aim of this study was to gain an understanding of the physiological conditions which favor the production of the LIPs and MNPs by developing an unstructured mathematical model for mycelial pellet cultures of *P. chrysosporium*. Key requirements for the model were that it was valid during secondary metabolism, incorporated Michaelis-Menten kinetics for respiration and considered mass transfer limitations within the mycelial pellets.

2.2 Kraft bleach plant effluents (BPE).

Formation of BPEs

The process of paper manufacturing begins with a forest. After cutting, logs are trucked to the mill, debarked and then chipped to uniform 1 inch squares. The chips are steam heated, mixed with sulfide and caustic and cooked for 3 hours at elevated temperature and pressure (340° F. and 165 psi at one Michigan mill). This process dissolves 90% of the lignin present in the wood. When the chips are flashed to atmospheric pressure, they explode, and form brown wood pulp which has the color and consistency of a wet grocery bag. The wood pulp is bleached to make white pulp for the production of fine printing papers.

Kraft bleach plant effluents (BPE) are formed when residual lignin is removed from the brown pulp during the bleaching process. This occurs in a series of crosscurrent stages using chlorine, caustic soda, sodium hypochlorite and chlorine dioxide (Figure 2.3). After each stage, dissolved impurities are washed from the pulp and blended together. Collectively, this waste stream is known as the bleach plant effluent (BPE) which is part of the over 3 billion gallons of wastewater discharged by the paper industry annually in the U.S (EPA report #600/8-80-042a). At one typical paper mill in southwestern Michigan, 17.5 gallons of wastewater is generated per pound of paper produced.
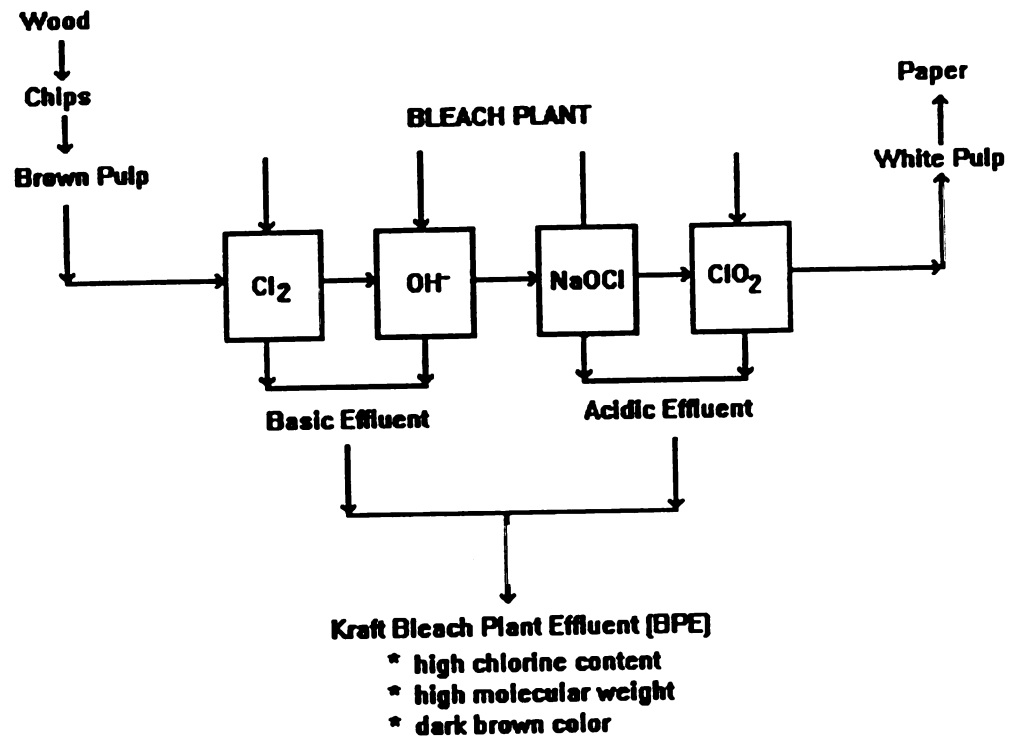
Figure 2.3   The process of brown pulp bleaching and the formation of kraft bleach plant effluents (BPE) at a Michigan paper mill.

Chemically, BPE consists of chlorinated degradation fragments of lignin. The molecular weight of these fragments ranges from 200 to over 100,000 daltons with high molecular weight species predominating. The toxicity of this material has been debated (Eriksson and Kolar, 1985). The predominantly high molecular weight of BPE makes it difficult to enter cells and it is not directly toxic to aquatic species. However some of the monomeric units of the BPE polymer, like chlorinated phenols and guiacols, are known to be toxic and carcinogenic. The rate of degradation of the high molecular weight chloro-lignin polymer in the environment, however, is not known. BPE contains some small molecular weight chlorinated aromatic compounds (Huynh *et al.*, 1985, Roy-Arcand and Archibald, 1991) and dioxins. Additionally, the dark brown color of BPE is aesthetically undesirable and limits the penetration of sunlight in streams and lakes. Furthermore, BPE increases the chemical and biological oxygen demand of receiving waters. Modification of the paper bleaching process using oxygen rather than chlorine as a bleaching agent may reduce the amount of BPE produced in the future, however chlorine bleaching will still be necessary to produce fine quality white paper as exemplified by the paper you now have before you (Messner *et al.*, 1990).

Treatment technologies for BPE

Many techniques for BPE treatment have been studied, however most pose economic or technical difficulties that have not been overcome. Dewatering and burning BPE is difficult since the high chlorine content requires special incinerators and dioxin formation is a problem (Michigan paper mill personnel). Ultrafiltration, carbon adsorption, high molecular weight amine precipitation (Gupta and Bhattacharya, 1985) and lime precipitation have proven too costly to implement (Royers *et al.* 1985; Gupta and Bhattacharya, 1985). Adsorption to fly ash, an electrical power generation waste, has been shown to be economically feasible based on laboratory scale tests (Gupta and Bhattacharya, 1985) however this material is considered hazardous and in some cases

toxic. A treatment process called rapid infiltration, wherein color is adsorbed and precipitated by flow through soil has been successfully implemented at an industrial scale in Canada (Swaney, 1983). None of these approaches destroys the BPE polymer in the process. The chloro-lignin material is simply concentrated and land-filled or dispersed into the environment and still poses a pollution problem.

Recently, a laboratory scale chemical oxidation process has been tested which shows promise (Sun *et al.*, 1989). In this process BPE is concentrated using ultrafiltration and is treated at 150° C. with sodium hydroxide and oxygen at 150 psi for 40 to 60 minutes. The process reportedly removes 70 to 80% of total organic chlorine and 60 to 70% of color and significantly reduces the molecular weight of the BPE (Sun *et al.*, 1989). However this process requires stoichiometric quantities of chemical reagents.

Studies have shown that few, if any bacterial organisms significantly degrade lignin (Forney, 1978). Ericksson and Kolar *et al.* (1985) measured the evolution of $^{14}CO_2$ from a high molecular weight fraction of ^{14}C-labelled synthetic BPE by bacteria isolated from an aerated lagoon which received paper mill effluents. They reported that less than 4% of the labelled carbon was converted to CO_2 in 90 days. Nevertheless, as pointed out by Roy-Arcand and Archibald (1991), the use of enzyme-based treatment would offer distinct advantages over physical and chemical processes in that only catalytic and not stoichiometric amounts of reagents would be needed.

2.3 Degradation of BPE by white-rot fungi.

P. chrysosporium and other white-rot fungi play key roles in environmental lignin degradation (Reddy, 1984). These organisms are the fastest known lignin degraders and among them *Phanerochaete chrysosporium* has been chosen as a model organism for the study of lignin degradation (Kirk and Farrell, 1987; Boominathan and Reddy, 1991). Kirk *et al.* (1978) examined the culture parameters influencing the ligninolytic activity of *P. chrysosporium*. Ligninolytic activity increased 2 to 3 fold in oxygen flushed cultures

as compared to air-flushed cultures and was negligible in cultures sparged with 5% oxygen. *P. chrysosporium* did not grow on lignin alone and ligninolytic activity was dependent on the presence of a metabolizable carbon and energy source like glucose or cellulose. Nitrogen sufficient cultures (24 mM) exhibited only 25-35% of the ligninolytic activity as compared to nitrogen-limited (2.4 mM) cultures.

Lundquist *et al.* (1977), first demonstrated the potential of white-rot fungi to degrade industrial lignin compounds. They showed that cultures of *P. chrysosporium* could degrade synthetic ^{14}C labelled bleached kraft lignins and other industrially modified lignins to $^{14}CO_2$. Approximately 40% of the ring-labelled and 31% of the side chain labelled carbon from synthetic BPE was recovered as labelled $^{14}CO_2$ after 42 days of treatment. Eaton *et al.* (1980) used stationary cultures of *P. chrysosporium* to degrade the E1 stage effluent (first alkaline stage after chlorination) of BPE which represents the majority of the bleach plant color. This effluent was decolorized 60% in four days and the biochemical and chemical oxygen demand of the effluent was reduced by approximately 40%. Huynh *et al.*, (1985) and Roy-Arcand and Archibald (1991) have demonstrated that low molecular weight chlorinated components of BPE such as chloroguiacols, chloroaldehydes and chlorophenols are removed by *P. chrysosporium* and *Coriolus versicolor* during the decolorization process. In addition studies have demonstrated that during the decolorization process, the molecular weight of the BPE polymer is reduced (Lackner *et al.*, 1991).

Many examples of bioreactor systems for BPE treatment exist. Eaton *et al.* (1983), Sundmann *et al.* (1981) and Chang *et al.* (1983) presented a series of articles describing the development of a rotating biological contactor system for BPE decolorization. The patented process uses *P. chrysosporium* immobilized on rotating discs. The discs are partially submerged in BPE which is diluted by the addition of growth nutrients. Campbell (1983) evaluated this process at an industrial scale and found that the cost for treatment would be $18/ metric ton dry pulp. The EPA is currently testing this mycelial

color removal (or MyCoR) process at the pilot plant scale (Susan Strohofer, personnel communication). Another bioreactor system called MYCOPOR, was developed by Messner *et al.* (1990) and uses sintered glass bead immobilized *P. chrysosporium*. This system decolorized, dechlorinated and reduced the BOD of BPEs by 60%, 70% and 85% respectively. An aerated lagoon process for BPE treatment by pellets of *P. chrysosporium* has also recently been evaluated (Prouty, 1989) in which a treatment cost of $4/ metric ton dry pulp was reported. In addition small-scale bioreactor systems have been developed for the production of LIP and MNP using stirred tank (Michel *et al.*, 1990) air-lift (Bonnarme and Jefferies, 1990) and by immobilized fungus reactor configurations (Linko, 1988).

Livernoche *et al.* (1983) studied the ability of a different white rot fungus to decolorize BPE. They reported that *Coriolus versicolor* could decolorize BPE by 80% after three days of incubation. Immobilization of *C. versicolor* in calcium alginate gel beads increased the rate of decolorization, and a lab scale fluidized bed reactor system was successfully tested. Royer *et al.*, (1985) described a continuous process utilizing mycelial pellets of *Coriolus versicolor* which decolorized E1 effluents by 50% in 15 h to 30 h and was operated for 24 days. Archibald *et al.* (1990) demonstrated that a wide variety of carbon sources could be used by *C. versicolor* during the decolorization process including glycerol, ethanol and crude carbohydrate sources like molasses and starch.

In summary, the white-rot fungi *P. chrysosporium* and *Coriolus versicolor* can rapidly decolorize, dechlorinate, and reduce the COD and BOD of bleach plant effluents. These organisms may prove valuable in industrial scale BPE waste treatment processes.

2.4 Enzymes involved in lignin biodegradation and BPE decolorization.

Phanerochaete chrysosporium produces a number of enzymes which are thought to play a role in lignin degradation. These enzymes include the lignin peroxidases (LIP), the manganese dependent peroxidases (MNP), glucose and glyoxal oxidases which are involved in hydrogen peroxide production and intracellular enzymes which complete the lignin mineralization process. *Coriolus versicolor* but not *Phanerochaete chrysosporium* produces the copper containing phenol oxidases known as laccases.

Two independent groups first isolated the enzymes which have come to be known collectively as lignin peroxidase (Tien and Kirk, 1984; Gold and Glenn, 1984). The extracellular lignin degrading enzymes (LIP) are secondary metabolites, first isolated from nitrogen-limited six day old cultures of *P. chrysosporium*. LIP non-specifically catalyzes several oxidations in the alkyl side chains of lignin related compounds including the Cα-Cβ bond of the propyl side chain of lignin model compounds. It is a heme containing glyco-protein requiring hydrogen peroxide for activity. Collectively these isozymes were called "ligninases". They share the ability to catalyze the oxidation of veratryl alcohol to veratryl aldehyde in the presence of hydrogen peroxide, a MW of between 39,000 and 43,000, cross reactions with polyclonal antibodies and pH optima of 2.5 to 3.0. The key reaction is the one electron oxidation of aromatic nuclei to produce unstable cation radicals.

Manganese peroxidases are a much less studied group of isozymes found in the culture fluid of *P. chrysosporium*. Kuwahara *et al.* (1984) and Tien and Kirk (1984) first isolated MNP. These enzymes are also glycosylated heme proteins but they catalyze the oxidation of Mn(II) to Mn(III), a highly reactive intermediate, in the presence of hydrogen peroxide. Mn(III) in turn can be stabilized by chelators, like lactate or malonate, and diffuse from the enzyme active site to attack phenolic substrates (Gold, 1991; Lackner *et al.*, 1991).

The production of both manganese peroxidases and lignin peroxidases is regulated by manganese and nutrient nitrogen. Bonnarme and Jefferies, (1990), found that the production of LIP varies inversely, and the production of MNP varies directly, with the manganese (Mn(II)) concentration in the culture media. Other fermentation parameters, such as glucose consumption and biomass production, are unaffected by manganese. Brown *et al.* (1990) reported manganese involvement in the transcriptional regulation of MNP expression by *P. chrysosporium*. Gold (1991) has reported the identification of manganese recognition sequences in the promoter regions of manganese peroxidase genes (but not lignin peroxidase genes).

The effect of nutrient nitrogen concentrations on ligninolytic activity is less clear. Fenn *et al.* (1981) and Kirk *et al.* (1978) showed that in nitrogen depleted cultures of *P. chrysosporium* addition of ammonium or glutamate repressed ligninolytic activity. Tien and Tu, (1987) established that nitrogen regulation acts at the level of lignin peroxidase gene transcription. LIPs were first isolated from nitrogen-limited cultures of *P. chrysosporium* (Tien and Kirk, 1983) but studies have reported ligninolytic activity in carbon-limited cultures where nutrient nitrogen is present in excess (Jefferies *et al.*, 1981) and have demonstrated LIP and MNP production in nitrogen sufficient cultures with glucose (Linko, 1988; Tonon *et al.*, 1990) and glycerol as the carbon sources (Tonon *et al.*, 1990). In general, the addition of glutamate has been shown to repress ligninolytic activity.

Beyond transcriptional level effects, the level of nutrient nitrogen has pronounced affects on the physiology of *P. chrysosporium*. The level of biomass, the size of pellets formed and the bulk rates of substrate utilization and respiration are much greater in nitrogen sufficient cultures as compared to nitrogen limited cultures (see Appendix 8). Thus besides affecting peroxidase gene transcription, the level of nutrient nitrogen may affect peroxidase production at a physiological level by altering culture conditions so that the production of the peroxidases is unfavorable.

Laccases are produced by many white rot fungi and in particular *C. versicolor*. These copper containing enzymes do not require hydrogen peroxide for activity and have been implicated in the dechlorination of chlorophenols and chloroguaicols found in BPE (Roy-Arcand and Archibald, 1991). In addition, laccases polymerize many phenol containing substrates. Laccases have been implicated in the decolorization of BPE by cultures of *C. versicolor* (Archibald *et al.*, 1990).

Surprisingly, despite the numerous studies of the ligninolytic system and the decolorization of BPE by the white-rot fungus *P. chrysosporium* the roles of the extracellular LIPs and MNPs in BPE decolorization, dechlorination and degradation have not been determined. Neither LIP nor MNP have been shown to decolorize BPE *in vitro*, although both enzymes have been shown to degrade lignin model dimer compounds in cell free systems (Kirk and Farrell, 1987). Paice and Jurasek (1984) demonstrated that horseradish peroxidase (HRP) could catalyze the decolorization of BPE. The same authors have claimed that peroxidases are not involved in the decolorization of BPE by *Coriolus versicolor* (Archibald *et al.*, 1990) by demonstrating that oxygen scavengers, hydrogen peroxide scavengers, catalase and compounds which affect peroxidase expression such as veratryl alcohol, nitrogen and manganese have no affect on decolorization of BPE by *Coriolus versicolor*. Recently, laccases of *C. versicolor* have been shown to dechlorinate and polymerize chlorophenols and chloroguiacols found in BPE (Roy-Arcand and Archibald, 1991).

Peroxidase activities in decolorization studies using *P. chrysosporium* are generally not reported and demonstration of the involvement of LIP and MNP in the decolorization of BPE has not been shown to date. One possible explanation for this is that the veratryl alcohol oxidation assay, the simplest and most widely used assay for lignin peroxidase activity, gives poor results when minute quantities of BPE are added to the assay mixture (Michel, unpublished results). To a lesser extent, the presence of BPE also interferes with assays for manganese peroxidase activity. A major focus of this study was to determine

the roles of the lignin and manganese peroxidases in BPE decolorization by *P. chrysosporium*. To accomplish this, the production of the LIPs and MNPs was controlled using manganese, nutrient nitrogen and mutant strains which are defective in their ability to produce LIP and MNP (Boominathan *et al.*, 1990; Kim and Reddy, 1990) and the affect on BPE decolorization was examined. The activities of the extracellular peroxidases were assayed in control cultures without added BPE and the presence of the peroxidases in BPE amended cultures was confirmed using gel electrophoresis.

2.5 Research Objectives

1. To study mass transfer limitations in mycelial pellet cultures of *P. chrysosporium* and understand their effect on the production of LIPs and MNPs.

2. To develop an unstructured kinetic model describing growth, substrate utilization and respiration by mycelial pellets of *P. chrysosporium* during the lag, primary growth, secondary metabolism and death phases.

3. To apply the extracellular peroxidases of *P. chrysosporium* to the decolorization of bleach plant effluents and investigate the roles of MNP and LIP in BPE decolorization.

CHAPTER III

THEORETICAL

3.1 Kinetic Model Development

In this section the development of a kinetic model for batch cultures of mycelial pellets of *P. chrysosporium* is presented. The model describes the unsteady-state glucose (G), nutrient nitrogen (N), oxygen (C_l), polysaccharide (pG) and carbon dioxide concentrations as well as the culture dry weight (X), the characteristic mycelial pellet radius (R) and the oxygen effectiveness factor (E), given the initial glucose, nutrient nitrogen and oxygen concentrations and the initial inoculum dry weight. The model is applicable to any mycelial pellet culture where intraparticle oxygen mass transfer is rate-limiting.

Typically, nitrogen-limited cultures of *P. chrysosporium* proceed through four phases. Following a short lag phase, a primary growth phase, during which the cultures grow rapidly. When the limiting substrate (nutrient nitrogen) is exhausted from the medium, and glucose is present in excess, the cultures enter a secondary metabolic phase during which the MNPs and then the LIPs are produced. Cell autolysis occurs during the death phase. A set of rate equations is presented for each of these life-cycle phases. Culture respiration, which is shown to be the rate limiting process under most conditions, is described using a separate set of equations which are valid during both the primary growth phase and secondary metabolism.

The critical model assumptions are that pellets are spherical, monodisperse and of constant density during the primary growth and secondary metabolic phases, that the transfer of oxygen into pellets occurs solely by means of molecular diffusion, and that cell respiration follows Michaelis-Menten kinetics. A summary of the kinetic model equations is presented in Figure 3.1.

	Lag Phase	Primary Growth	Secondary Metabolism	Death Phase
Biomass (X) (g/m^3)	$X = X_o$	$\dfrac{dX}{dt} = E_{MM}\,\mu_{max}\,X$	$\dfrac{dX}{dt} = -f_x\dfrac{dG}{dt}$	$-\dfrac{dX}{dt} = k_{aut}(X - X_f)$
Nutrient Nitrogen (N) (g/m^3)	$N = N_o$	$-\dfrac{dN}{dt} = Y_{n/x}\,E_{MM}\,\mu_{max}\,X$	$N = 0$	$N = 0$
Glucose (G) (g/m^3)	$G = G_o$	$-\dfrac{dG}{dt} = Y_{g/x}\dfrac{dX}{dt} + Y_{gO2}\,R_{O2}$	$-\dfrac{dG}{dt} = \left[\dfrac{Y_{gO2}}{1-f_x\cdot f_{pg}}\right] R_{O2}$	$G = 0$
Polysaccharide (pG) (g/m^3)	$pG = 0$	$pG = 0$	$\dfrac{dpG}{dt} = -f_{pg}\dfrac{dG}{dt}$	$-\dfrac{dpG}{dt} = k_{pg}\,X$
Respiration rate (RO$_2$) (g/m^3 media/s)	$R_{O2} = 0$	$R_{O2} = E_{MM}\left[\dfrac{V_{max}\,C_l}{K_m + C_l}\right]\left[\dfrac{V_{pel}\,\eta}{V_l}\right]\left[\dfrac{G}{K_s + G}\right]$		$R_{O2} = -\left[\dfrac{1}{Y_{g/O2}}\right]\dfrac{dpG}{dt}$
CO$_2$ evolution rate (RCO$_2$) (g/m^3 media/s)	$R_{CO2} = 0$	$R_{CO2} = Y_{CO2/O2}\,R_{O2}$		
Dissolved oxygen (C$_l$) (g/m3)	$C_l = C_{lo}$	$\dfrac{dC_l}{dt} = \dfrac{R_{O2}\,V_l}{V_l + H\,V_m}$		

Figure 3.1 Summary of kinetic model equations for mycelial pellet cultures of *P. chrysosporium*.

Lag phase

Relatively little change in the biomass, glucose or oxygen concentration is seen immediately after inoculation in agitated submerged cultures of *P. chrysosporium.* During this lag phase, tiny mycelial pellets form. The process of pellet formation, involving the aggregation of hyphal fragments, is complete within eight hours after culture inoculation and the total number of these spherical pellets does not increase after this period (Michel *et al.,*1990). Furthermore, these pellets exhibit a fairly uniform size which is dependent on the rate of agitation. The total specific pellet volume and hence pellet density, is constant for pellet diameters up to 0.005 m (Liebeskind *et al.,*1990, Michel *et al.,*1990). This is in contrast to previous studies of *P. chrysogenum* where pellet density varies with pellet size (Kobayashi *et al.,* 1973; van Suijdam *et al.,* 1982) or position (Wittler *et al.,* 1986) as a result of autolysis at the pellet center. Thus, at a specific biomass concentration the characteristic pellet radius and pellet volume can be calculated using Equations 1 and 2.

(1)

$$R = \left(\frac{X}{\frac{4}{3}\pi\rho\eta} \right)^{\frac{1}{3}}$$

(2)

$$V_{pel} = \frac{4}{3}\pi R^3 = \frac{X}{\rho\eta}$$

Primary Growth Phase

Growth proceeds exponentially after the lag phase if nutrients are non-limiting. The growth rate and the uptake rate of nutrient nitrogen are given by the exponential growth law and the yield coefficient $Y_{n/x}$ which represents the grams of biomass formed per gram of ammonium consumed (Equations 3 and 4).

$$R_X = \frac{dX}{dt} = \mu_e X \tag{3}$$

$$R_n = -\frac{dN}{dt} = Y_{n/x}\, \mu_e\, X \tag{4}$$

As reported by other investigators (Kobayashi *et al.*, 1973; Pirt, 1966), the oxygen concentration in the pellets may become growth limiting. The effective specific growth rate (μ_e) is related to the maximum growth rate (μ_{max}) by Equation 5 (vanSuijdam *et al.*,1982),

$$\mu_e = E\, \mu_{max} \tag{5}$$

where the oxygen effectiveness factor (E) is defined as the observed rate of respiration divided by the rate that would be observed without mass transfer limitations. The calculation of the effectiveness factor is described in section 3.3. If the effectiveness factor is near unity, the biomass concentration can be calculated as a function of time by integrating Equation (3).

$$\ln\left(\frac{X}{X_0}\right) = \mu_{max}\,(t - t_{lag}) = \mu_{max}\,t - \mu_{max}\,t_{lag} \tag{6}$$

This is a linear equation such that a plot of $\ln(X/X_0)$ versus time during the primary growth phase will reveal μ_{max} and t_{lag} as its slope and x-intercept respectively.

Glucose serves as both a carbon and energy source for *P. chrysosporium* during primary growth. It is used for energy via respiration and for biomass production (Equation 7).

$$Rg = -\frac{dG}{dt} = Rg_{respiration} + Rg_{growth} \tag{7}$$

The amount of glucose used for biomass formation during primary growth can be calculated using the yield coefficient $Y_{g/x}$ which represents the grams of glucose consumed per gram of biomass produced (Equation 8).

$$Rg_{growth} = Y_{g/x}\,\frac{dX}{dt} \tag{8}$$

The rate of glucose uptake for respiration under aerobic conditions is proportional to the rate of oxygen utilization. The yield coefficient $Y_{g/O2}$ represents the grams of glucose consumed divided by the grams of glucose respired (Equation 9).

$$Rg_{respiration} = Y_{g/O2} \; R_{O2} \tag{9}$$

Secondary metabolism

In nitrogen-limited cultures, the onset of secondary metabolism coincides with the depletion of nutrient nitrogen from the medium (Jefferies et al.,1981). The production of extracellular MNPs and then LIPs occurs only during this phase. The production of these enzymes as well as the total ligninolytic activity (^{14}C-lignin to $^{14}CO_2$) is significantly enhanced by high oxygen partial pressures (Barlev and Kirk,1981; Dosoretz et al.,1990a; Dosoretz and Grethlein,1991; Reid and Seifert,1982; Kirk and Farrell,1987). In the classic case, no cell growth occurs during this phase. However, in cultures of P. chrysosporium, the culture dry weight slowly increases after nitrogen is depleted. Polymerization of glucose in the media to cell-bound and soluble $\beta,1-4$ glucan has been shown to occur (Dosoretz et al.,1990a; Dosoretz and Grethlein, 1991; Leisola et al.,1982) which is also affected by the oxygen partial pressure (Dosoretz et al.,1990a). The primary metabolic activity of the cell during this period, however, is respiration. The total rate of glucose uptake during secondary metabolism is given by Equation 10.

$$Rg = - \frac{dG}{dt} = Rg_{respiration} + Rg_{growth} + Rg_{polyG} \tag{10}$$

The glucose metabolism factors f_x, f_{pg} and f_r represent the fractions of glucose consumed used for biomass, polysaccharide synthesis and respiration, respectively, during secondary metabolism (Equations 11 a,b,c).

$$\tag{11a}$$

$$Rg_{biomass} = -f_x \frac{dG}{dt}$$

$$Rg_{polyG} = -f_{P\mathbf{g}} \frac{dG}{dt} \tag{11b}$$

$$Rg_{respiration} = -f_r \frac{dG}{dt} = Y_{g/O2} \, R_{O2} \tag{11c}$$

The total rate of glucose consumption is given by Equation 12.

$$Rg = -\frac{dG}{dt} = -f_x \frac{dG}{dt} - f_{P\mathbf{g}} \frac{dG}{dt} + Y_{g/O2} \, R_{O2} \tag{12}$$

Simplifying Equation 12 gives the total rate of glucose consumption as a function of the rate of culture respiration (Equation 13).

$$Rg = -\frac{dG}{dt} = \left(\frac{Y_{g/O2}}{1 - f_x - f_{P\mathbf{g}}} \right) R_{O2} \tag{13}$$

Death Phase

In aerobic batch cultures of many fungi, a decline in cell mass occurs due to cell autolysis when the carbon energy source is exhausted. In nitrogen limited cultures of *P. chrysosporium*, proteases (shown to degrade LIPs and MNPs) are released during the beginning of the death phase (Dosoretz and Grethlein,1991). Although glucose has been depleted, carbon dioxide evolution continues during the death phase. To account for this the assumption was made that polysaccharide produced during secondary metabolism is used as an energy source by non-autolyzed cells (Equation 14).

$$Rg = -\frac{dpG}{dt} = k_{P\mathbf{g}} X \tag{14}$$

The rate of cell dry weight decrease is expressed using a first order rate constant (k_{aut}) (Equation 15). The amount of biomass remaining after all biological activity has ceased is X_f, this is assumed to be a fraction of the maximum biomass attained.

$$Rx = -\frac{dX}{dt} = k_{aut}(X - X_f) \tag{15}$$

During the death phase oxygen is no longer a limiting nutrient and the effectiveness factor is not needed. To provide maintenance energy, polysaccharides formed during secondary metabolism are respired (Equation 16).

$$R_{O2} = - \left(\frac{1}{Y_{g/O2}} \right) \cdot \frac{dpG}{dt} \tag{16}$$

3.2 Determination of the rate limiting process in mycelial pellet cultures of *P. chrysosporium*

Previous studies of mycelial pellet growth and respiration have shown that the mass transfer of oxygen into mycelial pellets may become diffusion limited. A schematic representation of the process of oxygen mass transfer in mycelial pellet cultures is presented in Figure 3.2. Oxygen must continuously move from the gas phase to the liquid phase, from the bulk liquid to the pellet surface, and from the pellet surface to the interior portion of the pellet where respiration occurs. Due to its low solubility in water (32.9 g/m^3 in water at 39° C), oxygen can quickly become depleted within the mycelial pellet. The mass transfer of substrates is analyzed for mycelial pellet cultures of *P. chrysosporium* in the following section.

Estimation of external and intraparticle mass transfer resistances.

The contributions of the gas-liquid, liquid-pellet, and intra-particle mass transfer limitations can be estimated by direct measurement of gas and liquid phase substrate concentrations, and by calculating the dimensionless Biot number (Bi) and observable modulus (Φ) (Bailey and Ollis, 1986). If the rate of oxygen transport from the headspace to the liquid phase is much greater than the bulk rate of oxygen consumption, the concentration of oxygen in the liquid phase and head-space can be related using Henry's law (Equation 17).
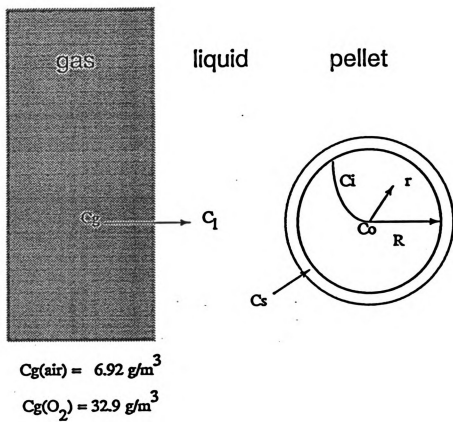
Figure 3.2   The process of mass transfer and reaction in mycelial pellet cultures.

$$C_l = H\,C_{hs} \qquad (17)$$

The value of the Henry's law constant can be estimated by dividing the solubility of oxygen in cell-free media by the ideal gas concentration in the headspace (Equation 18).

$$H = \frac{C_{sat}(T)RT}{MW\,P} \qquad (18)$$

The external and intraparticle mass transfer resistances can be compared based on the Biot number (Bailey and Ollis, 1986) (Equation 19).

$$Bi = \frac{k_l R}{3\,De} \qquad (19)$$

For Biot numbers greater than 100, the effects of external mass transfer resistance are not significant (Bailey and Ollis, 1986).

The dimensionless observable modulus (Equation 20) can be used to estimate the relative importance of the intraparticle mass transfer resistances of substrates without prior knowledge of intrinsic kinetic parameters (Bailey and Ollis, 1986).

$$\Phi = \frac{v}{De\,C_l}\left[\frac{R^2}{9}\right] \qquad (20)$$

For values of Φ less than 0.3 the effectiveness factor is approximately one and the diffusion and reaction of substrate in the pellet is reaction limited. For Φ greater than 0.3, intraparticle diffusion resistance limits the reaction rate (Bailey and Ollis, 1986).

3.3 Model for the intraparticle diffusion and reaction of oxygen in mycelial pellets.

If diffusion occurs only by means of molecular diffusion, the diffusion and reaction of oxygen in a spherical mycelial pellet can be modelled using the following second-order differential equation and boundary conditions.

$$\frac{dC}{dt} + De\left(\frac{d^2C}{dr^2} + \frac{2}{r}\frac{dC}{dr}\right) = v \tag{21}$$

$$@\ r = R,\ C = Cs$$

$$@\ r = 0,\ \frac{dC}{dr} = 0$$

De is the effective diffusivity of oxygen in the mycelial pellet and v is the rate of oxygen utilization for respiration. Various methods have been used to solve the pseudo-steady state form (dC/dt=0) of this differential equation (Kobayashi et al.,1973, Moo-Young and Kobayashi,1972, van Suijdam et al.,1982, Yano et al.,1961). The solutions are commonly represented in terms of an effectiveness factor, defined as the observed reaction rate divided by the rate without mass transfer limitations. In sealed shake flask cultures the pseudo-steady state assumption is not valid over long time periods (>1/2 hr) since the oxygen concentration and mycelial pellet size change with time.

Prediction of oxygen concentration profile in mycelial pellets.

During the time period when a microelectrode is being used to measure the oxygen profile in a mycelial pellet, the pseudo-steady state form of Equation 21 can be used. A finite difference approach was used to approximate this form of Equation 21 (Carnahan et al.,1969).

$$\frac{C_{i-1} - 2C_i + C_{i+1}}{\Delta r^2} + \frac{C_{i+1} - C_{i-1}}{i\Delta r^2} = \frac{v}{De} \tag{22}$$

The boundary conditions are $C_0 = C_1$ and $C_n = C_s$. Solving for C_{i+1} gives an expression for the oxygen concentration profile in the pellet (Equation 23).

$$C_{i+1} = \left[\frac{i}{i+1}\right]\left[2C_i + \left[\frac{1}{i} - 1\right]C_{i-1} + \frac{v(C_i)\Delta r^2}{De}\right] \tag{23}$$

By choosing an appropriate model for respiration, the concentration profile within the pellet can be calculated using a shooting algorithm. The oxygen concentration at the pellet center (where $dC/dr = 0$) in the range zero to C_s is used to start the algorithm and the surface concentration is calculated. The center concentration is changed until the calculated surface concentration converges to the known value ($C_n = C_s$). If a small step size ($n=100$) is used this approximationt yields an accurate solution ($<0.01\%$ error) to the pseudo-steady state form of Equation 21. The oxygen concentration profile can be measured using an oxygen microelectrode (Revsbech and Ward, 1983). Intrinsic kinetic parameters are determined by fitting experimental data to Equation 23.

Calculation of the effectiveness factor for Michaelis-Menten kinetics.

The generalized effectiveness factor (E), valid for any rate equation and spherical geometry, can be calculated at time t using Equation 24.

$$E = \frac{\sum_{i=0}^{n} \left(v(C_i)\, (r_i^3 - r_{i-1}^3)\right)}{v(C_s)\, R^3} \tag{24}$$

For most microbial cultures, the Michaelis-Menten equation adequately describes the respiration kinetics (Equation 25).

$$v = \frac{Vmax\, C_1}{[Km + C_1]} \tag{25}$$

Although Equation 23 provides a simple means of estimating kinetic parameter values from oxygen profile data, calculation of the oxygen effectiveness factor at each succesive time point in the integrated model using Equation 24 proved very time

consuming (over 2 hours for one batch culture simulation using an IBM Model 50 Z computer). Therefore, for the integrated kinetic model the approximation derived by Moo-Young and Kobayashi (1972) was used to calculate effectiveness factors for Michaelis-Menten kinetics ($E_{M.M.}$) at successive time increments. This approximation is based on the more easily calculated zero-order (E_O) and first order (E_1) effectiveness factors (Equation 26).

MICHEALIS-MENTEN ORDER:

$$E_{M.M.} = \frac{E_O + \left[\frac{Km}{Cs}\right] E_1}{1 + \left[\frac{Km}{Cs}\right]} \tag{26}$$

If the intrinsic Michaelis-Menten kinetics are known, the zero order (E_O) and first order (E_1) effectiveness factors can be easily calculated using Equations 27 and 28 (Bailey and Ollis,1986).

ZERO ORDER:

$$E_O = 1 \qquad \text{for;} \quad R\left[\frac{Vmax}{6\,De\,Cs}\right]^{\frac{1}{2}} \le 1$$

$$\tag{27}$$

$$E_O = 1 - \left[1 - \frac{6\,De\,Cs}{Vmax\,R^2}\right]^{\frac{3}{2}} \quad \text{for;} \quad R\left[\frac{Vmax}{6\,De\,Cs}\right]^{\frac{1}{2}} > 1$$

FIRST ORDER:

$$E_1 = \frac{1}{\phi}\left[\frac{1}{\tanh\phi} - \frac{1}{3\phi}\right] \qquad \text{where: } \phi = \frac{R}{3}\left[\frac{Vmax}{De\,Km}\right]^{\frac{1}{2}} \tag{28}$$

Using the effectiveness factor, the rate of oxygen uptake by pellets of *P. chrysosporium* (rO_2) can be calculated based on the liquid phase oxygen concentration (C_l) (Equation 29). A Monod expression is added to account for the decrease in the respiration rate at low glucose concentrations.

$$r_{O2} = E_{M.M.} \left[\frac{V_{max} C_l}{K_m + C_l} \right] \left[\frac{G}{K_s + G} \right] \tag{29}$$

The bulk rate of respiration (R_{O2}) can be calculated using the characteristic pellet volume (V_{pel}), and the pellet number (η) (Equation 30).

$$R_{O2} = r_{O2} V_{pel} \eta \tag{30}$$

During respiration, glucose is metabolized to carbon dioxide. The rate of CO_2 produced can be calculated using a yield coefficient ($R_{CO2} = Y_{CO2/O2} R_{O2}$; where $Y_{CO2/O2}$ = 44/32 = 1.38). The carbon dioxide balance assumes that all CO_2 accumulates in the gas phase. The total amount of CO_2 in grams which has accumulated in the gas phase is given by equation 31.

$$CO_2 = 1.38 \, V_l \int_0^t \frac{X}{\rho} E_{M.M.} \left[\frac{V_{max} C_l}{K_m + C_l} \right] dt \tag{31}$$

Unsteady state oxygen balance in sealed cultures.

In sealed shake flask cultures the gas phase is flushed daily with oxygen. As the oxygen is consumed for respiration, the total amount in the flask decreases. The amount of oxygen in the gas phase plus the amount in the liquid phase equals the total oxygen in the flask at time t (Equation 32).

$$\text{total } O_2 = C_l V_l + C_{hs} V_{hs} \tag{32}$$

Since the gas and liquid phase concentrations are near equilibrium, the Henry's law relation can be substituted into Equation 32 to give the following expression (Equation 33).

$$\text{total } O_2 = C_l (V_l + H V_{hs}) \tag{33}$$

A differential expression for the change in the liquid phase oxygen concentration as a function of time is obtained by combining Equation 33 and the bulk rate of respiration (R_{O2}).

$$\frac{dC_l}{dt} = \frac{R_{O2} V_l}{V_l + H V_{hs}} \tag{34}$$

Thus an approximate solution to Equation 21 can be obtained by numerically integrating Equation 34 and recalculating the respiration rate, the effectiveness factor and the liquid phase oxygen concentration at each successive time point. The mycelial pellet radius can be determined based on the substrate balances, the biomass balance and the pellet density.

Determination of Effective Diffusivity of Oxygen (De) in Mycelial Pellets.

The value of the diffusivity of oxygen within the mycelial pellet is critical to the accurate determination of the kinetic parameters for respiration. However, a number of different values for the pure solute diffusivity of oxygen in water D (DO_2-H_2O) have been reported in the literature (Table 3.1).

Table 3.1 Reported values of the diffusivity of oxygen in water.

$D_{O_2-H_2O}$ (m²/s)	T (C)	Reference	Comments
2.9 x 10⁻⁹	39⁰	Perry *et al.*, 1984	reported error ± 20%
1.8 x 10⁻⁹	20⁰	Yano *et al.*, 1961	cites Perry *et al.*, 1950
1.8 x 10⁻⁹	20⁰	Kobayashi *et al.*, 1973	cites Yano *et al.*, 1961
2.1 x 10⁻⁹	25⁰	Jordan *et al.*, 1956	direct measurement.
1.7 x 10⁻⁹	25⁰	Jordan *et al.*, 1956	10% sucrose solution.
3.2 x 10⁻⁹	n.r.	Phillips, 1966	assumes 0.85 void fraction
3.4 x 10⁻⁹	39⁰	Wilke-Chang equation value	(see Perry et. al. 1984)
2.2 x 10⁻⁹	n.r.	Bailey and Ollis, 1986	
2.0 x 10⁻⁹	25⁰	Wittler *et al.*, 1986	

n.r.- value not reported

Because of the uncertainty in this value and the possibility of a reduced value of the diffusivity within the pellets due to a void fraction less than unity, the diffusivity of oxygen within mycelial pellets of *P. chrysosporium* was measured directly.

A stirred bath technique was used to determine the effective diffusivity in mycelial pellets based on a method described by Cresand *et al.* (1988) developed for the measurement of glucose diffusivity in cell matrices. Crank (1975) has detailed various stirred tank experiments for the determination of effective diffusivities. In one such experiment a slab initially free of solute is contacted with a well stirred solution (Figure 3.3). By measuring the decrease of the solute concentration in the liquid phase, the uptake rate by the slab and the diffusivity of the solute can be calculated. Assuming Fickian diffusion and a well mixed liquid phase, the concentration in the slab can be represented using the following equation and boundary conditions,

$$\alpha = \frac{V_l}{V_{slab}}$$

$$\Omega = \frac{\text{total pellet volume}}{\text{slab volume}}$$

D_c

D V_l

Deionized water

Magnetic stir bar

2 % Agar with suspended, killed mycelial pellets

Magnetic Stir plate
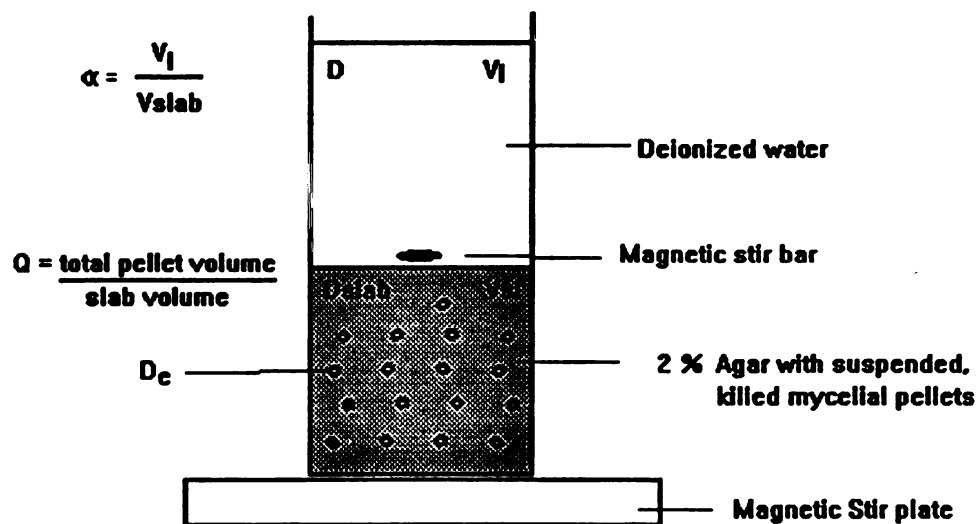
Figure 3.3   A schematic representation of an apparatus for measuring the effective diffusivity in mycelial pellets.

$$\frac{dC}{dt} = D_{slab} \frac{d^2C}{dx^2}$$

(35)

B.C.s $C=0$ at $t=0$, $C=Cb$ at $x=0$, $\frac{dC}{dx} = 0$ at $x=1$

where 1 is the slab thickness, Cb is the uniform bulk solute concentration in the liquid and x is the distance from the interface. A mass balance on the liquid phase gives Equation 36.

$$\alpha \, 1 \, \frac{dCb}{dt} = D_{slab} \left[\frac{dCb}{dt}\right]_{x=0}$$

(36)

B.C. $Cb = Co$ at $t=0$

where α is equal to V_l/V_{slab}, the liquid volume divided by the slab volume. These Equations can be solved using a Laplace transformation (Crank, 1975). The solution is written in terms of M_t, the amount of solute in the slab at time t and M_{inf} the amount of solute in the slab when the slab and liquid are in equilibrium where q_n are non-zero positive roots of Equation 38.

$$\frac{M_t}{M_{infinity}} = 1 - \sum_{n=1}^{infinity} \left[\frac{2\alpha(1+\alpha)}{1+\alpha+\alpha^2 q_n^2} \exp\left[\frac{-D_{slab} \, t}{l^2} q_n^2\right] \right]$$

(37)

$$\tan q_n = -\alpha \, q_n$$

(38)

Thus, if Mt/Minf is known at time t, then D_{slab}, the effective diffusivity in the slab can be calculated since α, t and 1 are known.

To determine De (the effective diffusivity in the pellets) a theoretical relationship derived by Maxwell (1973) can be used. This heat transfer equation was derived for the effective conductivity in a medium composed of periodically spaced spheres. The diffusivity analog, where no reaction is taking place, is given by Equation 39.

$$\frac{D_{slab}}{D} = \frac{\frac{2}{De} + \frac{1}{D} - 2Q\left(\frac{1}{De} - \frac{1}{D}\right)}{\frac{2}{De} + \frac{1}{D} + Q\left(\frac{1}{De} - \frac{1}{D}\right)} \tag{39}$$

In this equation, D is the diffusivity of oxygen in water, D_{slab} is the overall slab effective diffusivity, De is the effective diffusivity in the spheres (or pellets) and Q is the ratio of the total pellet volume to the slab volume. By plotting D_{slab}/D for a number of different values of Q, a curve is generated which is a function of De. The curve can be fit by selecting the appropriate value of De. According to Cresand et.al. (1988) the uncertainty in the value determined using the above approach is approximately 5% if the error in the concentration measurements is minimal.

3.4 Model for the decolorization of Kraft bleach plant effluent.

The decolorization of BPE was modelled using an apparent first order rate constant. A first order model was used because the initial rate of decolorization was found to be proportional to the initial BPE concentration, for synthetic BPE concentrations below 4000 C.U. (see results). This model was also used for reasons of mathematical simplicity. The rate of decolorization was modelled using the Equation 40.

$$\tag{40}$$

$$\frac{d\,C.U.}{dt} = k\,(\,C.U.\ -\ C.U._f)$$

The value of the apparent rate constant (k) was determined fitting experimental data to the integrated form of Equation 40.

CHAPTER IV

MATERIALS AND METHODS

4.1 Microorganisms.

The microorganisms used in this work were strains of the white-rot basidiomycete *Phanerochaete chrysosporium*. The wild-type strains used were BKM-F-1767 (ATCC 24725) and ME-446 (ATCC 34541). In addition mutant strains derived from ME-446 were used. These had the phenotypes lip⁻ (Boominathan *et al.*, 1990) and lip⁻ and mnp⁻ (Kim and Reddy, 1990). All strains were obtained from the laboratory of Dr. C.A. Reddy, of the Department of Microbiology and Public Health, Michigan State University and were maintained on 2% malt agar extract slants, pH 4.5 (Kelley and Reddy, 1986).

4.2 Culture conditions.

Experiments were conducted in shake flask cultures using asceptic techniques. The culture conditions used were as described by Michel *et al.* (1991). The defined culture medium contained diammonium tartrate (2 to 117 g/m^3 ammonium) as the nitrogen source and glucose (5000 to 15000 g/m^3) as the carbon source. The media also contained 2000 g/m^3 of KH_2PO_4, 1450 g/m^3 of $MgSO_4*7H_2O$, 132 g/m^3 of $CaCl_2*2H_2O$, 1.0 g/m^3 thiamine hydrochloride, 500 g/m^3 Tween 80 (not added in stationary starter cultures), 20 mM acetate (pH 4.5) and 0.4 mM veratryl alcohol. The following trace elements were also added: 142 g/m^3 of nitrolotriacetate trisodium salt, 70 g/m^3 of NaCl, 36.9 g/m^3 (12 ppm) of $MnSO_4*H_2O$, 12.6 g/m^3 of $CoCl_2*6H_2O$, 7.0 g/m^3 of $FeSO_4*7H_2O$, 7.0 g/m^3 of $ZnSO_4*7H_2O$, 1.1 g/m^3 of $CuSO_4*5H_2O$, 0.7 g/m^3 of $AlK(SO_4)_2*12H_2O$, 0.7 g/m^3 of H_3BO_3 and 0.7 g/m^3 of $Na_2MoO_4*2H_2O$. Unless mentioned otherwise, all the media contained 12 ppm Mn(II) as $MnSO_4$. In some experiments Mn(II), added as $MnSO4$, was varied to give 0, 12, 40 or 100 ppm.

Shake flask culture conditions.

Inoculated media (85 ml) were dispensed into sterile 250 ml rubber stoppered Erlenmeyer flasks. The inoculum consisted of a 10% (v/v) of homogenized mycelia which was grown in static cultures using the media described above with 10,000 g/m^3 glucose and 39 g/m^3 ammonium (as diammonium tartrate) but without Tween 80. All cultures were grown at 39° C. The cultures were agitated at 173 RPM on a shaker table (New Brunswick Gyrotory G-10) with 2.5 cm of eccentricity. The headspace (165 ml) of the flasks was flushed daily with oxygen for approximately 3 minutes at a flow rate of 1 l/min (Michel *et al.* 1990).

Bioreactor conditions.

The bioreactor system used consisted of a 5 liter Bioflo II (New Brunswick Sci. Co.) with a total volume of 6.3 liters. The culture conditions were as described by Michel *et al.* (1990). Agitation was provided by a marine impeller at a rate of 100 to 350 rev min^{-1}, no baffles were used. The reactor contents were sampled through the top-plate. For dry weight measurements a sample volume of greater than 50 ml was used. CO_2 evolution was measured by sealing the reactor without sparging for 24 hours, and sampling through the top plate using a pressure-lok syringe (Precision Sampling Corporation.). The respiration rate was also measured by transiently stopping the oxygen flow and measuring the decrease in the oxygen concentration in the culture fluid with time using a galvanic oxygen electrode.

4.3 Substrate Assays.

Glucose was measured as reducing sugar by the dinitrosalicylic acid (DNS) method using D-glucose as the standard (Miller, 1959). Samples were centrifuged and diluted and a 3.0 ml of a prepared DNS reagent solution was added. The assay mixture was

boiled for 5 minutes, cooled and the 595 nm absorbance was measured against an assay mixture blank.

Ammonium concentration was determined using an ammonium electrode (Orion model#95-12). Total carbohydrates were determined using the phenol-sulfuric acid assay as described by Leisola *et al.* (1982). For determining mycelial dry weight cultures were vacuum filtered through tared GF/C grade filter paper, rinsed with 100 ml deionized water and dried at 105° C to a constant weight.

The oxygen concentrations in the culture fluid and head space were measured using a polaragraphic oxygen electrode (Ingold, model #531) which was calibrated with oxygen and nitrogen sparged deionized water at 39° C. Respiration rate measurements were made by pouring one entire culture (85 ml) into a hydraulically full stirred vessel (respirometer) and measuring the decrease in oxygen concentration with time using a strip chart recorder with a chart speed of 20 cm/h or 50 cm/h. Stirring was provided by a magnetic stir bar rotating at approximately 120 min^{-1}. The rate of oxygen depletion was determined by measuring the slope of the oxygen depletion curve.

Acetate, ethanol and methanol concentrations (see Appendix 19 and 20) were determined using gas-liquid chromatography (Varian, model 3700, flame ionization detector). Samples were centrifuged, mixed with 4 parts 3N phosphoric acid and a volume of 5µl was injected. The injector, column and detector temperatures were 140° C, 125° C and 150° C, respectively. Peak areas were measured using an integrator (Hewlett-Packard, model HP-3396A).

Oxygen profile measurement

Oxygen profiles within mycelial pellets were measured using oxygen microelectrodes with tip diameters of approximately 3 µm generously donated by Dr. Peter Revsbech of the Center for Microbial Ecology (Revsbech and Ward, (1983). The electrode was connected to a chemical microsensor (picoammeter) and was calibrated with oxygen and nitrogen, sparged into distilled water. To determine the oxygen

concentration profile, a pellet was removed and placed onto a plate of agar-solidified extracellular culture fluid (15 ml). Liquid extracellular culture fluid (15 ml) was added to the surface of the agar and the system was equilibrated to air. Oxygen measurements were made by inserting the microelectrode into the pellet using a micromanipulator (0.01 mm gradations). In some cases a well was made in the agar gel using a Pasteur pipet. The microelectrode penetration procedure was monitored using a stereo dissecting microscope. The micromanipulator was also used to measure the diameter of the pellet being probed. The procedure was conducted in a 39° C. incubator room

The gas in the headspace was sampled with a pressure-lok syringe (Precision Sampling Corporation) and carbon dioxide was measured using a gas chromatograph (GOW-MAC series 350, thermal conductivity detector) fitted with a Porapak Q 80/100 column (helium carrier gas, column temperature 90° C). A sample volume of 1 to 5 µl was injected.

Manganese determination.

Manganese was measured using atomic absortion spectroscopy (Varian SpectrAA model AA-20) at a wavelength of 279.5 nm. One entire culture (85 ml) was filtered through GF/C grade filter paper to remove pellets and precipitated manganese solids. The filtrate, or soluble manganese fraction, was used undiluted, diluted 1:3 or diluted 1:10 with D.I. water (depending on initial manganese concentration). The precipitated and mycelially bound manganese was solubilized by adding an equal volume (85 ml) of 0.1 M HCl to the filter paper and stirring. Once the insoluble manganese had dissolved, this fraction was collected by vacuum filtration through the same filter paper.

4.4 Product Assays.

LIP and MNP activity.

LIP activity was determined spectrophotometrically by measuring veratryl alcohol oxidation to veratryl aldehyde at pH 2.5, room temperature (23° C.) and a wavelength of 310 nm as described by Tien and Kirk (1984). MNP activity was measured as described previously at a wavelength of 610 nm (Kuwahara *et al.*, 1984; Michel *et al.*, 1991) at 30° C. The sample volume was 10 to 40 μl, the pH was 4.5 and the reaction time was 4 min. A unit of MNP activity was defined as one μmol of phenol red oxidized per liter per minute, using an extinction coefficient of 4460 M^{-1} cm^{-1} (Michel *et al.*, 1991). MNP activity was also assayed using remazol blue. 10-40 μl of sample was added to 400 μl of buffer (125 mM), 400 μl of 5 g/l chicken albumin, 100 μl of 0.17 g/l $MnSO_4$ and 200 μl of 0.25g/l remazol blue. The reaction was started by adding 100 μl of 1 μM H_2O_2. The absorbance difference at 595 nm was measured over a 4 minute period.

The total protein concentration of the culture filtrate was measured using the Bradford Method employing bovine serum albumin as a standard. A commercially available reagent was used (Protein Assay, Bio-Rad, Richmond CA).

pH optima of LIP and MNP.

The pH optima of LIP and MNP were determined by buffering day 6 culture fluid, containing high levels of both LIP and MNP activity, with tartarate (10 mM) or acetate (20 mM) to 10 pH values between 2 and 7.2. The two enzymes exhibited different pH optima. LIP activity peaked at pH 2.5 and MNP peaked at pH 4.5 to 5.0. Interestingly, MNP activity at pH 2.5 was reduced by more than 80% compared to its activity level at pH 4.5. Also, LIP activity at pH 4.5 was reduced by more than 90% compared to its activity level at pH 2.5 (Figure 4.1).
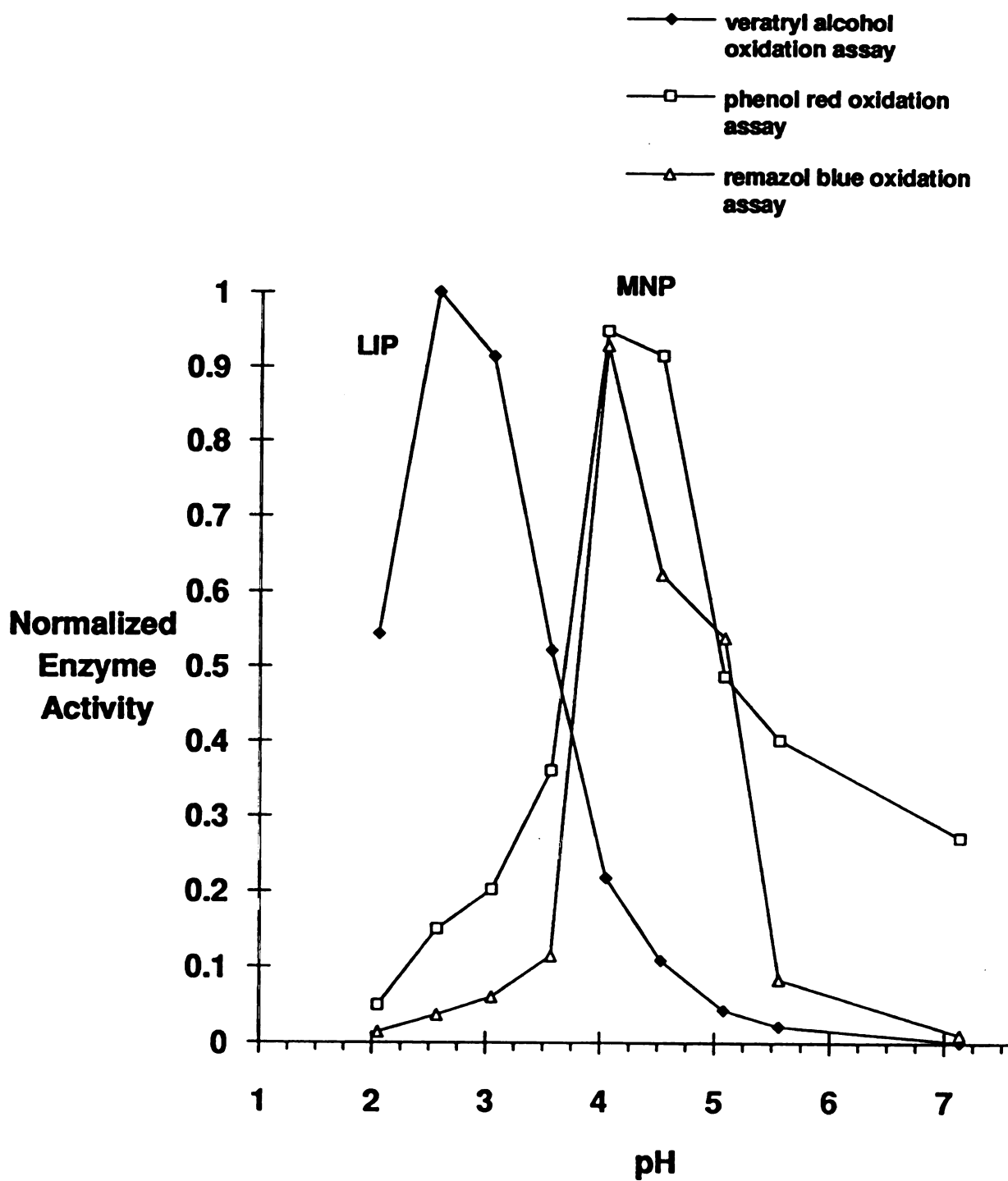
Figure 4.1 Lignin peroxidase and manganese peroxidase enzyme activities as a function of pH. Samples were buffered with acetate (0.1 M) for pH 4 to 7 or tartarate (0.1 M) for pH 2 to 3.5.

Pellet characteristics.

To measure pellet size, pellet density and pellet number (concentration), a known volume of culture fluid with pellets was poured into a Petri dish, photographed and enlarged. The total number of pellets was counted and the diameters of a group of twenty pellets were measured, scaled and averaged using the Sauter equation (Michel *et al.*, 1990). There was little difference in the values of the Sauter characteristic pellet radius and the radius determined by simply averaging the measured radii. Pellet sizes were also measured using a micromanipulator and a stereo dissecting microscope.

SDS-PAGE electrophoresis.

Extracellular proteins were identified using sodium dodecyl sulfate-polyacrylamide gel electrophoresis (SDS-PAGE) as previously described (Kelley and Reddy, 1986). Samples (2.0 ml) were removed from cultures and concentrated to 200 μl using a Centricon ultrafiltration unit (Amicon Div., W. R. Grace & Co., Danvers, MA) with a 10 kD molecular weight cut-off. The concentrated samples were applied to a 4% stacking/10% running gel and the proteins were stained with Coomasie brilliant blue.

Fast protein liquid chromatography.

To separate and purify MNP and LIP proteins, the extracellular fluid from active, 4 or 6 day-old cultures was frozen overnight to precipitate polysaccharides, centrifuged, concentrated to approximately 5% of the original volume by ultrafiltration, and dialyzed against 2 liters of 10 mM acetate buffer (pH 6). The concentrated enzyme solution was applied a Mono Q column (Pharmacia, Uppsala, Sweden) at a flow rate of 0.2 to 1.0 ml/min and eluted using a gradient of acetate buffer from 10 mM to 1.0 M. Heme proteins were detected by continuous monitoring at 409 nm. Fractions (0.5 ml) were collected using a programmable fraction collector.

4.5 Preparation and characteristics of Kraft bleach plant effluents

Two types of Kraft bleach plant effluent (BPE) were used, an industrial BPE obtained from a U.S. pulp mill and a synthetic BPE. The synthetic BPE was prepared from a high grade (less than 1% ash) commercially available Kraft lignin (Indulin AT, Westvaco Co.) as described by Lundquist et al., (1977). Briefly the procedure employed was as follows: Indulin AT (3.83 g), was dissolved in 150 ml of 0.14 M NaOH, 25.5 ml of 0.6 M H_2SO_4 was added with stirring, and the lignin material was precipitated. Chlorine water [668 ml of 8.1% (v/v) Chlorox] was added, and the solution was agitated for 1 h in a shaker bath at 25° C. The solution was removed from the shaker bath and stripped with nitrogen gas via a gas dispersion tube, to remove excess chlorine. After 2 h, 213 ml of 1.0 M NaOH was added, and the mixture was incubated for 2 h in a shaker bath at 30° C. Next, the solution was acidified to pH 2.5 using 0.6 M H_2SO_4 (approximately 128 ml) and deionized water was added to bring the mixture to a volume of 1.5 L. The effluent generated using this protocol was considered typical of the effluent from an industrial kraft bleach plant (Lundquist et al., 1977).

Both industrial and synthetic BPE were concentrated under vacuum using a Rotavapor-R (Brinkmann) to approximately 12% of their original volume. The pH was adjusted to 4.5 using 1.0 M NaOH and the solutions were stored at 4° C until used. After concentration the effluents contained 56,000 to 69,000 standard platinum cobalt units of color (C.U.). The concentrated BPE solutions were generally added to cultures of P. chrysosporium to give a final concentration of 3,000 C.U (624 C.U. = 1 g BPE/liter). Typically, industrial bleach plant effluents contain 3,000 to 10,000 C.U.

BPE Color measurement.

The measurement of decolorization of both fungal-treated and untreated BPE was based on the NCASI standard method (NCASI, 1971). The standard Platinum-Cobalt color solution (500 color units) was prepared by dissolving 0.2492g of K_2PtCl_2 and 0.2 g of $CoCl_2 \cdot 6H_2O$ in a mixture of 20 ml concentrated HCl and 50 ml of D.I. H_2O. After dissolving, the mixture was diluted to total volume 200 ml.

To measure color, samples were diluted in phosphate buffer (pH 7.6), centrifuged for 15 min at 10,000 x g, and the absorbance at 465 nm was measured as previously described (NCASI, 1971). The conversion factor used was 4015 std Pt-Co color units (C.U.) per 1.0 absorbance unit at 465 nm (cm^{-1}). Color on the mycelium was measured by homogenizing 10 parts buffer to 1 part centrifuged mycelial pellets, and then filtering through GF/C grade filter paper (Whatman Paper Ltd., Maidstone, England). In some instances adjustment of the pH of fungal treated BPE led to the precipitation of extracellular polysaccharides. When this occured the data were disregarded.

Solubility of BPE

The solubility of both synthetic and industrial BPE was determined as follows; 2.0 ml of concentrated BPE was added to 9.0 ml of complete media. The pH was adjusted to values between pH 2.5 and pH 7 using 1 M HCl or 1 M NaOH. These solutions were mixed vigorously, allowed to sit for 30 minutes, mixed again and then cetrifuged for 10 minutes at 14,000 x g. After centrifugation, 0.5 ml aliquot each supernatant was immediately removed and mixed with 1.0 ml of phosphate buffer (pH 7.6). The absorbance of each sample was then measured at 465 nm. Industrial BPE was more soluble at pH 2.0 to 7.0 than synthetic BPE prepared as described above (Figure 4.2).
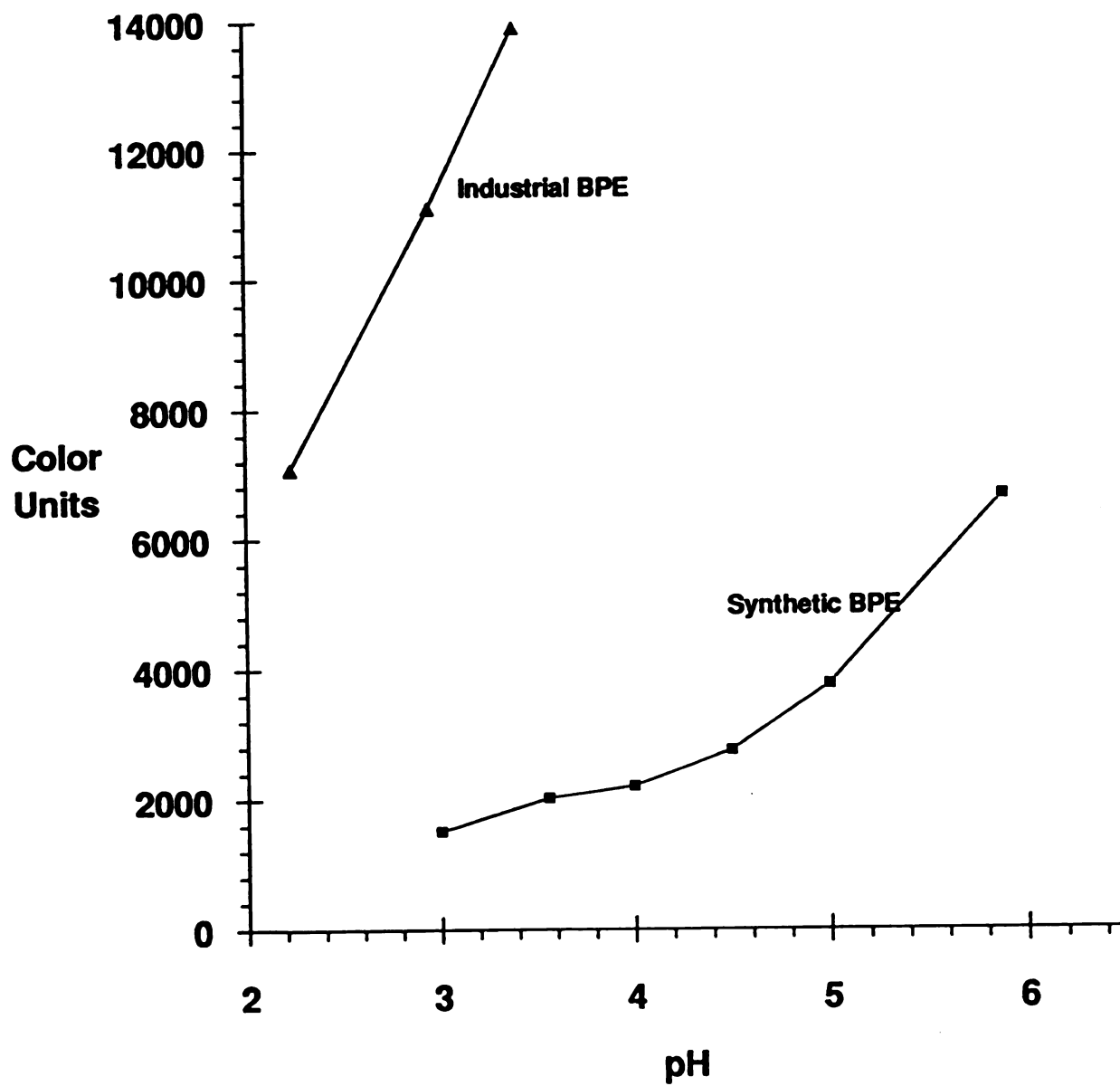
Figure 4.2   The solubilities of synthetic BPE and industrial BPE in culture medium as a function of medium pH.

Molecular weight of BPE.

The molecular weight of the colored material in the plant and synthetic BPE was estimated using ultrafiltration. Samples of BPE (1 ml, 1200 C.U.) were mixed with 3 ml 0.1M KOH to solubilize all precipitates. After centrifugation (no precipitates observed) 2 ml of the solutions were applied to disposable ultracentrifuge tubes with a molecular weight cut-off of 10,000 daltons. After centrifugation for 2 hours both the upper (>10000 MW) and lower (<10000 MW) fractions were diluted back to the original 2 ml using buffer (pH 7.6) and 465 nm absorbance was measured. For both industrial and synthetic BPEs, more than 90% of the color remained in the upper part of the tube indicating that most (>90%) of the colored material in the BPE had a molecular weight greater than 10,000 daltons.

4.6 Computational methods.

The complete kinetic model equations were analytically or numerically integrated using Euler's method with a time increment of 1 h. A BASIC computer program calculated X, G, N, C, pG, $E_{M.M.}$, total culture CO_2, total culture O_2 and characteristic pellet radius (R) as a function of time (Appendix 21). The data were transferred to a spreadsheet (EXCEL) and plotted. This was compared to experimental data for X, G, N, total culture CO_2 and pellet size (Appendix 15). The Michaelis-Menten effectiveness factor was determined using the method of Moo-Young and Kobayashi (1972).

Another computer program, (Appendix 22) calculated the oxygen concentration gradient within a mycelial pellet, given the pellet radius and liquid phase oxygen concentration. This program solved the Equations for diffusion and reaction of oxygen within a mycelial pellet using Michaelis-Menten kinetics. A shooting algorithm was used with Newton-Raphson convergence. The program was used to determine values of V_{max} and Km as described by Michel *et al.* (1992a).

CHAPTER V

A model for submerged, peroxidase producing, mycelial pellet cultures

of *Phanerochaete chrysosporium*

Part I: Results

5.1 Culture characteristics of mycelial pellet cultures of *P. chrysosporium*.

Patterns of growth (culture dry weight and pellet radius), glucose and nitrogen (ammonium) depletion, carbon dioxide evolution and oxygen depletion, and the production of extracellular peroxidases were determined for nitrogen-limited, mycelial pellet cultures of *P. chrysosporium* BKM-F-1767 (Figure 5.1a-d). The organism grew rapidly during the first 24 hours after inoculation (doubling time=5.2 h) and the nutrient nitrogen (ammonium) concentration decreased steadily to undetectable levels within 24 hours. The glucose concentration in the medium decreased in a linear fashion between days 2 and 8 of incubation and was completely depleted by day 10 (Figure 5.1a). The total culture carbohydrate concentration (Appendix 4) closely followed the glucose concentration between days 0 and 5. From day 5 to day 9, total carbohydrates exceeded total culture glucose due to the formation of polysaccharides. Between days 1 and 9 there was a steady increase in culture dry weight from approximately 1,000 g/m^3 on day 1 to approximately 2,000 g/m^3 on day 9. Concurrently, the size of the mycelial pellets increased from an average diameter of 1.5 mm to 2.1 mm (Figure 5.1c).
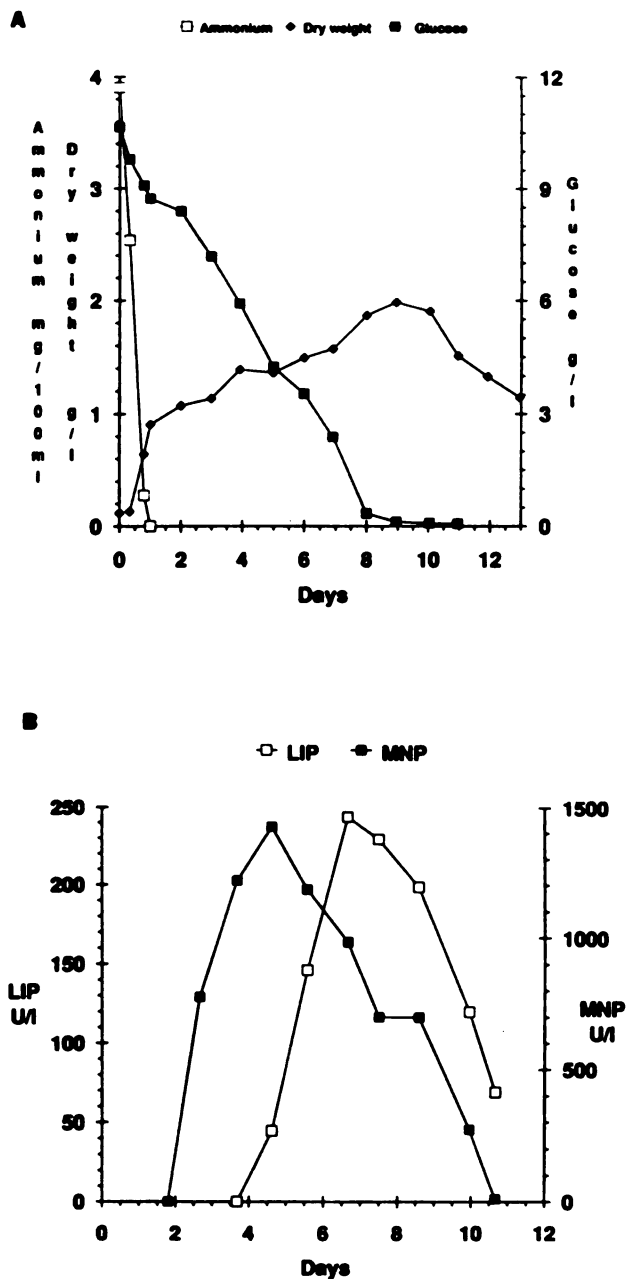
Figure 5.1   Biomass production, nitrogen and glucose utilization, and production of extracellular peroxidases in agitated, nitrogen-limited (2.2 mM) cultures of *P. chrysosporium* BKM-F-1767. A. Time course of ammonium, glucose, and biomass (culture dry weight). Values represent averages for triplicate cultures.
B. Time course of lignin peroxidase (LIP) and manganese peroxidase (MNP) activities and total extracellular protein concentration.
C. Mycelial pellet size.
D. Carbon dioxide evolved and oxygen utilized.

C
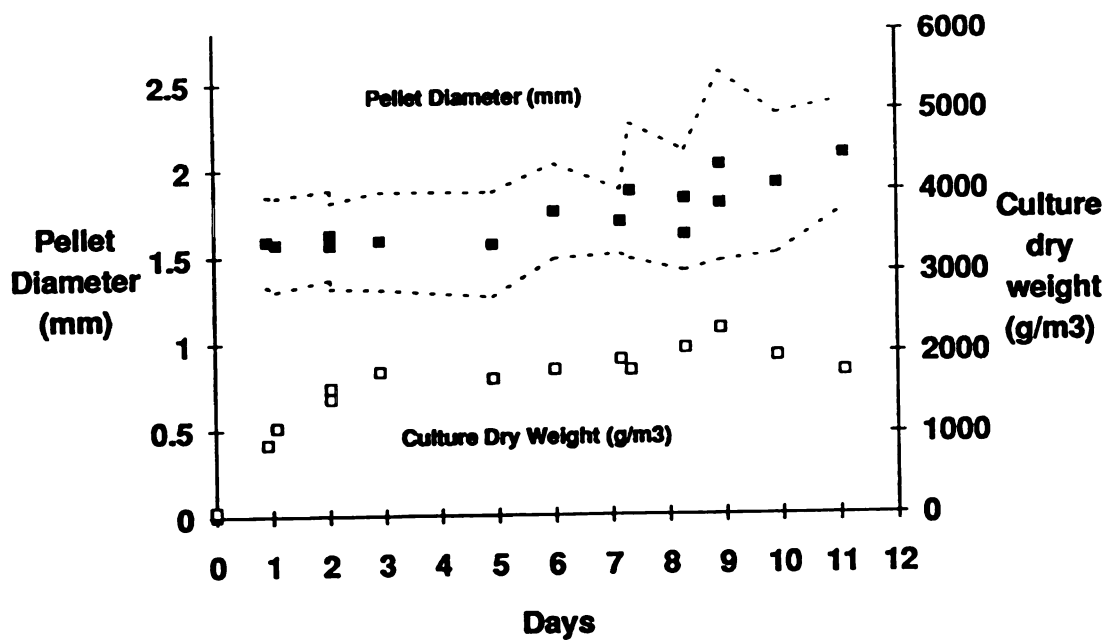
D
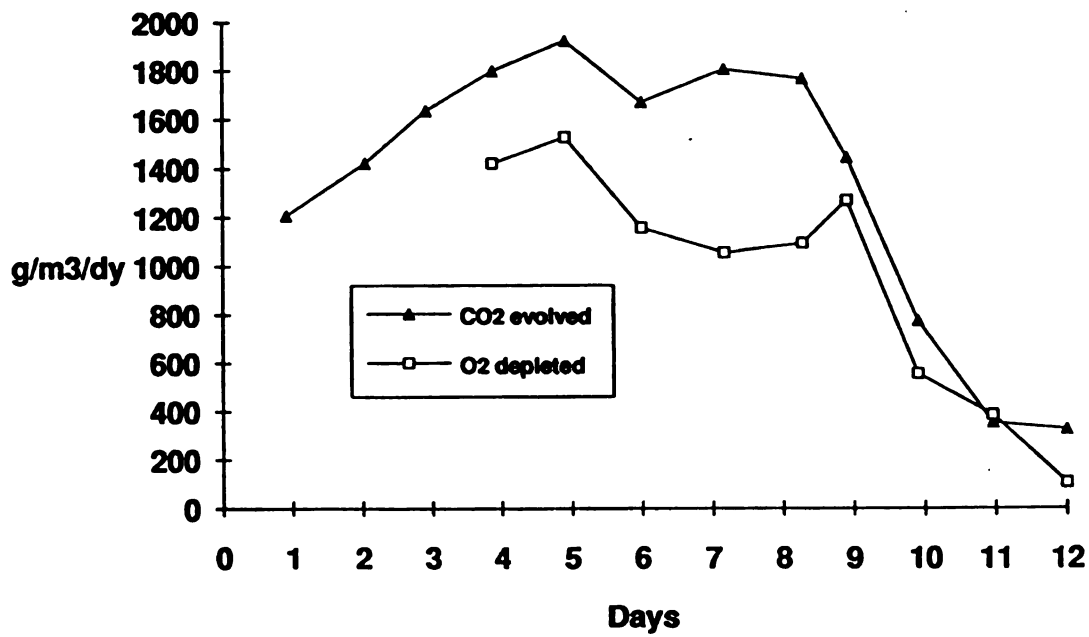
After glucose depletion on day 10, the culture dry weight decreased rapidly, probably due to cell autolysis and/or cell wall polysaccharide utilization (Boominathan and Reddy, 1991; Kirk and Farrell, 1987). Acetate, which is used as a buffer and has been shown to increase the production of LIP and MNP compared to other buffers (Michel *et al.*, 1988), was not detectable after 3 days (Appendix 4).

The concentration of CO_2 in the headspace (measured daily before culture oxygenation) also gradually increased during secondary metabolism from day 1 to day 9. The depletion of oxygen from the headspace paralleled the evolution of CO_2 with a nearly 1:1 O_2/CO_2 molar ratio, characteristic of aerobic metabolism (Figure 5.1d).

The extracellular peroxidases of *P. chrysosporium* are widely implicated in lignin degradation and in the detoxification of a variety of toxic aromatic compounds (Kirk and Farrell, 1987; Lamar *et al.*, 1990; Valli *et al.*, 1991, Eaton, 1984, Bumpus *et al.*, 1985; Lin and Wang, 1990). Therefore, the time courses of MNP and LIP activities as well as total extracellular protein were determined. The depletion of nutrient nitrogen (Figure 5.1a) coincided with the onset of secondary metabolism and the production of extracellular peroxidases (Figure 5.1b). In agreement with other studies (Dosoretz *et al.*, 1990a, Michel et al., 1991), MNP activity was first detected in the extracellular culture fluid between day 2 or 3 of incubation, increased to a maximum on day 4 or 5, and declined to low levels by day 11 (Figure 5.1b). LIP activity, on the other hand, first appeared between days 4 and 5, reached a maximum between days 6 and 7 and then rapidly declined. This decline in LIP activity during secondary metabolism has been reported to be due to degradation of LIP proteins by a protease induced under starvation conditions (Dosoretz *et al.*, 1990b). The observed loss of peroxidase activity between days 8 to 11 also corresponded to the depletion of glucose in the culture fluid. Total extracellular proteins, which are initially high due to mycelial disruption during homogenizing, declined throughout the primary growth phase but gradually increased

during secondary metabolism on days 5 through 8 as the MNP and LIPs were produced (Appendix 4).

The concentration of soluble manganese in cultures declined to low levels one day after MNP's were first produced (Figure 5.2). The appearance of a brown mycelial coloration coincided with this decrease in soluble manganese. Most of the manganese, which was soluble before MNPs were produced, was found in an insoluble fraction associated with the mycelia by day 5. Cultures without manganese in the medium did not form the brown coloration, nor did high nitrogen cultures containing 12 ppm Mn, where no peroxidase activity was detected. Thus manganese deposition in these cultures seems to be related to the production of MNP and not due to simple physical precipitation. After the addition of BPE (see chapter 6), the brown coloration was observed to diminish substantially and then reappear after the BPE had been decolorized.

5.2 Estimation of mass transfer resistances in mycelial pellet cultures of *P. chrysosporium*.

The overall resistance to the mass transfer of substrates in a submerged mycelial pellet culture (Figure 3.1) can be examined in terms of a series of resistances involving a gas film and a liquid film for the gas liquid interface, a liquid film around the mycelial pellets and intraparticle diffusion (Kobayashi et al., 1973). In most studies of respiration by mycelial pellets the oxygen concentration at the pellet surface (C_s) is assumed to be equal to the bulk liquid concentration (C_l) (Metz and Kossen,1977). This assumption has rarely been validated. In theory, the relative importance of the film mass transfer resistance can be estimated by calculating the Biot number (Equation 19). Experimentally, the bulk and surface concentrations of oxygen can be directly measured using oxygen microelectrodes. The Biot number for oxygen, assuming a hypothetical worst case of very small pellets (R=0.5 mm) and a low value for the mass transfer coefficient (k_l = 0.0005 m/s), is 250. For a Biot number greater than 100, the external
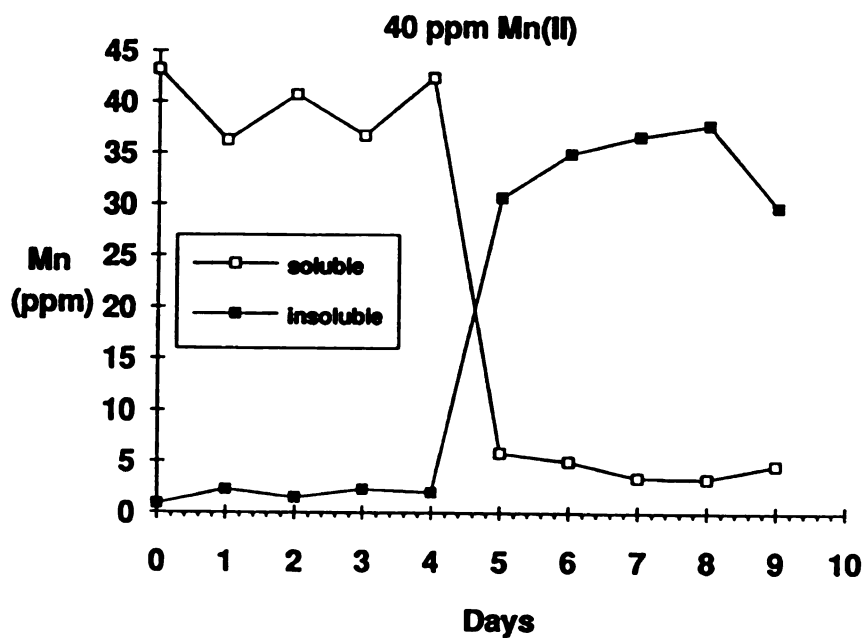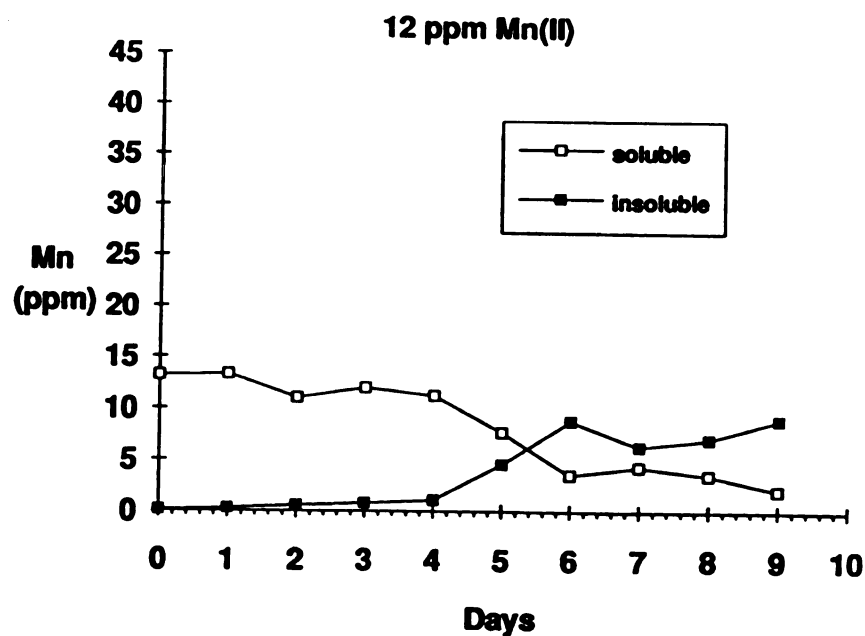
Figure 5.2   Soluble and insoluble manganese concentration as a function of time in nitrogen-limited cultures of *P. chrysosporium* initially containing 12 ppm and 40 ppm Mn(II).

mass transfer resistance is negligible compared to the intraparticle mass transfer resistance (Bailey and Ollis, 1986) and the pellet surface concentration is approximately equal to the bulk liquid concentration. Measurements using an oxygen microelectrode confirmed this finding. There was a negligible decrease in the oxygen concentration as the microelectrode was moved from the bulk liquid phase to the pellet surface. Likewise, for both ammonium and glucose substrates, the Biot number indicated that the substrate concentration at the pellet surface was not significantly different from the bulk liquid substrate concentration.

To confirm Henry's law equilibrium for oxygen (Equation 18), the gas phase and liquid phase oxygen concentrations were measured in active cultures using a polarographic oxygen electrode. The liquid phase oxygen concentration was never significantly different than the corresponding gas phase equilibrium concentration. This implies that the rate of oxygen transfer into the liquid phase by means of diffusion is much faster than the bulk rate of culture respiration and that Equation 18 is valid. Van Suijdam et al. (1982) reported that in mycelial pellet cultures of P. chrysogenum, the gas-liquid mass transfer coefficient (k_{la}) dropped rapidly above pellet volume fractions of 40%. In this study the pellet volume fraction never exceeded 10%.

The dominant mass transfer resistance in shake flask cultures of P. chrysosporium was the intraparticle diffusion of oxygen. This was shown by calculating the observed moduli (Φ) which compares the rate of reaction to the rate of substrate diffusion (Equation 20). For Φ values less than 0.3 the resistance to intraparticle mass transfer is negligible and the process is reaction limited. For Φ values greater then 0.3, the process is diffusion limited. Typical observed oxygen uptake rates with worst case assumptions of large pellets (R=.0015 m) and liquid phase oxygen concentration of 1.5 g/m^3, gives a Φ value of 10.5 (Table 5.1). By comparison, the observable modulus for glucose is 0.16 using typical observed glucose uptake rates with worst case assumptions of large pellets (R> 1.5 mm) and a low bulk glucose concentration (G<500 g/m^3). The observed

modulus for ammonium during primary phase growth using worst case assumptions is 0.13 (Table 5.1).

Table 5.1. Observable moduli for substrates of *P. chrysosporium* using worst case assumptions.

	Oxygen	Glucose	Ammonium
v (g/m^3 pellet/s)	0.18	0.29	0.01
D^a (m^2/s)	2.9×10^{-9}	9×10^{-10}	2.1×10^{-9}
C_l (g/m^3)	1.5	500	3
R (m)	0.0015	0.0015	0.0008
Φ	**10.5**	**0.16**	**0.13**

[a] Pure solute diffusivity in water at 39 C from Perry *et al.* (1984).

Determination of the effective diffusivity of oxygen in mycelial pellets of *P. chrysosporium*

The effective diffusivity (De) of oxygen in mycelial pellets was determined using a stirred cell apparatus as described in section 3.2. A group of pellets which had been killed by suspension in 1% glutaraldehyde was immobilized in 2% agar. The suspension was poured into the bottom of a 50 ml graduated cylinder to 20 ml (l= 0.06m) and after the gel had solidified, nitrogen saturated liquid was added above the gel, the apparatus was sealed, and the system was allowed to equilibrate for 3 days. The liquid was then replaced by an equal volume of liquid (α=1) which was air saturated. A polarographic oxygen electrode was placed into the liquid and the apparatus was sealed. A small magnetic stir bar resting on the gel matrix mixed the liquid phase. The decrease in the oxygen concentration was monitored using a strip chart recorder for six hours. Five different pellet volume fractions were used corresponding to Q values of from 0 to 0.4. Since the effective diffusivity of oxygen in a 2 wt% agar gel has been shown to be 99%

of the value in water (An Lac *et al.*, 1986), the diffusivity of oxygen in the 2% agar slab without pellets was assumed to be 2.9×10^{-9} m^2/s.

The results using this procedure were disappointing when compared to theoretical predictions. During some runs the calculated diffusivity in the slab (D_{slab}) was too large (greater than D). For other runs the diffusivity was less than D by two orders of magnitude. These inconsistent results were attributed to problems eliminating all oxygen bubbles from the diffusion cell apparatus, the effect of pressure on the oxygen electrode output, the diffusion of air into the apparatus and the sloughing away of the agar gel from the cylinder. After many attempts this technique was abandoned.

To try and overcome these problems, the diffusivity of glucose into the slab was measured. This technique eliminated the problems associated with the oxygen electrode, the air bubbles and the diffusion of air into the apparatus. Glucose was assayed using the DNS assay. Initially the slab was free of glucose and contained 20 vol% pellets (Q=0.2). To start the experiment 30 ml of a 5 g/l glucose solution was added above the slab (α=1) and the apparatus was placed in a 39° C room with stirring. After 48 hours, a sample was removed and compared to the initial sample. The value of M_t/M_{inf} calculated based on experimental data was 0.432 and the calculated value for the diffusivity of glucose in the pellet-agar matrix slab was 9.5×10^{-10} m^2/s. This compares well to the literature value for the diffusion of glucose in water of 9×10^{-10} m^2/s (Cresand *et al.*, 1988). Subsequent attempts to measure the effective diffusivity were unsuccessful due to deterioration of the gel matrix over the 48 hour period. Since the diffusivity of glucose into this 20 vol% pellet agar slab was not significantly different than the diffusivity of glucose in water, the effective diffusivity of glucose in mycelial pellets of *P. chrysosporium* (De) was assumed to be equal to the pure liquid diffusivity (D). At this point the effective diffusivity of oxygen in the pellets was assumed to be equal to the pure liquid diffusivity of oxygen. Thus for all culture modelling the value of the effective diffusivity used was 2.9×10^{-9}

m^2/s which is the value given by Perry *et al.* (1984) and Jordan *et al.* (1956) for the diffusivity of oxygen in water at 39° C.

5.3 Determination of kinetic model parameter values

The kinetic parameter values for the kinetic model were determined in nitrogen-limited cultures as described in section 5.1. The physical characteristics of these cultures were as presented in Table 5.2.

Table 5.2. Physical characteristics of agitated, submerged mycelial pellet culture of *P. chrysosporium.*

Characteristic	Value
Temperature	39° C
Liquid Phase Volume (V_l)	$8.5 \times 10^{-5} \ m^3$
Head Space Volume (V_{hs})	$1.65 \times 10^{-4} \ m^3$
Pellet number[a] (η)	$7.3 \pm 1.1 \times 10^6 \ m^{-3}$
Pellet density[b] (ρ)	$6.5 \pm 3.0 \times 10^4 \ g/m^3$
Diffusivity[c] (De)	$2.9 \times 10^{-9} \ m^2/s$
Henry's law constant (H)	37.8
Solubility of oxygen at 39° C	$32.9 \ g/m^3$

[a] Values were experimentally determined and reported as a mean ± one standard deviation.

[b] Value used for computer modelling ± the range of experimentally observed values.

[c] Literature value for the diffusivity of oxygen in water at 39° C (Perry *et al.* 1984)

A summary of the determined growth model parameter values is presented in Table 5.3. The methods used to determine the model parameters are described in the following sections (5.3 and 5.4).

Table 5.3. Kinetic model parameter values.

Parameter	Definition	Value	Equations
Respiration			
V_{max}	Michaelis-Menten coefficient	0.76 ± 0.10 g/m^3 pellet/s	25, 27, 28, 29
K_m	Michaelis-Menten coefficient	0.5 ± 0.3 g/m^3	25, 26, 28, 29
$Y_{g/O2}$	Theoretical yield coefficient	0.92 g/g	9, 13, 16
$Y_{CO2/O2}$	Theoretical yield coefficient	1.38 g/g	31
Primary Growth			
t_{lag}	Length of the lag phase	$2.8 \pm 0.2 \times 10^4$ s	6
μ_{max}	Growth rate constant	$3.9 \pm 0.3 \times 10^{-5}$ s^{-1}	5, 6
$Y_{g/x}$	Growth yield for glucose	0.92 ± 0.1 g/g	8
$Y_{n/x}$	Growth yield for ammonium	0.04 ± 0.1 g/g	4
Secondary Metabolism			
f_{pg}	Polysaccharide from glucose	0.04 ± 0.03 g/g	11a, 12, 13
f_x	Biomass from glucose	0.12 ± 0.01 g/g	11b, 12 13
f_r	Glucose for respiration	0.84 ± 0.03 g/g	11c
Death Phase			
k_{aut}	Autolysis rate constant	$2.5 \pm 0.5 \times 10^{-6}$ s^{-1}	15
k_{pg}	Polysaccharide utilization constant	$0.4 \pm 0.1 \times 10^{-6}$ s^{-1}	14

Kinetic coefficients for the lag phase and primary growth phase.

To determine μ_{max} and the length of the lag-time (t_{lag}), the natural log of the biomass divided by the average initial biomass concentration was plotted for the first 24 hours after inoculation (Figure 5.3). The slope and the x-intercept were determined using a linear regression technique (Appendix 10). As given by Equation 6, the length of the lag time (x-intercept) was 7.9 h and the maximum growth rate constant μ_{max} (slope), was equal to $3.9 \, e^{-5} \, s^{-1}$.

Yield coefficients during primary metabolism were determined as follows. The yield coefficient for nutrient nitrogen (Yn/x, Equation 4) was calculated by dividing the total nutrient nitrogen consumed, by the cell dry weight, at the end of the primary growth phase. The yield coefficient for glucose (Equation 8) was estimated based on the following assumptions. In fungi, inorganic nutrients account for 1% to 10% of the dry biomass (Aiba et al.,1973). In nitrogen limited cultures, nutrient nitrogen accounts for only 1% to 3% of the biomass. Therefore, the yield coefficient for glucose (Yg/x) during balanced growth was set at 0.92 g/g.

Kinetic coefficients for secondary metabolism.

The glucose metabolism factors (Equations 11 a,b,c) are used to determine the fate of glucose as it is used for polysaccharide production, biomass and respiration during secondary metabolism.
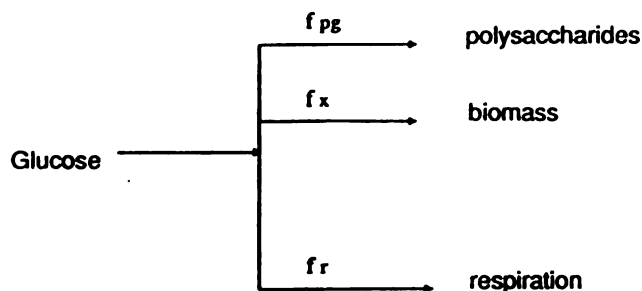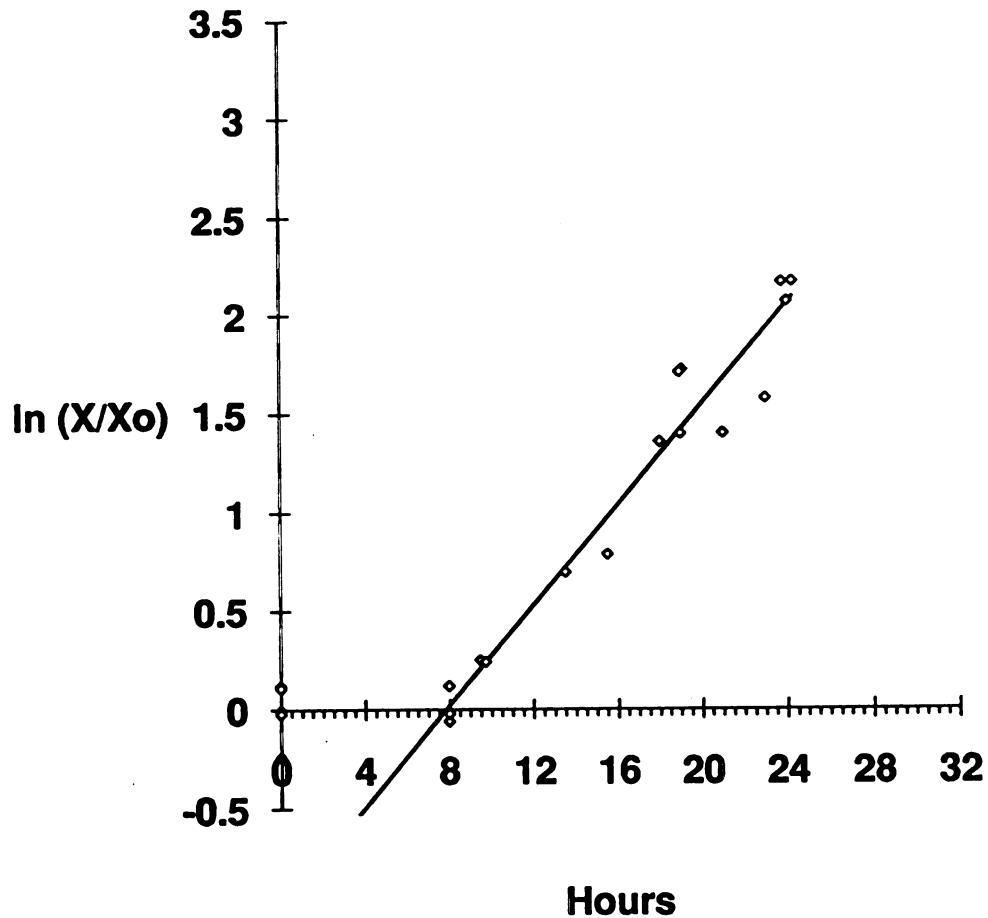
Figure 5.3   Plot of the logarithm of the biomass (X) divided by the average initial biomass (Xo,avg) as a function of culture age in nitrogen-limited mycelial pellet cultures of *P. chrysosporium*. This plot was used for the determination of μmax and tlag. Open diamonds are experimental data from cultures on four different occasions. The line is a linear regression fit of the data points (μ_{max}=3.9 x 10^{-5} s^{-1}, tlag=7.9 h).

Dosoretz *et al.*(1990a) showed that in submerged oxygen flushed cultures initially containing 10,000 g/m^3 glucose, approximately 400 g/m^3 of soluble polysaccharide is formed by the time of glucose depletion. Hence, a figure of 4% was used for the glucose consumed for soluble polysaccharide synthesis (f_{pg}=0.04). A small amount of biomass is produced during secondary metabolism corresponding to approximately 12% of the glucose consumed (f_x=0.12). The balance of the glucose consumed is used for respiration (f_r=0.84). The values of these factors are assumed to be fixed for the purposes of the model, however in reality these factors may change due to oxygen starvation or other metabolic or environmental conditions (see discussion).

The yield coefficients for oxygen and carbon dioxide from glucose used for respiration (Equations 9 and 31), were calculated based on the overall stoichiometry of respiration (Y_{CO_2/O_2}= 1.38, Y_{g/O_2}= .92).

$$C_6H_{12}O_6 + 6O_2 \longrightarrow 6CO_2 + 6H_2O$$
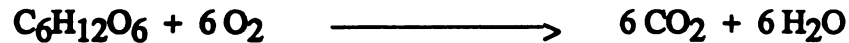
Kinetic coefficients for the death phase.

The rate constant for autolysis (k_{aut}) was estimated by curve fitting biomass data after glucose was depleted from the medium to a first order death rate Equation (Equation 15). The rate constant for polysaccharide utilization (k_{pg}) was calculated by measuring the rate of CO_2 evolution after glucose was depleted from the medium using the yield coefficients for respiration (Equations 14 and 16) and assuming that all CO_2 evolved is due to polysaccharide respiration. The final culture dry weight (X_f) was determined by measuring the biomass concentration 20 days after no respiration was detectable (Equation 15).

Mycelial pellet characteristics

The pellet density (ρ) was calculated from Equation 1 using experimental values for the characteristic pellet radius, pellet number and culture dry weight. Using the constant constant pellet density assumption, the model predicted characterisitic pellet radius (R) was calculated. The time course of the experimentally determined pellet radii

and the model predicted pellet radii using parameter values from Table 5.3 showed good agreement (Figure 5.4). During the death phase, pellet density decreased due to autolysis.

5.4 Determination of kinetic coefficients for the oxygen utilization model.

Three different approaches were used to determine the intrinsic Michaelis-Menten kinetic parameters for respiration; Vmax and Km (Equation 25). The values of both Vmax and Km were determined by fitting data for the oxygen concentration profile in mycelial pellets as determined using a microelectrode with the model Equation for the oxygen concentration profile (Equation 23). The value of Vmax was also determined by measuring the rate of oxygen depletion from the bulk liquid and calculating Vmax using Wilkinson's method. The values of Vmax and Km determined by oxygen profile modelling were checked by comparing the evolution of CO_2 predicted by the integrated kinetic model with experimental data for CO_2 evolution.

The oxygen concentration profiles within individual mycelial pellets were measured using an oxygen microelectrode as described in Methods. The data (see Appendix 12) were plotted using EXCEL software and compared to oxygen profile data generated using a computer simulation (see Equation 23 and Appendix 22). Values of Vmax and Km in the computer simulation were changed until the computer simulation profile most closely resembled the experimental data. Using this approach, the range of values of V_{max} were 0.76 ± 0.10 g/m^3/s and the range of values of Km were 0.5 ± 0.3 g/m^3. A typical oxygen concentration profile and the computer simulation curve which most resembled the experimental data is presented in Figure 5.5. In pellets with a diameter greater than 1 mm, the oxygen concentration decreased to undetectable levels well before the pellet center. However, the data were taken in an air atmosphere. In shake-flask cultures, the oxygen partial pressure was generally greater than 0.5 atm and the rate of autolysis due to oxygen starvation was probably negligible, since both culture dry weight and the rate of respiration increased during secondary metabolism.
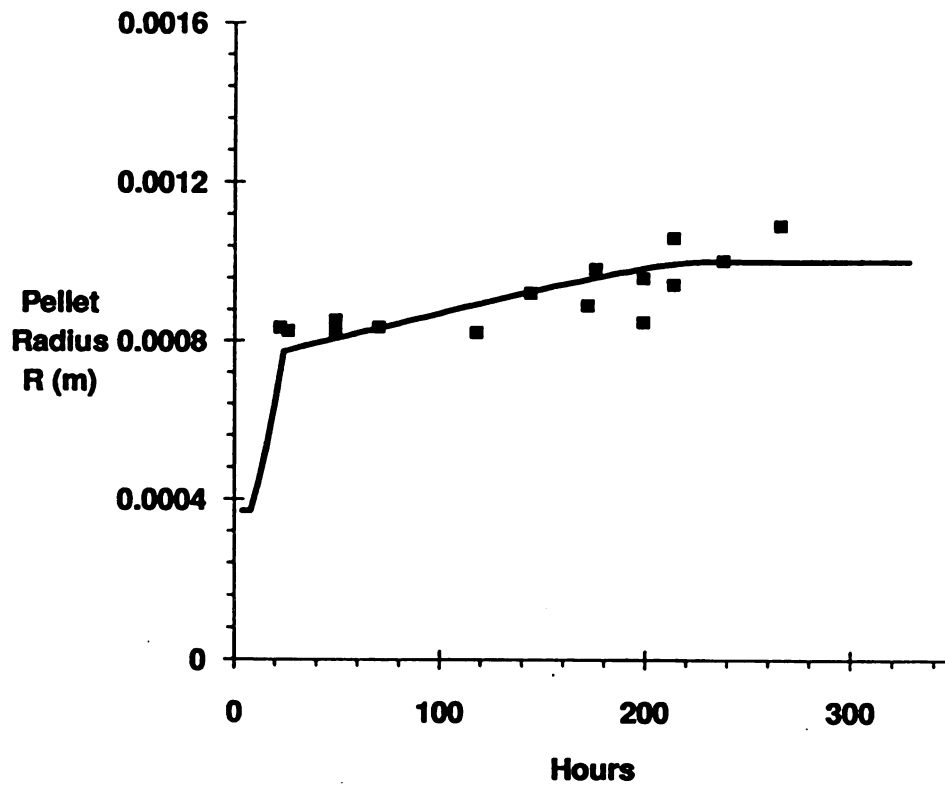
Figure 5.4   Mycelial pellet radius in submerged cultures of *P. chrysosporium* grown nitrogen-limited medium (Condition 2). solid line: kinetic model prediction. squares: experimental data points.

The evolution of carbon dioxide was measured by determining the concentration of CO_2 in the culture headspace every 24 hours before oxygenation. The data (see Appendix 13) were compared to CO_2 evolution as predicted by the integrated kinetic model. The model curve using the parameter values presented in Table 5.3 (V_{max} value of 0.76 $g/m^3/s$, Km of 0.5 g/m^3 and pellet density value of 65000 g/m^3 pellet), closely followed the CO_2 production data (Figure 5.6) except on the first day. This may be due to a faster rate of metabolism during the growth phase.

Respiration rate measurements were also made by pouring one entire culture into a full stirred vessel (respirometer) and measuring the decrease in the liquid phase oxygen concentration (C_l) with time using a polarographic oxygen electrode (Ingold, model #531) (see Appendix 14). To determine the rate of oxygen uptake (v), the slope of the depletion curve was measured at various oxygen concentrations (Figure 5.7). The apparent Vmax and apparent Km values were fit using the method of Wilkinson (1961). During primary growth, the apparent value of Vmax was 0.04 g/m^3 media/s. During secondary metabolism the apparent Vmax values ranged from 0.014 to 0.031 g/m^3 media/s while the apparent Km ranged from 1.5 to 8 g/m^3. The apparent Vmax dropped to 0.007±.002 g/m^3 media/s one day after the culture glucose level dropped below 1,000 g/m^3 and to 0.0001±.0001 g/m^3 media/s ten days later. By using appropriate pellet density and culture dry weight values, the oxygen depletion Vmax were averaged to give the specific apparent Vmax (0.77±0.23 $g/m^3/s$) (see Appendix 14). Note that mass transfer effects are not considered in the apparent Vmax and apparent Km values; however, if the effectiveness factor is near unity (the case at high C_l) the apparent Vmax and the intrinsic Vmax values should be comparable.

Some evidence indicated that oxygen transfer may occur by mechanisms other than diffusion in the respirometer apparatus. The rate of depletion of oxygen measured daily in cultures of *P. chrysosporium* was plotted against the liquid phase oxygen concentration (C_l) (Figure 5.8a). The overall oxygen depletion rate (R_{O2}) increased daily

with culture age until culture glucose was exhausted (Day 10). This agrees with CO_2 evolution data which also increased daily during secondary metabolism (see Figure 5.6). However, the depletion rate remained near the apparent Vmax value calculated using Wilkinson's method until the oxygen concentration was below 5 g/m^3. A model simulation (Fig 5.8b), indicates that respiration should have decreased from the apparent Vmax at around 20-30 g/m^3 oxygen due to intraparticle mass transfer limitations as represented by the effectiveness factor. One possible explanation of this finding is that the stirring rate in the respirometer is so rapid that pellets are disrupted to a filamentous form causing the effectiveness factor to become unity. In this case, the oxygen uptake rate would appear as it does in Figure 5.8c. This behavior more closely resembles the experimental results. Filaments of mycelia were observed after a period of stirring on most occasions. Another possibility is that the stirring rate in the respirometer induced convective diffusion into the pellets by causing the pellets to contract and expand.
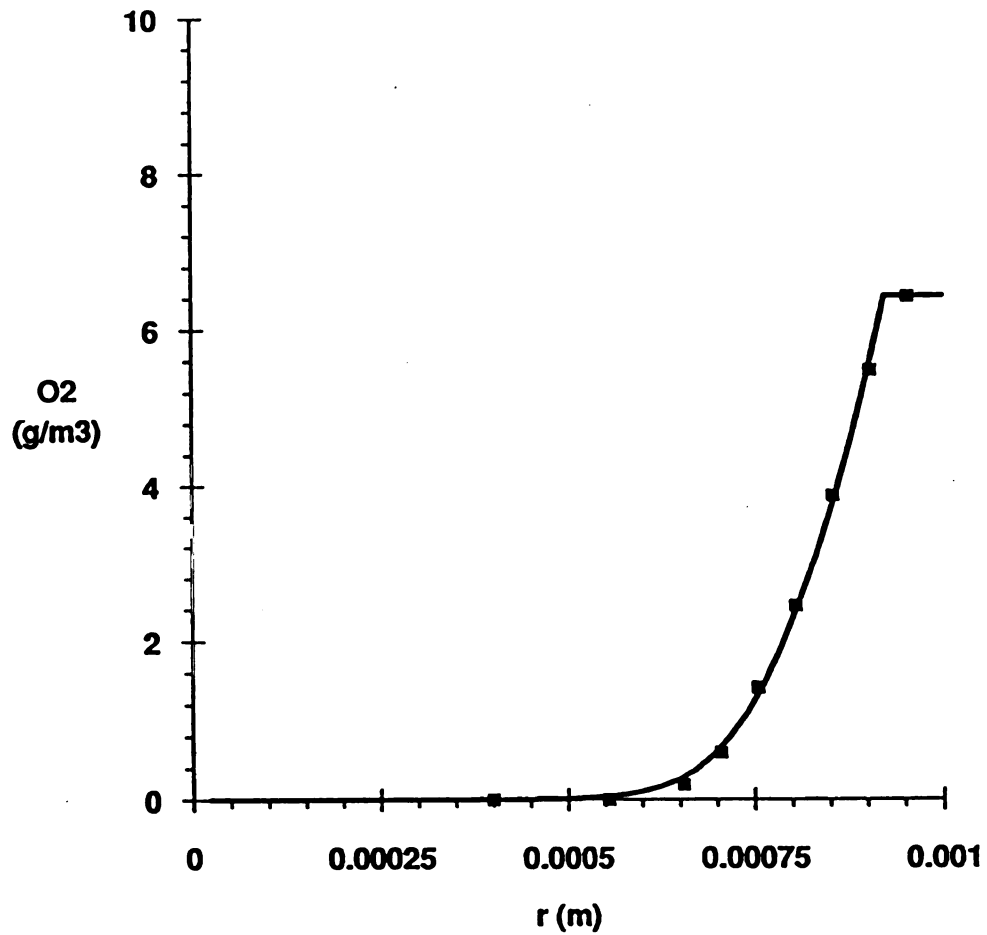
Figure 5.5   Oxygen concentration profile in a mycelial pellet of *P. chrysosporium* (diam.=.00185 m) as determined using an oxygen micro-electrode.

The solid line is as predicted by the kinetic model ($Km=0.5$ g/m^3, $V_{max}=0.76$ $g/m^3/s$, $De=2.9$ x 10^{-9} m^2/s).
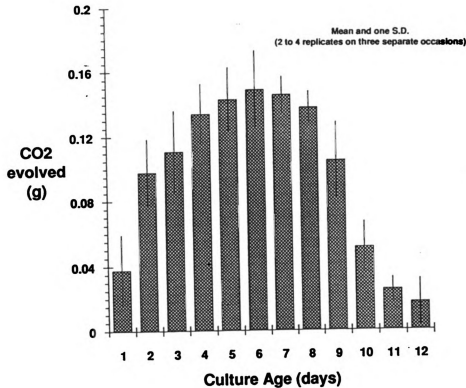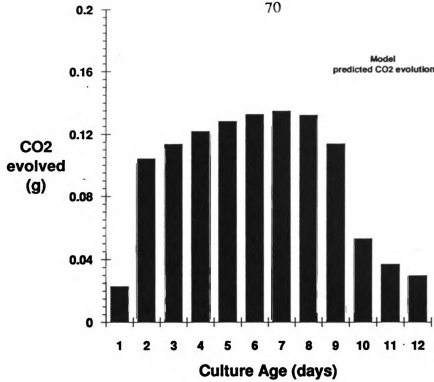
Figure 5.6   Carbon dioxide evolution in nitrogen-limited mycelial pellet cultures of *P. chrysosporium* (Condition 2). The solid bars are as predicted by the kinetic model (K_m=0.5 g/m^3, V_{max}=0.76 g/m^3/s, D_e=2.9 x 10^{-9} m^2/s.). Cross-hatched bars are experimental data.
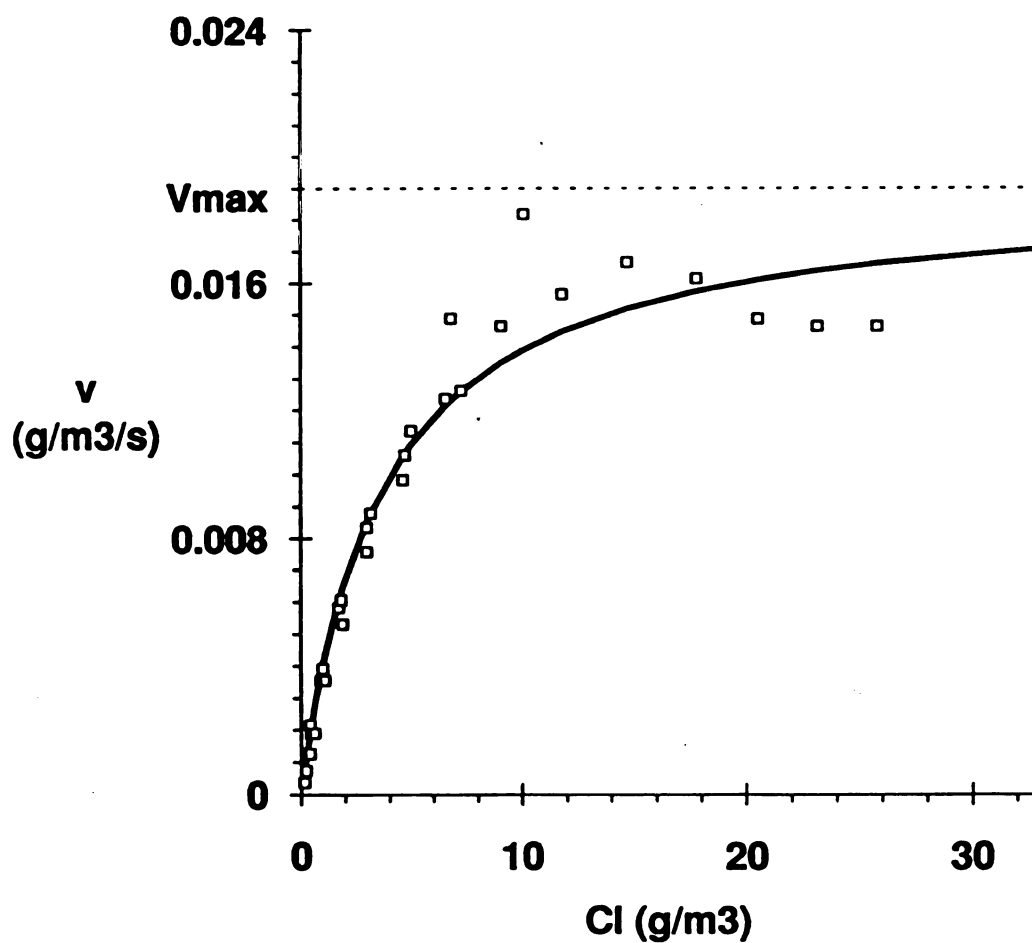
Figure 5.7   Typical plot of the rate of oxygen depletion (v g/m^3/s) from the culture fluid versus the liquid phase oxygen concentration (C$_l$ g/m^3) from nitrogen-limited, mycelial pellet cultures of *P. chrysosporium* as measured using a respirometer. Solid line is a curve fit using the method of Wilkinson (1961). Open squares are experimental data from three consecutive measurements.
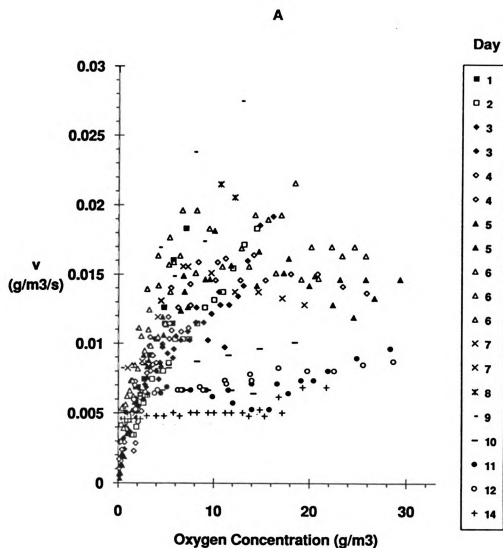
Figure 5.8   The rate of oxygen uptake by cultures of *P. chrysosporium* as a function of culture age as measured using a respirometer:
A. Experimental data.
B. Model prediction using kinetic parameter values from Table 5.3.
C. Model prediction assuming an effectiveness factor of one (Emm = 1) at all times.

B

C
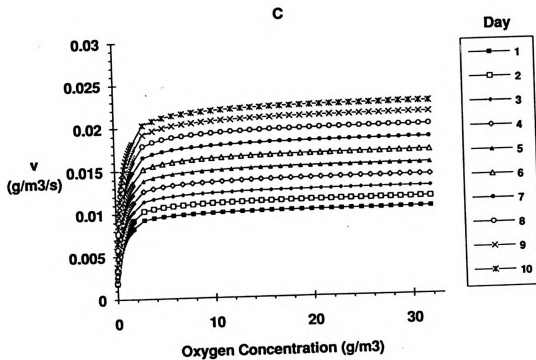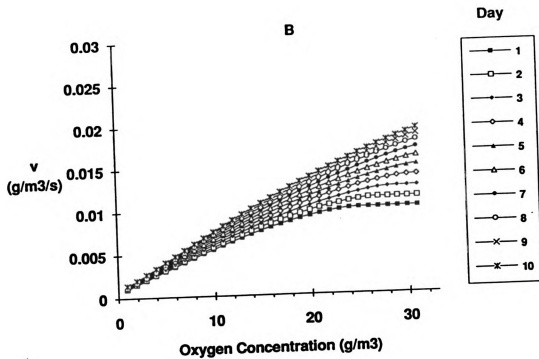
5.5 Model test cases

The complete kinetic model Equations describing growth, substrate utilization and respiration in shake flask cultures of *P. chrysosporium* were integrated and solved using a computer program (Appendix 21). Euler's method was used to approximate the differential Equations with a time increment of one hour. The kinetic parameters determined in the previous two sections were used (see Table 5.3). Batch cultures were grown with five different initial conditions to test the model fit (Table 5.4).

Table 5.4 Initial conditions for model test cases.

Condition	Description	Ammonium (g/m3)	Glucose (g/m^3)
1	Low glucose	39	5,000
2	Nitrogen-limited	39	10,000
3	High glucose	39	15,000
4	Very low nitrogen	2	11,000
5	3X basal nitrogen	117	11,000

In one set of experiments, three different initial glucose concentrations were used (conditions 1,2 and 3). The model closely predicted the glucose and biomass data for the three conditions (Figure 5.9). Nutrient nitrogen was completely depleted under each condition within 24 hours. The initial level of glucose had little effect on the specific rate of glucose or nitrogen uptake, the culture dry weight or the pellet size. The initial glucose concentration primarily affected the length of secondary metabolism. In low glucose cultures (condition 1), the onset of the death phase occured just 120 hours after inoculation. In high glucose cultures (condition 3) the length of secondary metabolism was extended by approximately 80 hours compared to basal glucose cultures and the onset of the death phase did not occur until 300 hours after culture inoculation.
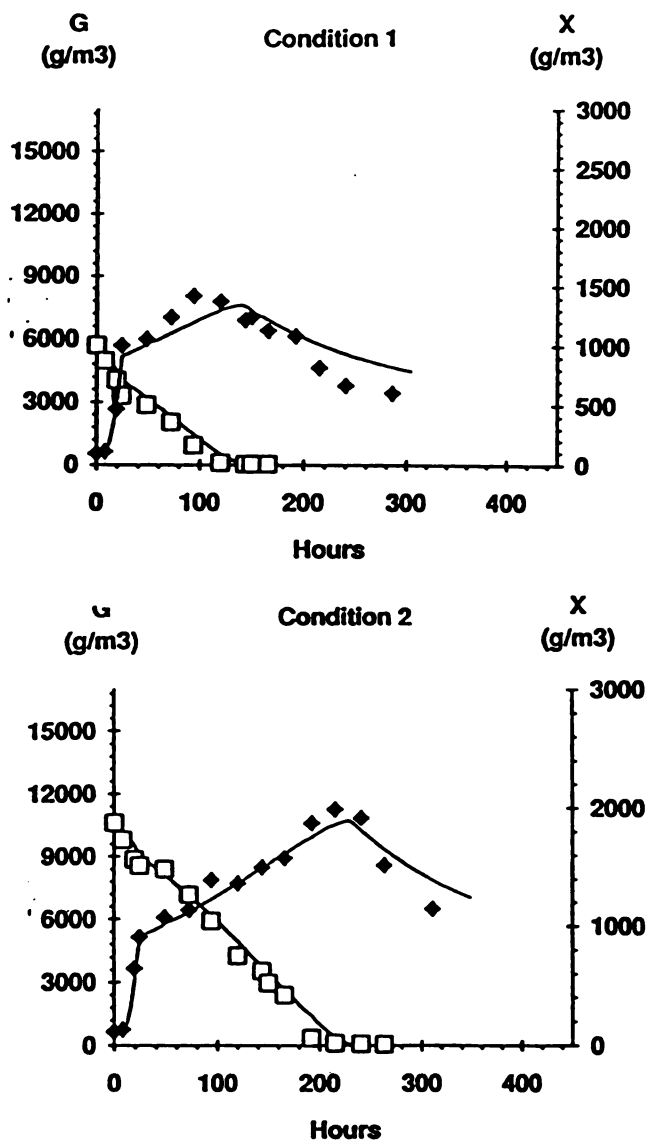
Figure 5.9   Culture dry weight (X), glucose concentration (G), and nutrient nitrogen (ammonium) concentration (N) as a function of time in cultures of *P. chrysosporium* grown under various initial glucose and nutrient nitrogen conditions. Solid lines are as predicted by the kinetic model. Open squares are experimental data for glucose, closed diamonds are experimental data for culture dry weight and open triangles are experimental data for ammonium.

A. Condition 1; G_0= 5,000 g/m^3, N_0= 39 g/m^3.

B. Condition 2; G_0= 10,000 g/m^3, N_0= 39 g/m^3.

C. Condition 3; G_0= 15,000 g/m^3, N_0= 39 g/m^3.

D. Condition 4; G_0= 11,000 g/m^3, N_0= 2 g/m^3.

E. Condition 5; G_0= 11,000 g/m^3, N_0=117 g/m^3.

Condition 4

Condition 3
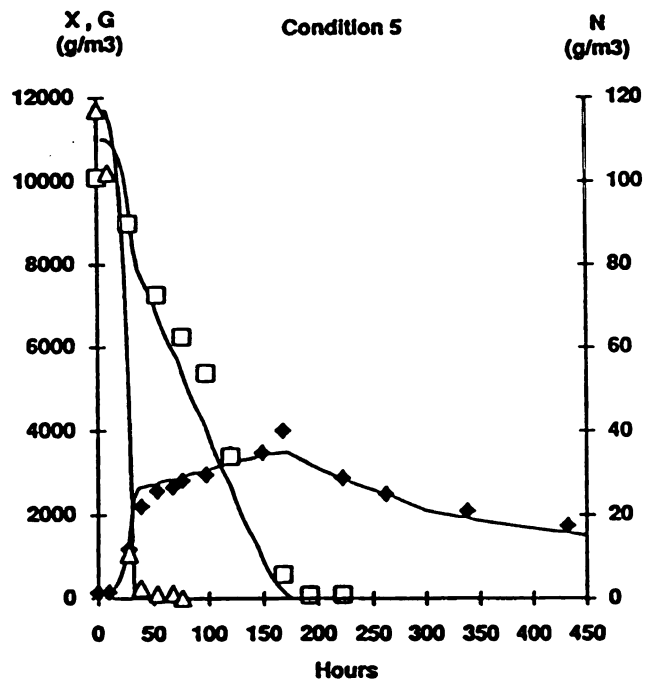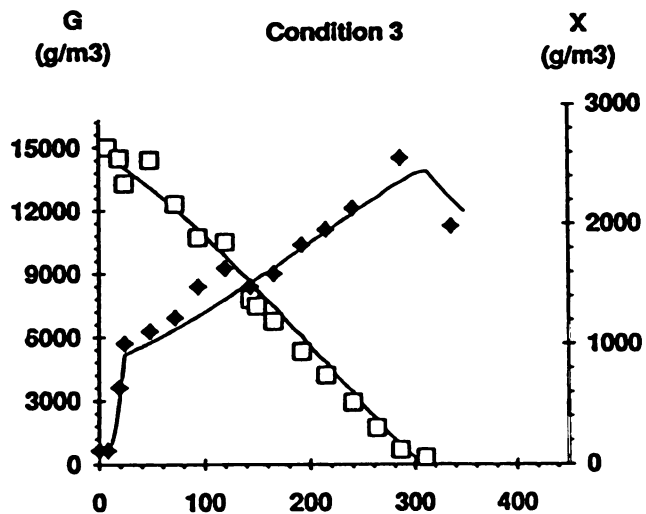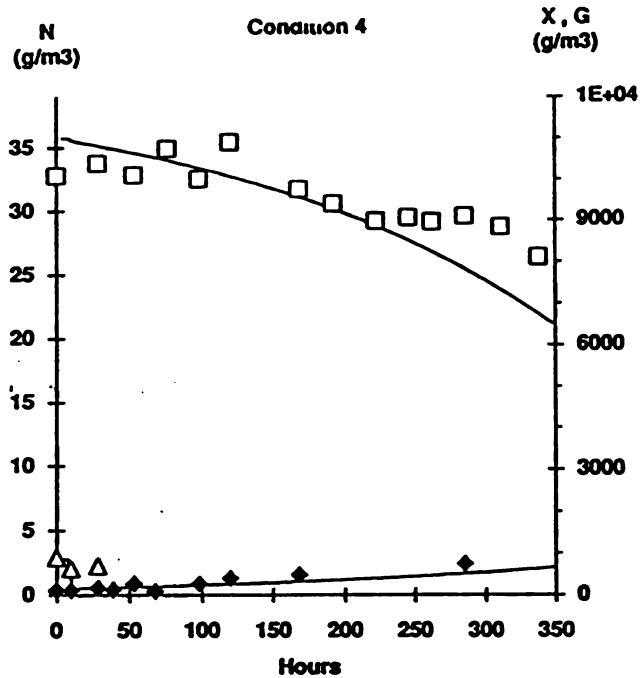
Condition 5

For conditions 1,2 and 3, the MNP activity reached a maximum of 2,500 U/l on day 3. The LIP activity in condition 1 cultures reached a maximum of 140 U/l on day 5. In conditions 2 and 3, LIP activity reached a maximum of 260 U/l and 310 U/l between days 5 and 6 respectively. A rapid decrease in biomass concentration and the disappearance of MNP and LIP activity coincided with the time of glucose depletion. This occurred at hour 140, 220 and 300 for the low glucose (condition 1), basal glucose (condition 2) and high glucose (condition 3) cultures respectively. Under identical initial conditions, Jones (1990) has shown that this kinetic model accurately predicts culture dry weight and glucose consumption by cultures of *P. chrysosporium* in a rotating biological contactor, when corrections are made for slab geometry.

A second set of initial conditions was tested in a subsequent experiment (conditions 4 and 5) to determine the model's ability to predict changes in the nutrient nitrogen concentration. When cultures were grown with very low levels of nutrient nitrogen, (2 g/m^3, condition 4), little total biomass was produced and glucose was consumed slowly (Figure 5.9d). In cultures grown in 3 times the basal level of nutrient nitrogen (117 g/m^3 ammonium, condition 5), nutrient nitrogen was depleted within 30 hours, glucose was depleted within 190 hours and the biomass concentration reached 3,000 g/m^3 (Figure 5.9e). Thus the level of nutrient nitrogen primarily affected the biomass level at the end of the primary growth phase. The biomass level, in turn, affected the rate of glucose metabolism and respiration. The integrated kinetic model accurately predicted the experimental data under these conditions.

Cultures grown in 39 g/m^3 ammonium (condition 2) produced the highest LIP activity (220 U/l) even though less biomass was produced than in the higher nitrogen cultures (condition 5). In condition 4 and 5 the LIP activity decreased to undetectable levels one day after the glucose concentration dropped below 400 g/m^3.

5.6 Bioreactor studies

Cultures were grown in a 6.8 l stirred tank reactor (BioFlo II, New Brunswick Scientific Co. Inc.) with a 2.3 l operating volume. This system had the same liquid to headspace volume ratio as the shake flask cultures described above. Oxygen was provided by daily flushing of the headspace of the reactor with oxygen, and the daily evolution of CO_2 was measured. Compared to control cultures grown in shake flasks, the bioreactor culture produced the same amount of biomass and had a similar pH profile but consumed glucose and evolved CO_2 much slower (Figure 5.10). The bioreactor culture produced significantly less MNP and no LIP. The large scale production of LIPs and MNPs is still hampered by the inability to produce the peroxidases in a scalable reactor configuration. This is primarily due to the organisms sensitivity to agitation (Michel *et al.*, 1990). The production of MNPs appeared to be less sensitive than the production of LIPs to culture and agitation conditions.
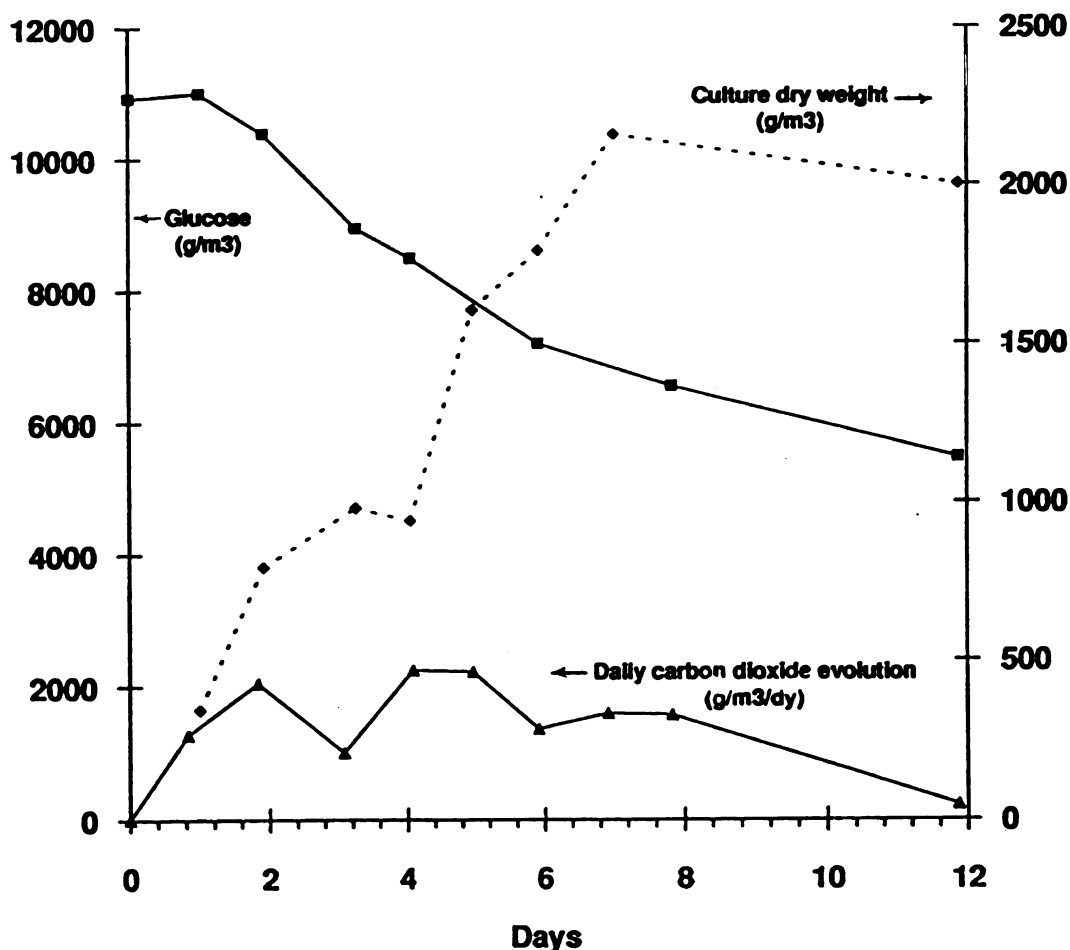
5.10 Characteristics of a stirred tank bioreactor culture of P. chrysosporium

Part II: Discussion

5.7 The life-cycle of cultures of *Phanerochaete chrysosporium*

Nitrogen-limited, peroxidase producing cultures of *P. chrysosporium* (Figure 5.1) displayed the classic characteristics of the microbial life-cycle. For approximately 8 hours immediately after inoculation, no significant growth occurred (Figure 5.1a). After 8 hours, the biomass increased exponentially (Figures 5.1a and 5.3) until the nutrient nitrogen was depleted. During secondary metabolism (or idiophase), the biomass, the rate of CO_2 evolution and oxygen depletion, and the mycelial pellet radius (Figure 5.4) increased slowly until the glucose was depleted from the medium. Both the lignin peroxidases (LIP) and manganese peroxidases (MNP) were produced during this period. Depletion of the carbon source from the medium on day 10 coincided with a decrease in the biomass, a substantial decrease in the rate of culture respiration and the disappearance of peroxidase enzyme activity. Clearly, the cultures proceeded through four distinct phases (Figure 5.1); a lag phase where little growth or metabolism occurred, a primary growth phase where growth was exponential and nutrient nitrogen and glucose were depleted, a secondary metabolic phase where glucose was depleted and culture respiration reached its highest rate, and a death phase where the biomass and metabolic activity diminished rapidly.

5.8 Kinetic model for mycelial pellet cultures

An integrated model based on the life-cycle phases accurately predicted a wide spectrum of culture characteristics using a minimal number of model parameters. In total, ten independent model parameters were used to describe the life-cycle of mycelial pellet cultures of *P. chrysosporium* (Table 5.3). These included growth rate constants, substrate utilization factors and respiration kinetic parameters. The reported parameter values are those which best fit the control culture data. Error estimates for the determined parameter values represent the range of observed values and are not standard deviations.

The "delayed" exponential growth law (Figure 5.3) predicted the level of biomass at the beginning of secondary metabolism within 10% of the experimentally determined value, however experimental data were not accurate enough to distinguish between different growth models such as the Monod model, the cube-root model or other models. This is due to error in the biomass determination of about $\pm$ 10% (see van-Suijdam *et al.*, 1982 for more discussion of this). However, unlike other commonly used growth models, the integrated kinetic model accounted for the depletion of limiting substrates which triggered the transition between life-cycle phases.

The model accurately predicted the pellet radius as a function of time when the pellet number (η) and pellet density (ρ) was known (Figure 5.4). A function relating pellet density and pellet size has been used by other investigators to account for the decrease in the pellet density which occurs as a result of autolysis within the mycelial pellets (Yano *et al.*, 1961, van-Suijdam *et al.*, 1982). A relationship of this type was not used here because previous studies have shown that for pellets of *P. chrysosporium* pellet density is constant up to pellet radii of 0.0025 mm. However, the error in the pellet number and size determinations were fairly large (S.D. $= \pm$ 15%) but the pellet size did not change substantially as it did in other studies (for instance in Yano *et al.*, (1961) pellets from less than 1 mm to greater than 10 mm were studied). This was due to the short period of growth in the nitrogen limited cultures. In addition, a wide range of pellet densities were observed for different experimental runs. Densities as low as 30,000 g/m^3 to as high as 90,000 g/m^3 were observed. The reason for this variation is not known. The effect of pellet density variation on the biomass, effectiveness factor, glucose uptake rate and pellet radius as predicted by the kinetic model is presented in Figure 5.11 . As pellet density decreases, the characteristic pellet size increases. Increases in pellet size results in lower oxygen effectiveness factors for respiration (Figure 5.11).
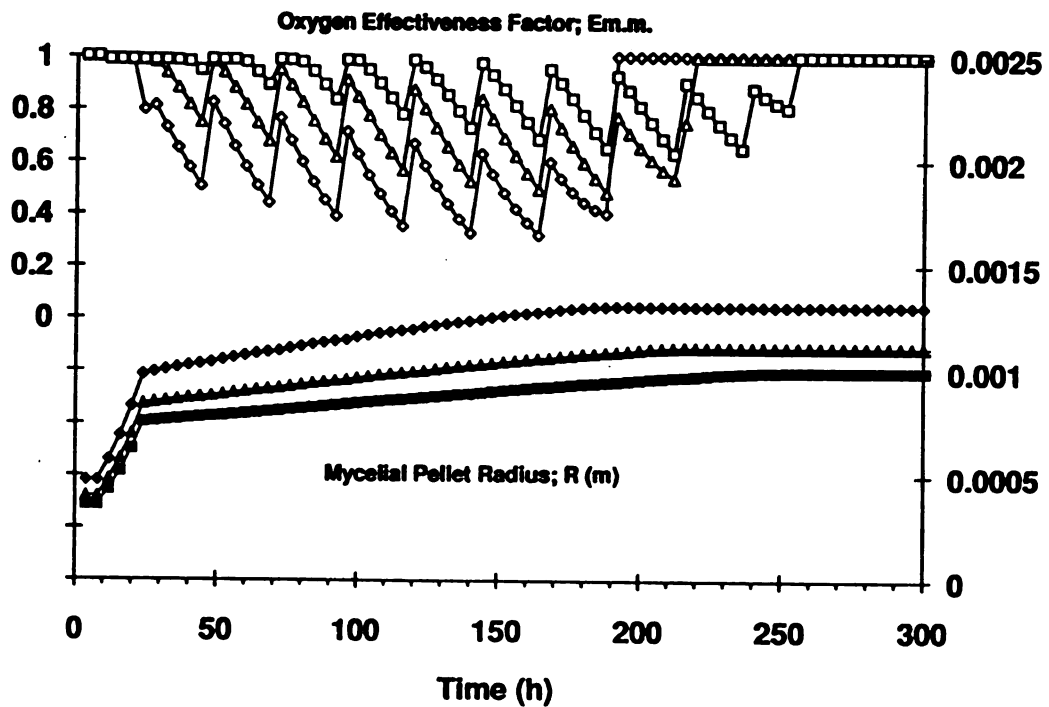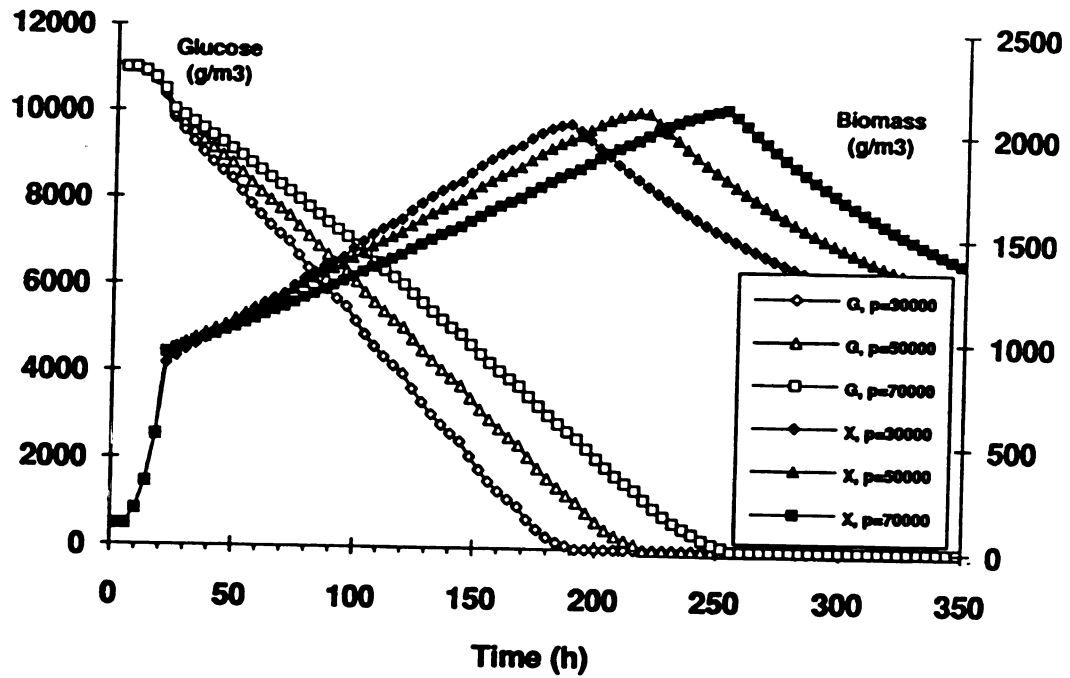
Figure 5.11 The effect of the mycelial pellet density (ρ) on the biomass, glucose uptake rate, oxygen effectiveness factor and mycelial pellet radius as predicted by the kinetic model.

5.9 Oxygen utilization in mycelial pellet cultures of *P. chrysosporium*.

The intrinsic kinetics parameters for respiration, V_{max} and Km, determined by three separate methods were in agreement. The values of the Michaelis-Menten kinetic parameters for respiration determined by modelling the oxygen concentration profile within pellets of *P. chrysosporium* (Figure 5.5) closely agreed with CO_2 evolution data (Figure 5.6) when the same parameters were used. To a lesser extent, oxygen depletion data (Figure 5.7 and 5.8) also agreed with kinetic parameter values determined by profile modelling. A wide range of kinetic parameter values (S.D.=30% of mean) were obtained using Wilkinson's method and data from the respirometer ($Vmax = 0.77 \pm 0.23$ g/m^3/s) (see Appendix 14). This may be due to disruption of the pellets within the respirometer apparatus (Figure 5.8). This agreement, and the fact that closure of the oxygen mass balance was obtained, gives added credibility to the kinetic parameter values determined for culture respiration.

In previous studies the oxygen utilization by fungal pellets has been studied only during the primary growth phase (Table 2.2). The rate constants for respiration in these previous studies are of the same order of magnitude as those determined here for *P. chrysosporium*. In the zero order model for pellets of *P. chrysogenum* developed by Phillips (1966) a rate constant of 0.56 g/m^3/s was reported. Van Suijdam *et al.* (1982) reported a maximum oxygen uptake rate of approximately 0.8 g/m^3/s for pellets of *P. chrysogenum*. These values compare to a V_{max} value for pellets of *P. chrysosporium* of 0.76 g/m^3/s. Both Yano *et al.* (1961) and Kobayashi *et al.*(1973), reported that the maximum specific oxygen uptake rate (QO_2max) for filamentous *A. niger* is 6.1×10^{-5} g/g/s. By comparison, for pellets of *P. chrysosporium* QO_2max was 1.2×10^{-5} g/g/s. It should be noted that the respiration kinetics determined in this work were for secondary metabolism and not for primary growth as in the previous studies.

The low Km value for respiration of 0.5 ± 0.3 g/m^3 found for pellets of *P. chrysosporium* is also in line with other studies. The value of Km reported for pellets of

A. niger by Kobayashi *et al.*(1973) was 0.1 g/m^3 and yeast cells typically have a Km of approximately 0.05 g/m^3 (Bailey and Ollis, 1986). Because of the very low value of Km for oxygen, a zero-order model (Km=0) for respiration has been used by some investigators (Phillips, 1966; van Suijdam *et al.*, 1982; Yano *et al.*, 1961; Wittler *et al.*, 1986) to model respiration in mycelial pellets. If a zero-order model is assumed for pellets of *P. chrysosporium*, then a critical pellet radius can be calculated where the center of the pellet first becomes oxygen starved. For mycelial pellets of *P. chrysosporium*, this radius is 0.86 mm in oxygen saturated medium and 0.40 mm in air saturated medium.

Wittler *et al.* (1986) showed that in a flow reactor, oxygen transfer in pellets of *P. chrysogenum* may occur by means of convection and eddy diffusion as well as by molecular diffusion. These methods of oxygen transfer were not considered in the model presented here, where in mildly agitated shake flask cultures were studied. However, in larger scale fermentations, with sparging and more turbulent mixing conditions, reactor hydrodynamics may significantly influence the oxygen mass transfer within the mycelial pellets. Respirometer results indicated that convection may play a role in oxygen mass transfer is rapidly agitated cultures of *P. chrysosporium* (see Figure 5.8)

For Michaelis-Menten kinetics, a three dimensional surface (Figure 5.12) provides a tool for quickly estimating the oxygen effectiveness factor in mycelial pellets of *P. chrysosporium* as a function of the characterisitic pellet radius (R) and the liquid phase oxygen concentration (C_l). The most favorable conditions for aerobic metabolism are represented by the plateau of the surface where the oxygen effectiveness factor (E) is near one. This region corresponds to small pellet radii and high dissolved oxygen concentrations.
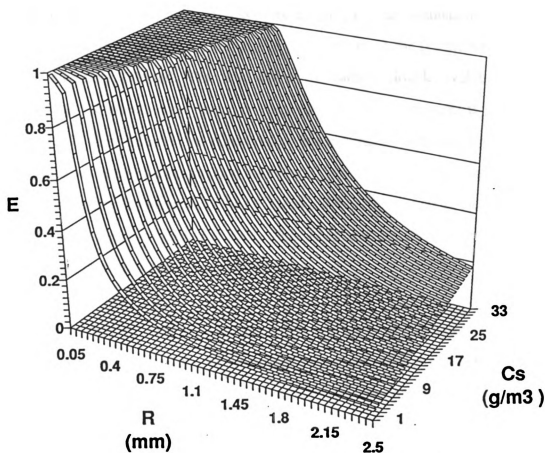
Figure 5.12   Three dimensional representation of the oxygen effectiveness factor (Emm) for mycelial pellets of *P. chrysosporium* as a function of the liquid phase oxygen concentration (C_l) and the characteristic pellet radius (R).

5.10 Kinetic model simulations

Models for LIP and MNP production are difficult to develop without detailed knowledge of the metabolic pathways involved and their genetic regulation. To study the effect of oxygen limitations on peroxidase production, computer simulations based on the kinetic model were conducted for various conditions in which the production of LIP and MNP is adversely affected. The time course of carbon dioxide evolution, oxygen depletion and the effectiveness factor in basal nitrogen-limited cultures is presented in Figure 5.13. In these cultures, the effectiveness factor remains near unity during primary growth (thus validating the assumption made for Equation 6) and drops to approximately 0.6 during secondary metabolism on day 9. Nearly 50% of the oxygen in the headspace is depleted between each oxygenation cycle. This simulation clearly reveals the unsteady state nature of fermentations in sealed shake-flasks.

Air-flushed cultures

In air-flushed cultures no LIP and 66% less MNP is produced. Furthermore, Dosoretz *et al.* (1990a) found that in air-flushed submerged cultures of *P. chrysosporium*, the rates of glucose depletion and carbon dioxide production decreased by 33% and 70% respectively compared to oxygen flushed cultures, while the biomass concentration reached 2,900 g/m^3 by day 8 and soluble polysaccharides doubled. A model simulation for air-flushed cultures using the kinetic parameters from Table 5.3 closely predicted the data for carbon dioxide production reported by Dosoretz *et al.* (1990a) but under-predicted the glucose utilization rate and the biomass concentration. The oxygen effectiveness factor for air-flushed cultures ranged from 0.1 to 0.6. Thus in air flushed cultures, more cells are oxygen limited and unable to respire glucose so the yield coefficients for glucose metabolism may be different. By adjusting the glucose metabolism factors accordingly (f_{pg}=0.25, f_x=0.3) the model closely predicted the results for CO_2 evolution, glucose consumption and biomass production as reported for
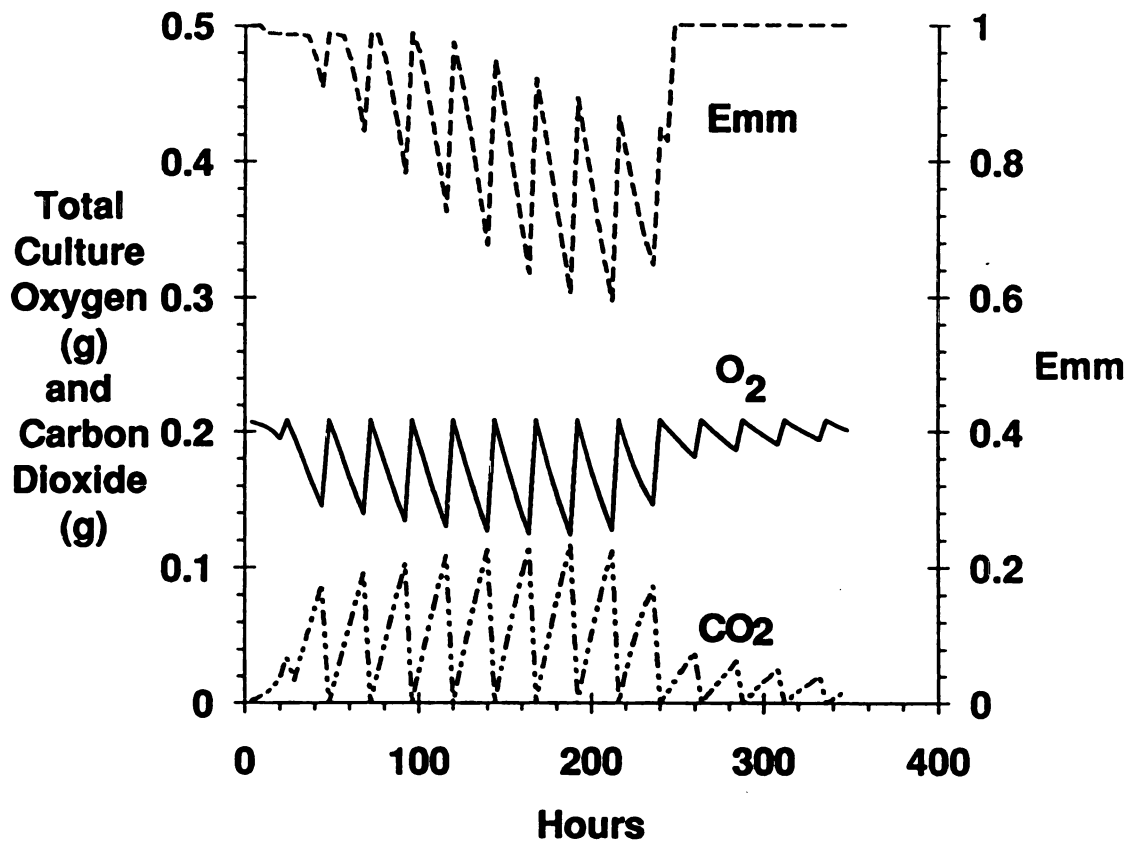
Figure 5.13   Total oxygen and carbon dioxide and oxygen effectiveness factor in nitrogen-limited cultures of *P. chrysosporium* as predicted by the kinetic model.
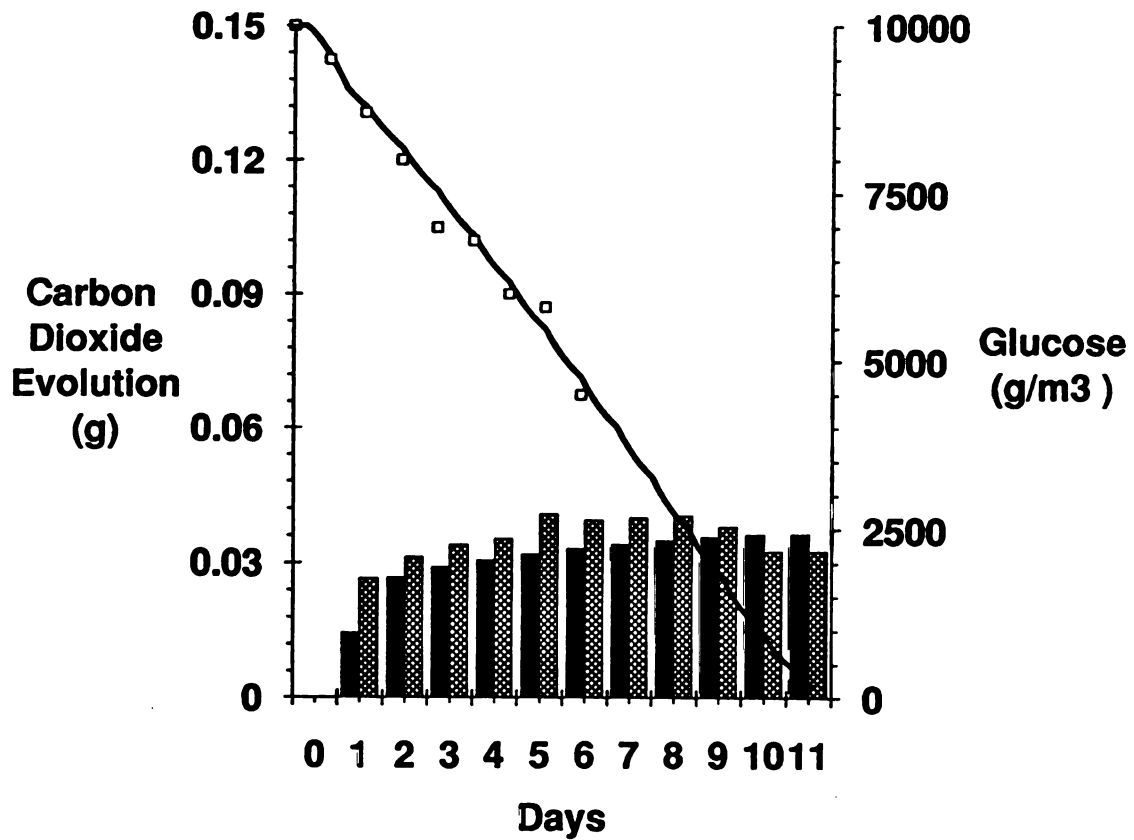
Figure 5.14   Glucose consumption and carbon dioxide production in air-flushed shake flask cultures of *P. chrysosporium* as predicted by the kinetic model (line and solid bars) and as reported by Dosoretz *et al.* (1990) (open squares and cross-hatched bars).

air-flushed cultures by Dosoretz *et al.* (1990a) (Figure 5.14). This finding suggests a relationship between the level of polysaccharides produced and the dissolved oxygen concentration within the mycelial pellets.

High nutrient nitrogen cultures.

A simulation for batch cultures grown in high nitrogen (390 g/m^3 ammonium) illustrates the effect of nutrient nitrogen sufficiency on pellet cultures of *P. chrysosporium*. According to the model simulation, culture glucose is exhausted much faster in these cultures and autolysis begins between days 2 and 3 (Figure 5.15). Thus, under this condition the cells are no longer in a secondary metabolic state when LIPs and MNPs are normally produced in control cultures. The fed-batch administration of glucose to such cultures to prolong secondary metabolism may not ameliorate this situation since the pellets have already grown to a large size (>2 mm diameter) and have an oxygen effectiveness factor of approximately 0.2 so that much of the center of the pellet is oxygen starved.

Large mycelial pellet cultures

A model simulation for cultures in which large mycelial pellets form (pellet diameter = 6 mm) is presented in Figure 5.16. This case is analogous to cultures grown under low rates of agitation (see Michel *et al.*, 1990). According to the model simulation, under this condition, nutrient nitrogen is depleted within 50 hours after inoculation. Also, during secondary metabolism, the rate of glucose depletion is markedly slower than the rate typically found in cultures with small pellets. The oxygen effectiveness factor drops precipitously to a value of 0.1 during the primary growth phase as the pellet size increases (Figure 6.6).
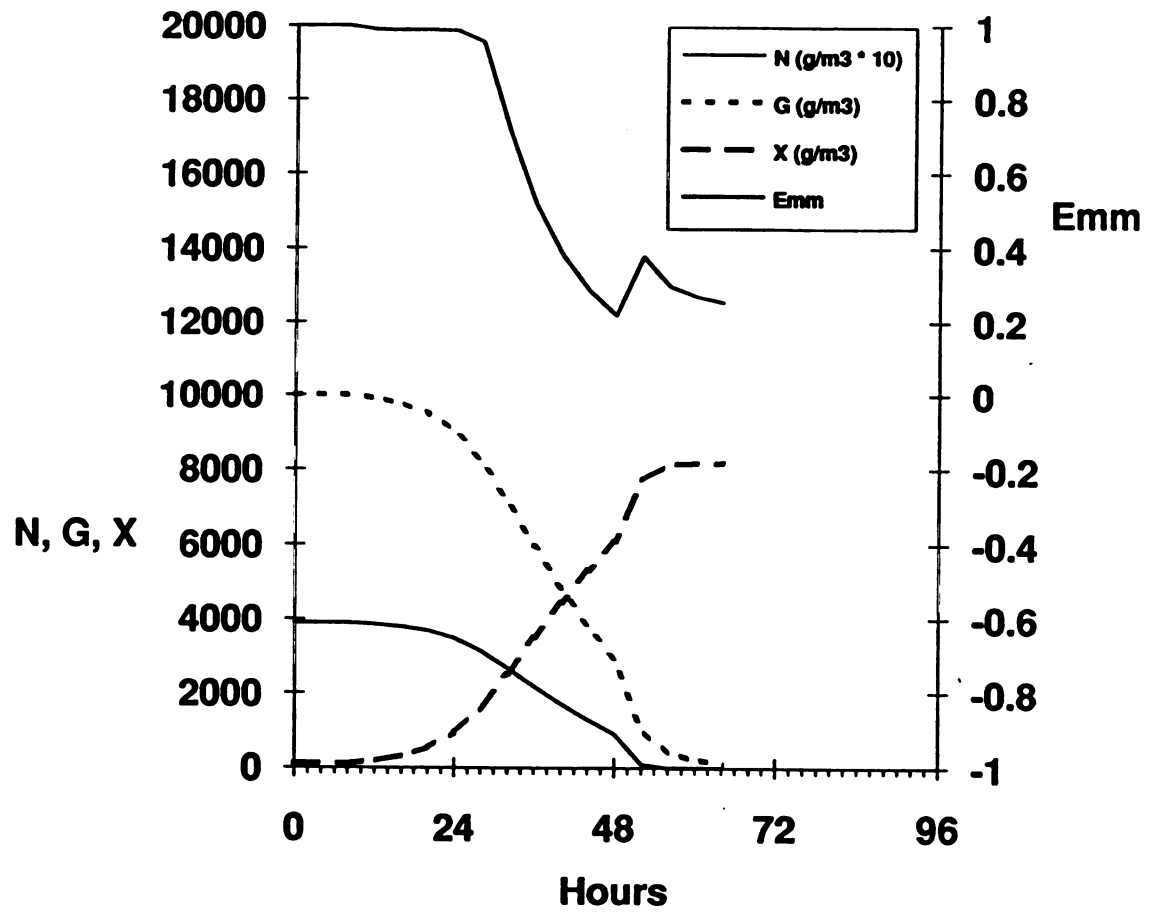
Figure 5.15 Model simulation for cultures grown in high nutrient nitrogen condition; $G_0=10000$ g/m^3, $N_0=390$ g/m^3.
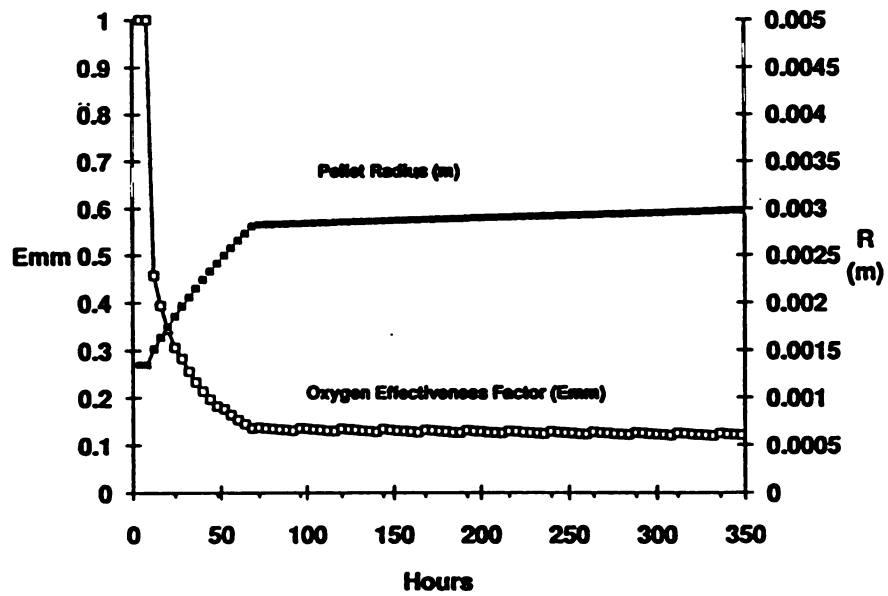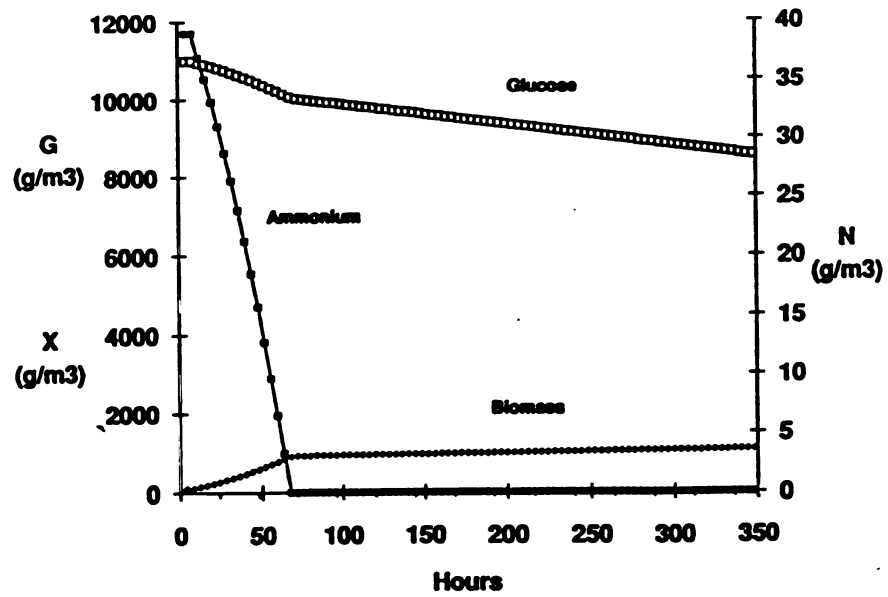
Figure 5.16   Kinetic model simulation for nitrogen-limited cultures of *P. chrysosporium* with large pellets (R=3mm). (This case is analogous to cultures of large pellets grown at low agitation speeds as described by Michel *et al.*, 1990).

Production of peroxidases by mycelial pellets with low effectiveness factors.

Cultures of *P. chrysosporium*, for which the kinetic model predicted a low oxygen effectiveness factor (E<0.4), produce much lower levels of LIP and MNP activity. For example, Dosoretz *et al.* (1990a) showed that in air-flushed cultures, (where the model predicts an oxygen effectiveness factor ranging from0.1 to 0.3), no LIPs and one third less MNPs were produced. In high nitrogen cultures where the oxygen effectiveness factor was less than 0.2 (Figure 5.16) no LIPs or MNPs were produced (see Figure 6.8). Furthermore, Michel *et al.*, (1990) found that large pellets (6 mm diam.), formed using low agitation rates, and for which the kinetic model predicts effectiveness factors of around 0.1, fail to produce LIPs. By comparison, cultures of *P. chrysosporium* where a high effectiveness factor is predicted by the kinetic model (small pellets and liquid phase oxygen concentrations near saturation), produce high levels of both LIP (200 to 300 U/l) and MNP (1000 to 2500 U/l). Therefore, oxygen limitations in mycelial pellets of *P. chrysosporium* appear to have a significant affect on the level of LIPs and MNPs produced. Unlike genetic regulation of peroxidase expression by manganese, veratryl alcohol and nitrogen, the effect of hyperbaric oxygen on cultures of *P. chrysosporium* appears to have a physiological basis.

CHAPTER VI

Application of the peroxidases of *Phanerochaete chrysosporium* to the decolorization of Kraft bleach plant effluents (BPE)

Part I: Results

6.1 Decolorization of BPE by cultures of *P. chrysosporium*.

Kraft pulp is typically bleached with chlorine and its oxides (Eriksson and Kirk, 1985). The effluent from this bleaching operation is called bleach plant effluent (BPE). Combined chlorination stage and extraction stage effluents from industrial and artificial sources were used in this study. The chromophoric (or color causing) material in these effluents has a high molecular weight and a low solubility in water. For both BPEs studied, over 90% of the color containing material had a molecular weight greater than 10,000 daltons. The solubility of synthetic and industrial BPE decreased with pH from 7.0 to 2.0. Synthetic BPE had a lower solubility than industrial BPE (see Figure 4.1). At pH 4.5, the solubility of synthetic BPE was approximately 4,000 C.U. corresponding to approximately 7 g BPE/l. Industrial BPE had a relatively high solubility. The solubility of industrial BPE was greater than 14,000 C.U. at pH 4.5 (Figure 4.1).

Industrial and synthetic BPE were added to nitrogen-limited cultures of *P. chrysosporium*. Addition of synthetic BPE to nitrogen-limited cultures (as described in section 5.1), on days 2 through 7 caused rapid decolorization of the BPE material (Figure 6.1). It was of interest that decolorization occurred on days 3 and 4 when no LIP activity was detectable in control cultures. The rate of decolorization reached a maximum
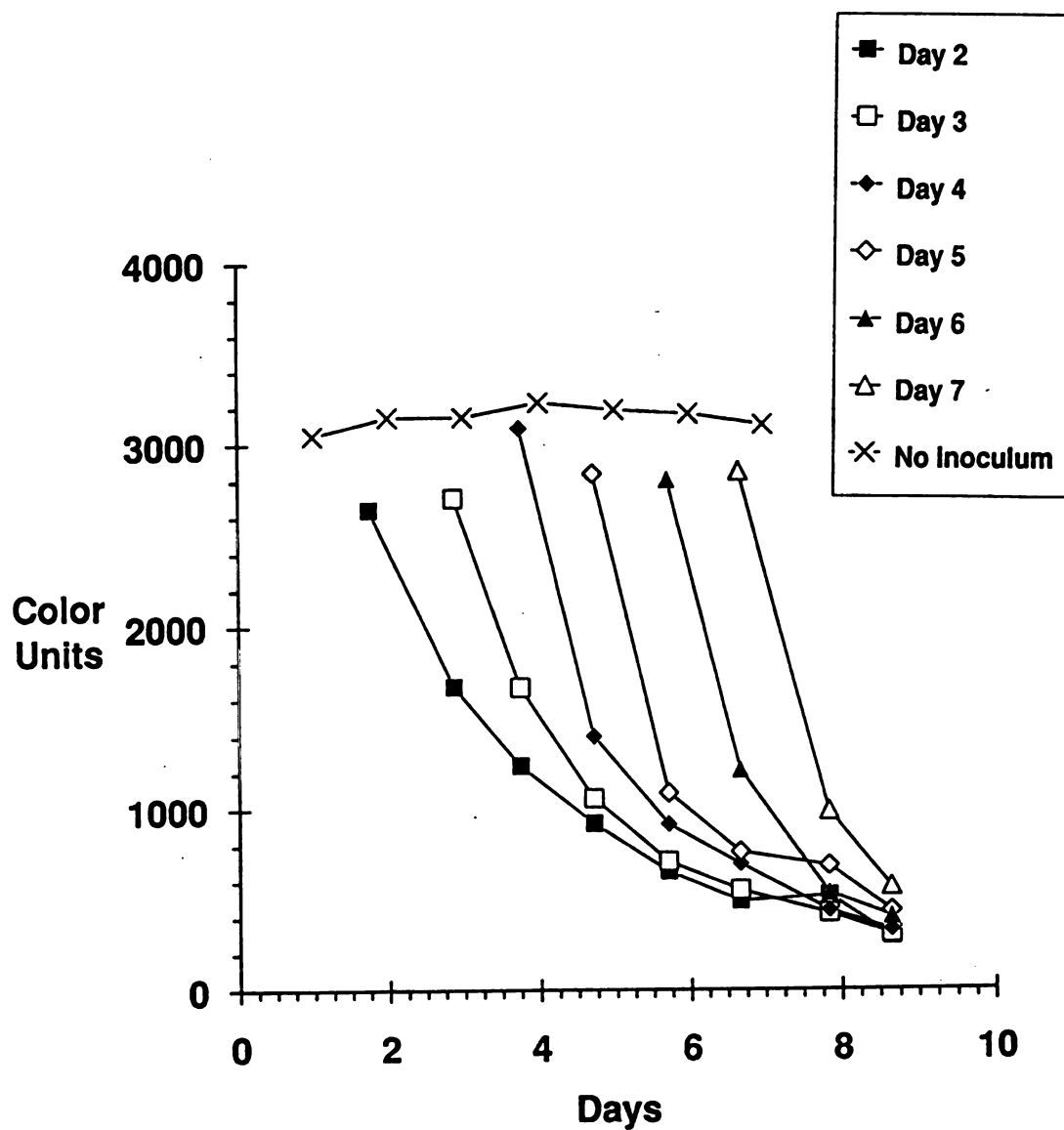
Figure 6.1   Decolorization of Kraft bleach plant effluent (BPE) when added to cultures on different days of incubation. Data for an uninoculated control are also presented. Values represent means for duplicate cultures.

between day 4 and 5 when MNP activity also reached its highest level and showed little or no increase in rate when the LIP activity reached its maximum between days 6 and 7. Thus, the rate of decolorization temporally paralleled MNP, rather than LIP activity. Industrial BPE showed a similar pattern of decolorization compared to synthetic BPE when it was added on day 4 (Figure 6.2). Incubation of synthetic or industrial BPE with autoclaved or filter sterilized culture fluid from day 6 cultures failed to show significant decolorization activity.

Apparent first order rate constants (see discussion of the first order model below) for daily decolorization data are presented in Table 6.1.

Table 6.1 Apparent first order rate constant for decolorization of Kraft BPE by cultures of *P. chrysosporium* as a function of the day of BPE addition.

Day of BPE Addition	k Apparent Rate Constant (dy^{-1})
2	0.35
3	0.45
4	0.70
5	0.75
6	0.75
7	0.75
8	0.80

The rates are highest (0.75 to .80 d^{-1}) on days 5 to 8 when both MNP and LIP are present. However, relatively high rate constants of 0.35, 0.45 and 0.70, respectively, were observed with 4 and 5 day-old cultures, which had little or no LIP activity. It was of interest that the apparent rate constant for BPE decolorization on day 4 of incubation
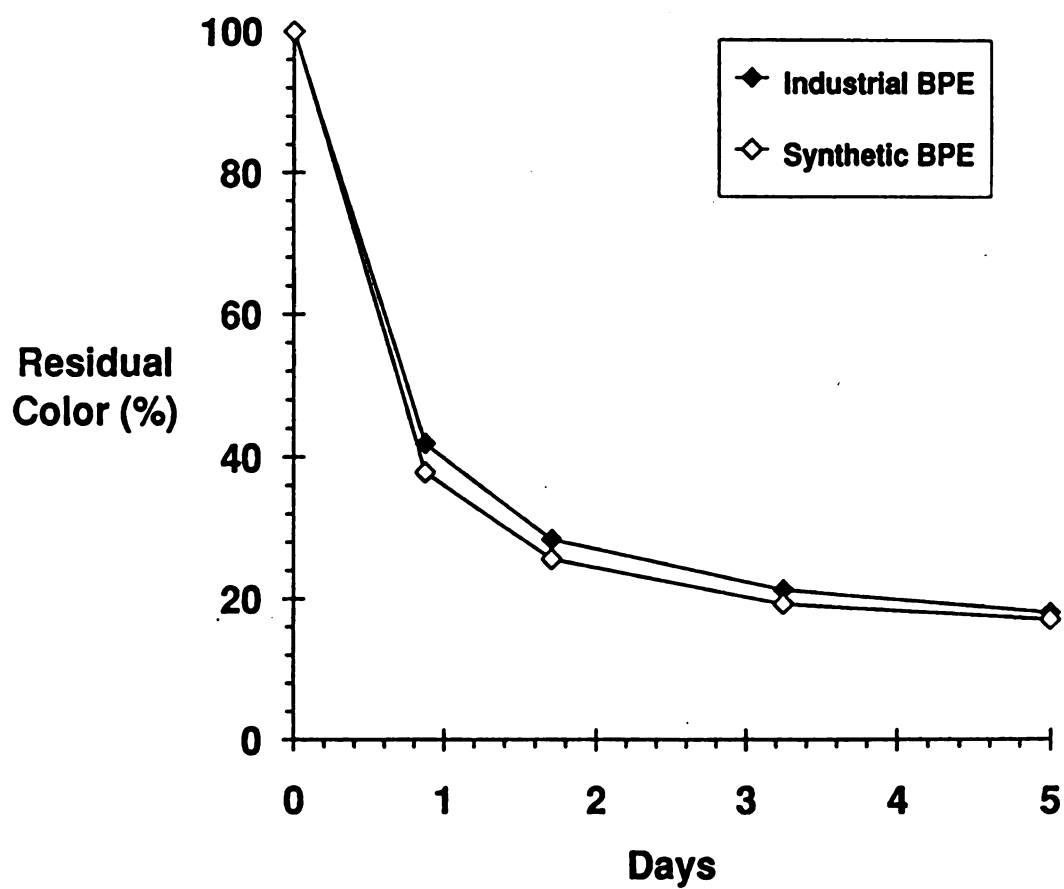
Figure 6.2   The decolorization of synthetic BPE and industrial BPE by nitrogen-limited, agitated cultures of *P. chrysosporium* BKM-F-1767. BPE was added to a final concentration of 3,000 C.U.

(when MNP activity is at or close to its maximum and the LIP activity is negligible) is >90% of that observed on days 6 and 7, when both LIPs and MNPs are present at relatively high levels.

In cultures to which BPE was added, LIP activity was never detected and MNP activity was difficult to detect by enzymatic assay, even after dialysis. Therefore, the pattern of extracellular LIP and MNP production was studied using SDS-PAGE electrophoresis. In agreement with activity assays, in control cultures without added BPE, MNP protein band ($Mr=43,000$ to $46,000$) appeared first (between days 2 and 3) whereas the LIP protein bands were not seen clearly until day 5 (Figure 6.3). On days 5 to 9 multiple MNP and LIP protein bands were evident in the culture fluid (Figure 6.3). Dass and Reddy (1990), have shown that in acetate buffered cultures the predominant MNP protein produced was H4 (43-46 kD) and the major LIP proteins produced were H2 and H6 (38-40 kD). Thus the primary MNP and LIP proteins will form discreet bands on an SDS-PAGE gel.

Although no LIP activity could be detected in industrial and synthetic BPE amended cultures, the LIP and MNP protein bands were similar to the protein bands observed in control cultures (Figure 6.4). The protein band representing MNP proteins was evident on days 4 through 7 while the protein bands representing LIP proteins were evident on days 5 through 7. Thus although LIP and MNPs are not always detectable by enzymatic assay, the proteins are present in the extracellular culture fluid of BPE amended cultures.

Concentrations of between 1,000 and 8,000 C.U. were added to nitrogen-limited cultures of *P. chrysosporium* on day 4. The initial rate of synthetic BPE decolorization was first-order below BPE concentrations of 4000 C.U. and zero-order above 4,000 C.U. This is in agreement with the findings of other investigators (Campbell *et al.*, 1983; Yin *et al.*, 1989). Attempts to fit the data using a Michaelis-Menten kinetic model did not give good results so a "first order below 4000 C.U./ zero-order above 4000 C.U." model
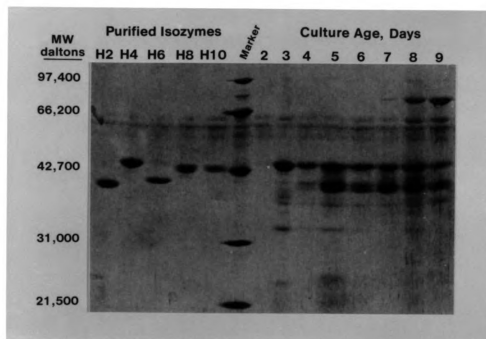
Figure 6.3   SDS-PAGE of extracellular culture fluid from *P. chrysosporium* cultures aged 2 to 9 days. Electrophoretic mobility of FPLC-purified LIP isozymes (H2, H6, H8, and H10) and MNP isozyme H4 is presented.
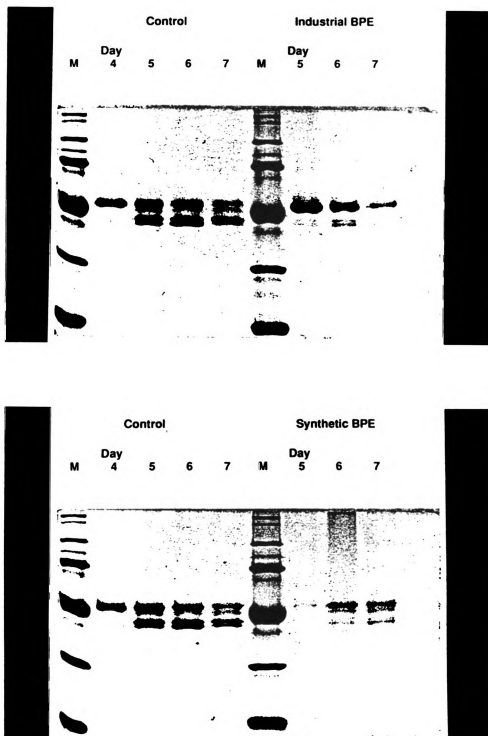
Figure 6.4 SDS-PAGE profile of extracellular fluid from control cultures on days 4 through 7 and from cultures which were amended with (A) industrial BPE and (B) synthetic BPE.
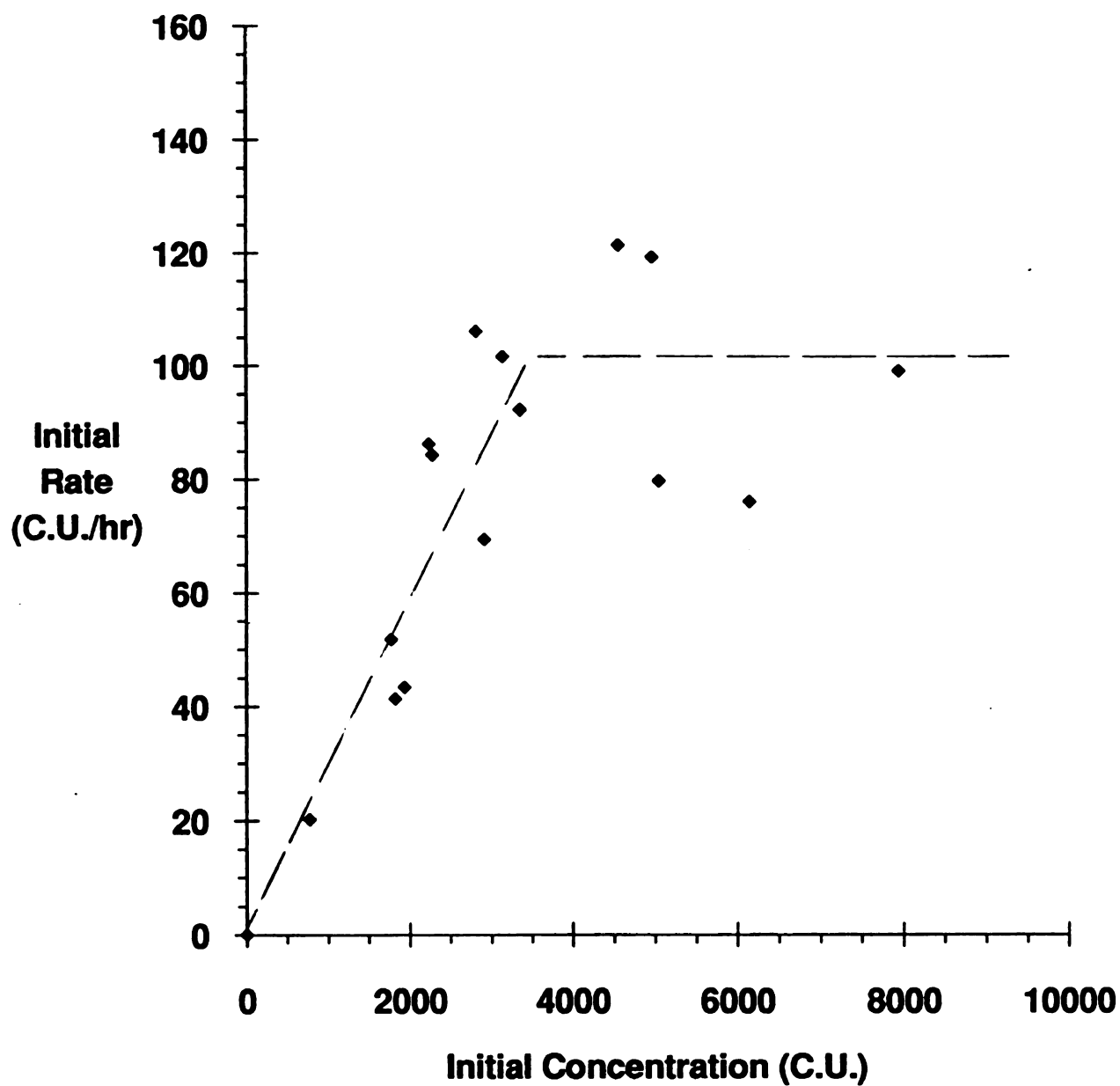
Figure 6.5   The initial rate of synthetic Kraft bleach plant effluent (BPE) decolorization as a function of initial BPE concentration. Synthetic BPE was added to nitrogen-limited cultures of *P. chrysosporium* 4 days after culture inoculation.

was employed (Figure 6.5). The first order rate constant (k) ranged from 0.8 to 0.5 dy^{-1} in this experiment. Interestingly, the concentration where the model switched from zero-order to first-order (4000 C.U.) kinetics coincided with the solubility of the synthetic BPE at pH 4.5 (see Figure 4.2). This finding suggests that the decolorization system acts on soluble BPE at a much faster rate than on insoluble BPE and that the reaction is pseudo-first order with respect to soluble BPE. Industrial BPE had a much higher solubility than synthetic BPE at pH 4.5 (>>14,000 C.U., see Figure 4.2). Previous kinetic models developed for BPE decolorization also use transition from zero-order to first-order kinetics (Campbell *et al.*, 1983; Yin *et al.*, 1989) but do not consider BPE solubility. Both Campbell *et al.* (1983) and Yin *et al.*(1989) used industrial BPEs which presumably have relatively high solubilities. However Yin *et al.* used an initial BPE concentration of 20,000 C.U. which may be near the solubility limit of industrial BPE at pH 4.5. Campbell reported that saturation of the fungal decolorization system occurred at between 4,000 and 6,000 C.U. in the MyCoR system. A first-order model was used to fit rate data in subsequent experiments where a final concentration of 3,000 C.U. of synthetic or industrial BPE was added to cultures.

6.2 Effect of varying manganese concentration on MNP and LIP production and BPE Decolorization.

It has been well-documented that high levels of nitrogen in the medium repress LIP and MNP production in cultures of *P. chrysosporium* (Gold *et al.*, 1989; Kirk and Farrell, 1987). More recently, manganese levels in the medium were shown to have a dramatic effect on the levels of production of MNPs and LIPs (Bonnarme and Jefferies, 1990; Brown *et al.*, 1990; Perez and Jefferies, 1990). High levels (40 ppm) of Mn(II) were shown to completely suppress LIP and enhance MNP production, whereas in the complete absence of Mn(II), no MNPs were produced but LIP production was essentially normal (Bonnarme and Jefferies, 1990; Brown *et al.*, 1990; Perez and Jefferies, 1990).

Varying concentrations of Mn(II) were added to nitrogen limited (2.4 mM) cultures of *P. chrysosporium* to determine the relative contribution of LIPs versus MNPs to BPE decolorization. The aim was to manipulate LIP and MNP levels using manganese and study the effect of these variations on BPE decolorization. Three levels of Mn(II) were added to cultures: 0, 12 and 100 ppm corresponding to low, basal and high Mn(II) levels. Basal Mn(II) cultures exhibited high MNP and LIP activity reaching maxima on days 4-5 and 6-7, respectively (Figure 6.6a,b). Low Mn(II) cultures exhibited relatively low MNP activity compared to high Mn(II) cultures and reached a maximum on day 4. In high Mn(II) cultures LIP activity was not detected but MNP activity was greater than that in basal Mn(II) cultures.

In high nitrogen (24 mM nitrogen) cultures containing 12 ppm Mn(II) neither MNP nor LIP activity was detected (Figure 6.6a,b) and no LIP and MNP bands were seen on the SDS-PAGE gel (Figure 6.7). SDS-PAGE analysis of the culture fluid from high manganese cultures [100 ppm Mn(II)] and basal manganese cultures [12 ppm Mn(II)] showed a single intense protein band (Figure 6.7) which appears to be an MNP protein based on its molecular size and the fact that neither the high Mn(II) nor the basal Mn(II) cultures displayed LIP activity on the day of BPE addition, i.e., on day 4 of incubation. In low manganese cultures on the other hand, faint bands corresponding to LIP and MNP proteins were seen.

When BPE was added to 4 day-old basal Mn(II) and high Mn(II) cultures, decolorization proceeded at a high initial rate (Figure 6.8). Significantly slower rates of decolorization were observed in low Mn(II) and high nitrogen cultures. A mass balance analysis 4 days after the addition of BPE showed approximately 8% decolorization in high nitrogen (nitrogen sufficient) cultures containing 12 ppm Mn(II), 27% decolorization in low Mn(II) cultures, 75% decolorization in high Mn(II) cultures, and 85% decolorization in basal Mn(II) cultures. The apparent first order rate constants (Table 6.2) for decolorization of BPE in cultures containing different levels of nitrogen

and Mn(II), showed that when LIP and MNP are not present little decolorization was observed. The absence of LIPs cultures had minimal effect on the decolorization rate whereas decreasing the activity of MNPs had a pronounced effect on the decolorization rate even when the LIPs were present (Table 6.2).

Table 6.2 Apparent first order rate constant for decolorization of BPE by *P. chrysosporium* as affected by nitrogen and manganese levels in the medium.

Nitrogen level (mM)	Mn(II) (ppm)	Predominant peroxidases	Decolorization rate constant $(dy^{-1})^b$
24.0	12	none	0.01
2.4	0	LIP	0.10
2.4	12	LIP, MNP	0.70
2.4	100	MNP	0.65

b Differences in rate constants of greater than 0.07 dy-1 are considered significant.
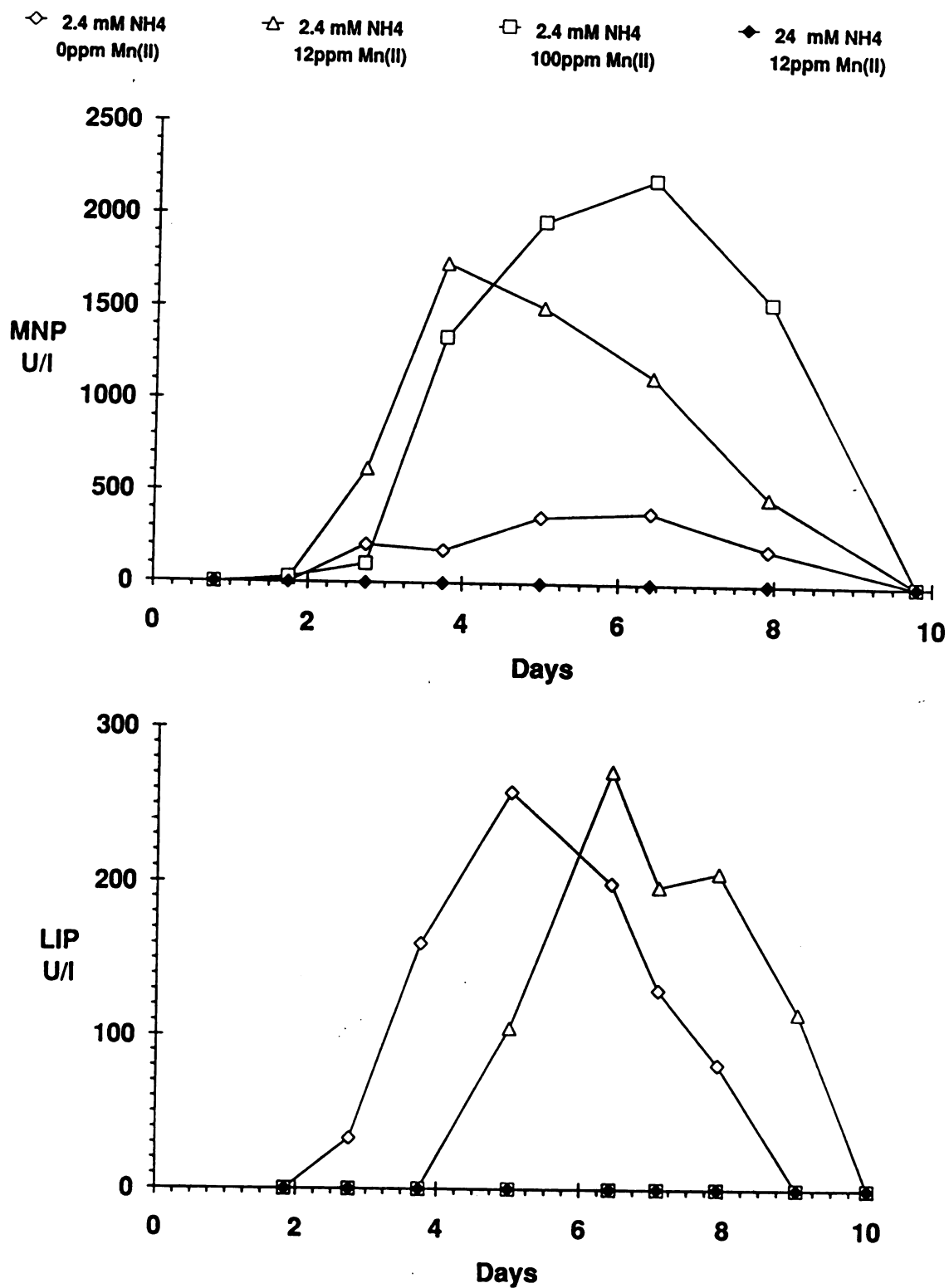
Figure 6.6   The effect of Mn(II) and nitrogen levels on LIP and MNP activities of wild type *P. chrysosporium*. Values presented are averages for triplicate cultures.   A. MNP activity. B. LIP activity.
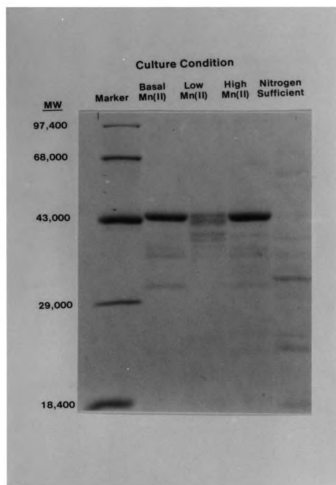
Figure 6.7   SDS-PAGE of peroxidases in extracellular culture fluid of *P. chrysosporium*, at the time of BPE addition, 4 days after incubation at 39° C. Mn(II) concentrations were 0 ppm, 12 ppm and 100 ppm, respectively, in low, basal and high Mn(II) nitrogen limited (2.4 mM N) cultures. Nitrogen sufficient (24 mM N) cultures contained 12 ppm Mn(II).
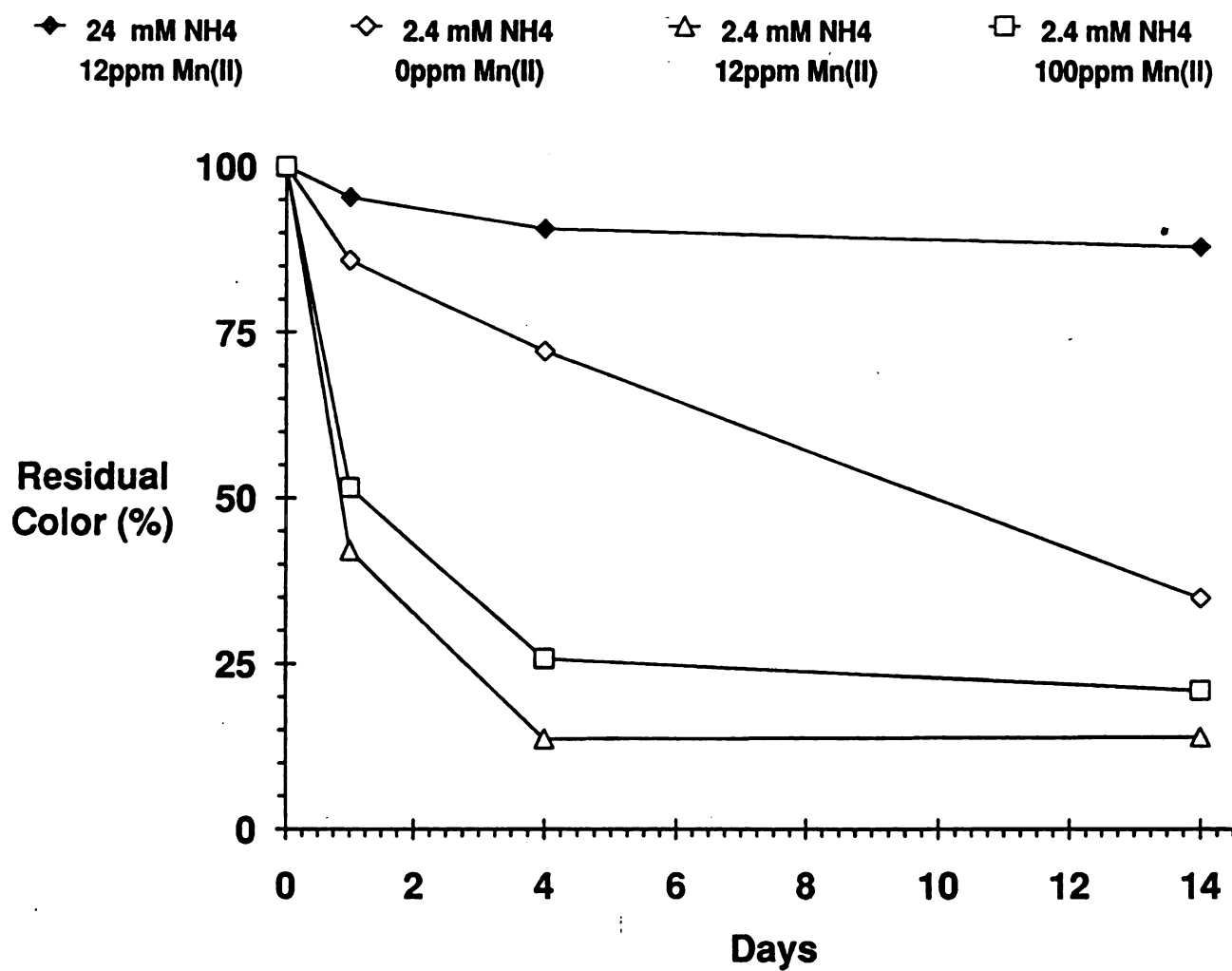
Figure 6.8   The effect of Mn(II) and nitrogen levels on BPE decolorization by cultures of *P. chrysosporium*. BPE was added on day 4 of incubation.

6.3 BPE decolorization by *lip* and *per* mutant cultures.

To further investigate the importance of extracellular peroxidases in BPE decolorization, two mutant strains (*per* and *lip*) and two wild-type strains (ME-446 and BKM-F 1767) of *P. chrysosporium* were compared based on their ability to decolorize BPE. The *per* mutant lacks the ability to produce extracellular peroxidases based on several lines of evidence. First, no MNP or LIP activity was detected in culture fluid of *per* mutant grown in low nitrogen basal medium whereas under identical conditions both MNPs and LIPs are produced in large amounts by the wild type. When concentrated culture fluid from the *per* mutant cultures was fractionated by SDS-PAGE, no LIP or MNP bands were evident (Figure 6.9). In the same gel, however, concentrated culture fluid from 4-day-old cultures of the *lip* mutant and the wild type showed a single band (corresponding to MNP). Moreover, FPLC analysis of the concentrated extracellular fluid from the *per* mutant cultures showed no LIP or MNP peaks. No physiological difference was found between the *per* mutant and the wild type (aside from a lack of MNP and LIP production). The *per* mutant consumed glucose at the same rate as the wild type, produced the same amount of cell biomass and formed mycelial pellets similar in size to those of the wild type. The *lip* mutant has been characterized previously (Boominathan *et al.*, 1990). It produces MNPs and H_2O_2 but lacks the ability to produce the LIPs. The wild type strains ME-446 and BKM-F 1767 produce both LIPs and MNPs.

BPE was added to the *per* mutant, *lip* mutant, and wild-type cultures two days after MNPs first appeared (generally day 4 of incubation) and the extent of decolorization was monitored daily for the next 5 days. The presence (or absence) of extracellular peroxidases was determined by SDS gel electrophoresis of concentrated culture fluid (Figure 6.9) and by LIP and MNP assays of control cultures without added BPE (Figure 6.10). SDS gel results showed that in *lip* and wild-type cultures a single protein band (at 46,000 MW) corresponding to MNP was present at the time of BPE addition. In the *per*

mutant culture, neither LIP nor MNP protein bands were evident (Fiogure 6.9). The MNP activities in the ME446, BKM-F-1767, *lip* mutant and *per* mutant cultures were 3,550, 2,200, 2,050 U/l and 0 U/l, respectively at the time of BPE addition (Figure 6.10). Only the wild-type cultures produced LIP activity (Figure 6.10).

The *per* mutant, exhibited negligible decolorization of BPE (Figure 6.11) while the wild-type strains exhibited rapid decolorization of BPE. The *lip* mutant (which produces MNPs only) showed about 80% of the decolorization activity exhibited by ME446. These results, consistent with the other data presented above, indicate that the extracellular peroxidases are important for BPE decolorization and that the MNPs play a predominant role in BPE decolorization by *P. chrysosporium*.

Further evidence of the involvement of MNP as opposed to LIP in BPE decolorization is given by the culture pH during decolorization. As determined in Methods (see also Appendix 3), the MNPs have their maximal activity at pH 4.5 while LIPs have their peak activity at pH 2.5. LIP activity at pH 4.5 is reduced by more than 90% compared to it's maximal activity. In the decolorization cultures the pH ranges from 4.5 to 5, the range where the MNPs are most active and LIP activity is reduced.

Culture Condition

BKM Basal Mn (II)	BKM Low Mn (II)	Marker	LIP⁻	Per⁻

MW

97,400 —

68,000 —

43,000 —

29,000 —
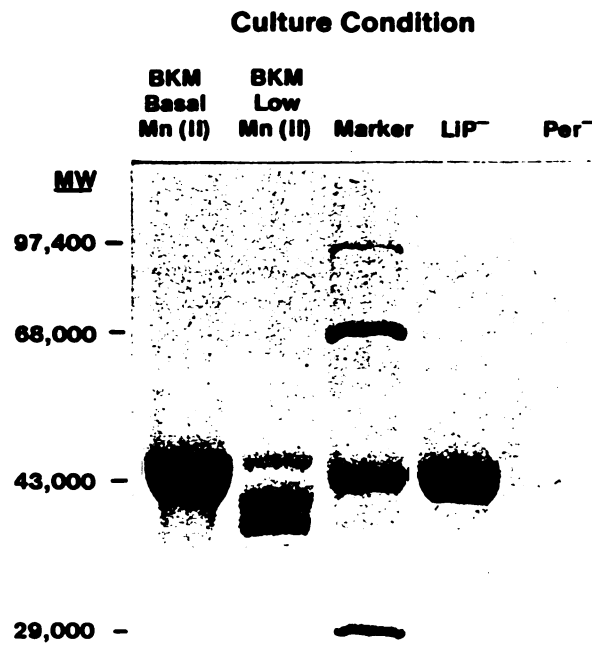
Figure 6.9   SDS-PAGE of peroxidases in extracellular culture fluid of *P. chrysosporium* wild type strain BKM-F-1767, a *lip* mutant strain and a *per* mutant strain at the time of BPE addition.
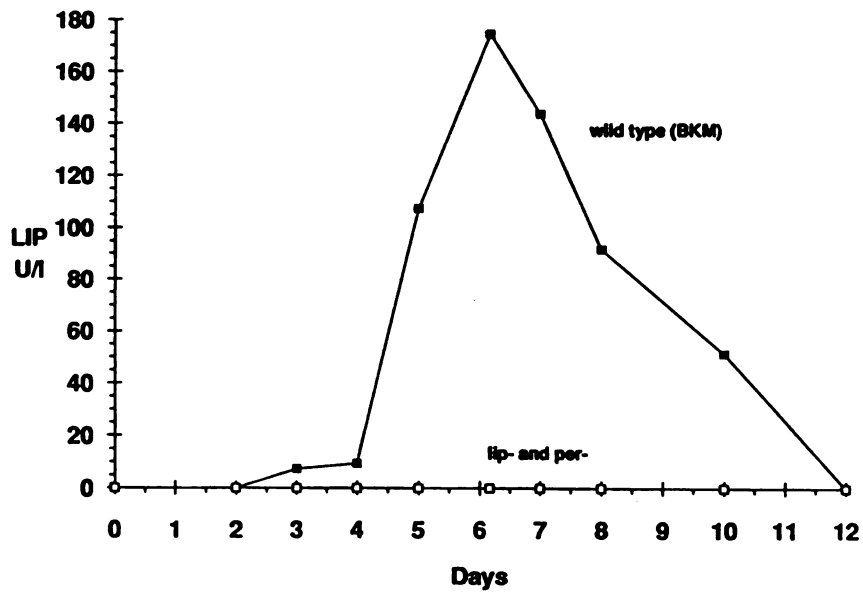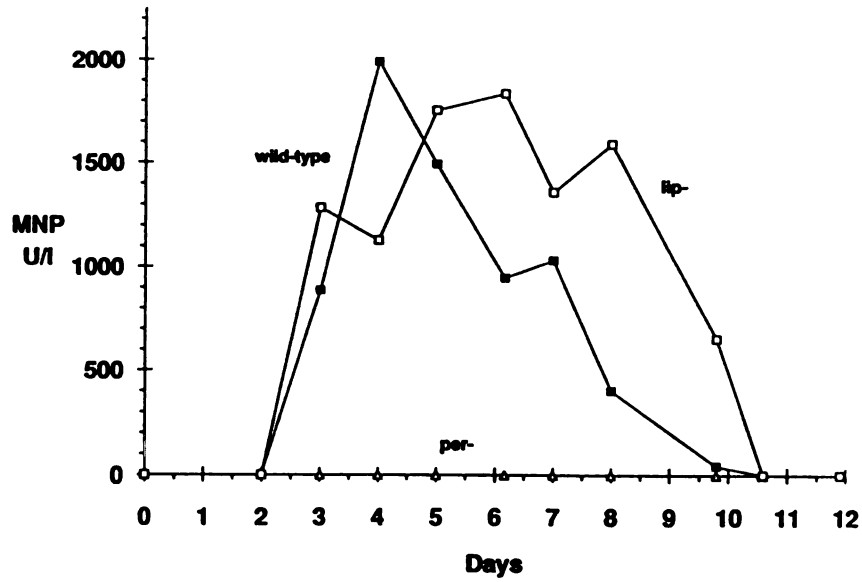
Figure 6.10   Lignin peroxidase (LIP) and manganese peroxidase (MNP) activities in wild-type (BKM-F-1767), lip⁻ mutant and per⁻ mutant cultures of *P. chrysosporium*. Cultures were grown in low nitrogen medium which contained 12 ppm Mn(II).
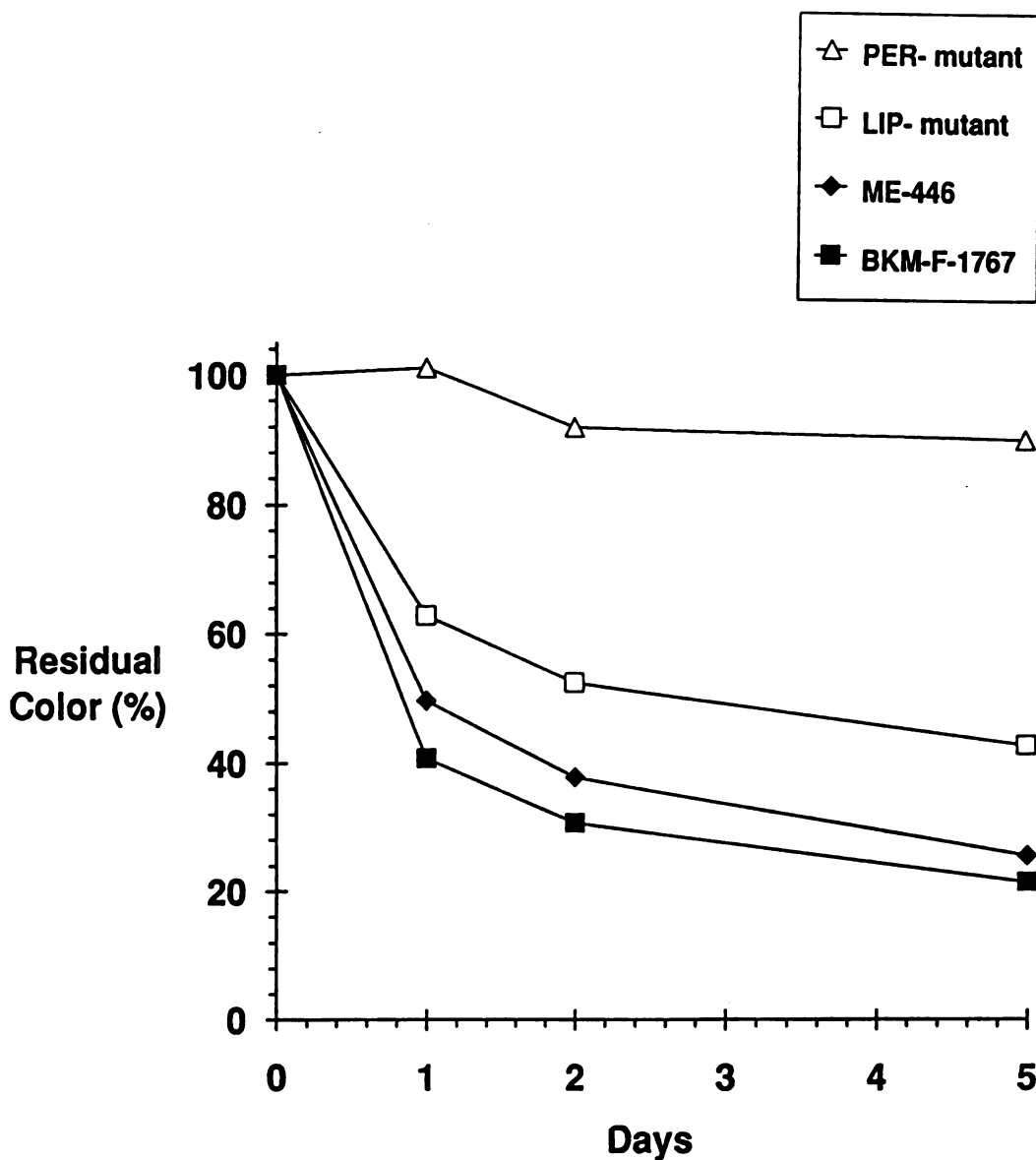
Figure 6.11   Decolorization of BPE by *P. chrysosporium* wild-type strains ME446 and BKM-F 1767 and two mutants, *per* and *lip* of ME446. BPE (3000 C.U.) was added to each of the cultures on the peak day of MNP activity and the extent of BPE decolorization was monitored each day for the next 5 days. The values shown are averages of duplicate cultures on two separate occasions.

6.4 *In vitro* decolorization of BPE.

A brief study was conducted of the ability of isolated MNPs and LIPs to decolorize BPE. Culture fluid from 5-day old nitrogen limited cultures with both LIP and MNP activity was collected and concentrated using ultrafiltration. This concentrated (10:1) enzyme solution was applied to an FPLC column and the MNPs and LIPs were eluted using an acetate gradient. The eluate was distributed using a fraction collector and individual fractions were assayed for LIP and MNP activity. A 300 μl aliquot of the MNP fraction (no LIP activity) and a 300 μl aliquot of a LIP fraction (H10) (no MNP activity) were added to test tubes containing 900 μl of BPE (722 initial color units), 40 μl of 8mM H_2O_2 and 60 μl of 5.2 g/l $MnSO_4$ and incubated overnight at 37 C. Control cultures with H_2O_2 only, with $MnSO_4$ and H_2O_2, and with H_2O_2, $MnSO_4$ and concentrated 5-day old culture fluid were also prepared. The results are shown in Table 6.3. Compared to the LIP and MNP activity in day 6 nitrogen limited cultures, the peroxidase activities in the *in vitro* experiments were a factor of three higher.

Table 6.3 Decolorization of Kraft BPE by FPLC purified peroxidases of *P. chrysosporium* in a cell free system.

Condition	Residual Color (%)[a]
H_2O	100 ± 1
$MnSO_4$, H_2O_2	99 ± 2
$MnSO_4$, H_2O_2, purified MNP	73 ± 4
$MnSO_4$, H_2O_2, purified LIP (H10)	110 ± 1
$MnSO_4$, H_2O_2, day 5 culture fluid	66 ± 5

[a] Values are means for triplicate samples ± one standard deviation.

The purified MNP preparation decolorized the BPE by approximately 27% in 20 hours. Similarly, 5-day old concentrated culture fluid containing both LIP and MNP activities decolorized the BPE by 34% in 20 hours. When purified LIP H10 was added to the BPE the color increased by 10% in 20 hours. Neither water, nor H_2O_2 and $MnSO_4$ showed any decolorization activity. In further experiments to demonstrate *in vitro* decolorization no decolorization activity was observed and this avenue of study was abandoned. (Note: Recently, Lackner *et al.* (1991) have demonstrated *in vitro* decolorization of BPE by MNP and Mn(III). In their reaction system the hydrogen peroxide was added at a slow rate to obviate enzyme deactivation. Furthermore, Michael Gold (personal communication) has indicated that acetate, which was used as a buffer, may interfere with the reaction cycle).

Part II: Discussion

6.5 Role of MNPs and LIPs in the decolorization of BPE.

Earlier studies have shown that *P. chrysosporium* as well as some other white-rot fungi rapidly decolorize BPE. Sundman *et al.* (1981) showed that BPE from the first alkali extraction stage after chlorination (E1 effluent) was decomposed to low molecular weight colorless products. *P. chrysosporium* was shown to degrade significant amounts of ^{14}C-labeled bleached kraft lignin to $^{14}CO_2$ (4,19). Campbell (1983) and Eaton *et al.* (1983) developed the MyCoR process which utilizes *P. chrysosporium* immobilized on partially submerged rotating discs to decolorize industrial BPE. Yin *et al.* (1989) examined the kinetics of BPE decolorization in the MyCoR process and indicated that BPE decolorization consisted of three distinct stages. The LIP or MNP activities were not reported in any of these previous studies. Furthermore, although Paice and Jurasek (1984) have shown that horseradish peroxidase can catalyze BPE decolorization, and Archibald *et al.*(1990) have implicated laccases of *C. versicolor* in BPE decolorization, the role of LIPs and MNPs of *P. chrysosporium* in the decolorization process has never clearly been established.

Results indicate that the extracellular peroxidases of *P. chrysosporium* play a key role in BPE decolorization by this organism. Little or no BPE decolorization was seen when *P. chrysosporium* was grown in high nitrogen medium which blocks production of both LIPs and MNPs (Figure 6.8) suggesting that these peroxidases are required for decolorization activity. This is independently supported by the experiment with the *per* mutant which lacks the ability to produce LIPs and MNPs but produces H_2O_2 comparable to the wild-type (Boominathan and Reddy, 1991). The fact that the *per* mutant shows negligible BPE decolorization (Figure 6.10) is consistent with the idea that extracellular peroxidases play a key role in BPE decolorization.

A determination of the relative contribution of LIPs versus MNPs to BPE decolorization was an important focus of this investigation. Several lines of evidence indicated that the MNPs play a predominant role in BPE decolorization by *P. chrysosporium*. First, a high degree of BPE decolorization was observed in the high Mn(II) wild-type cultures and in the *lip* mutant cultures, in which high levels of MNP activity, but no LIP activity, was seen (Figures 6.8 and 6.10) and LIP proteins were not evident on SDS-PAGE gels (Figures 6.7 and 6.9). Second, very low levels of BPE decolorization were observed in wild-type cultures grown without Mn(II) in which high levels of LIP and very low levels of MNP activity were seen (Figure 6.8). Third, BPE decolorization activity temporally paralleled the appearance of MNP rather than LIP activity in wild-type cultures containing 12 ppm Mn(II) (see Figure 6.1). For example, relatively high rates of BPE degradation are observed on days 3 and 4 of incubation in basal nitrogen-limited medium at which time little or no LIP activity is seen and LIP proteins were not present in the culture fluid (Figure 6.4). These results, in combination with results showing that peroxidases are necessary for decolorization to occur, conclusively show that MNPs play a more important role than LIPs in decolorizing BPE.

The results of this study indicating a minor role for LIPs and a major role for MNPs is an interesting contrast to earlier studies which showed that the LIPs play a major role in the degradation of synthetic ^{14}C-lignin to $^{14}CO_2$ whereas the MNPs play a minor role in this process (Boominathan *et al.*, 1990; Perez and Jefferies, 1990). Boominathan *et al.* (1990) showed that the *lip* mutant of *P. chrysosporium*, which lacks the ability to produce LIPs but produces a full complement of MNPs, exhibits only about 16% of the ligninolytic activity of the wild-type indicating that MNPs play a minor role in lignin degradation by *P. chrysosporium*. Perez and Jeffries (1990) showed that high levels of MNP activity but no LIP activity was seen when *P. chrysosporium* was grown in nitrogen-limited medium in the presence of 39.8 ppm Mn(II). These cultures exhibited only about 10 to 11% of the lignin degradation ability as compared to cultures grown in

low N medium containing 0.35 ppm Mn(II), which supports production of high levels of LIP but negligible levels of MNP activity. These apparent differences in contributions of LIPs versus MNPs to lignin degradation versus BPE degradation are quite interesting and unexpected. The observed differences in activities may reflect the differences in the two substrates (i.e. lignin and BPE). BPE is predominantly soluble, chlorinated, and partially degraded whereas the structure of DHP more closely resembles the insoluble native lignin polymer.

In conclusion, the results indicate that extracellular peroxidases are important for BPE decolorization by *P. chrysosporium* and that MNPs play a predominant role and LIPs play a relatively minor role in this decolorization process.

The appearance of a brown mycelial coloration has been used as a visual indicator of the onset of ligninolytic activity in cultures of *P. chrysosporium*. This brown coloration coincides temporally with the rapid disappearance from the culture fluid of soluble manganese (Figure 5.2) and with peak MNP activity (Figure 5.1b). When BPE is added to cultures with this brown coloration, the color disappears for a period of two or three days while the decolorization process occurs and then gradually reappears. Therefore based on these findings, and the results of Lackner *et al.* (1991), a simple reaction scheme was been postulated for the enzymatic oxidation of BPE and the formation of insoluble manganese by MNPs (Figure 6.12). Divalent manganese (Mn(II)), which is a component of the culture media, is enzymatically converted to reactive trivalent manganese (Mn(III)) by MNP and hydrogen peroxide. The trivalent manganese non-specifically oxidizes the BPE polymer leading to a variety of products and in the process is reduced back to divalent manganese. In the absence of oxidizable substrates like BPE or lignin, trivalent manganese, formed by the action of MNP, is converted via hydrolyzation and disproportionation to divalent and tetravalent manganese (Lackner *et al.*, 1991). Tetravalent manganese can react to form insoluble manganese salts such as manganese dioxide (MnO_2). These insoluble manganese salts give the pellets their

characteristic brown coloration during the onset of ligninolytic activity. This study is the first to relate a decrease in the concentration of soluble manganese with the appearance of the brown coloration on the mycelial pellets and adds credence to the idea that the brown coloration is due to deposits of solid MnO_2.
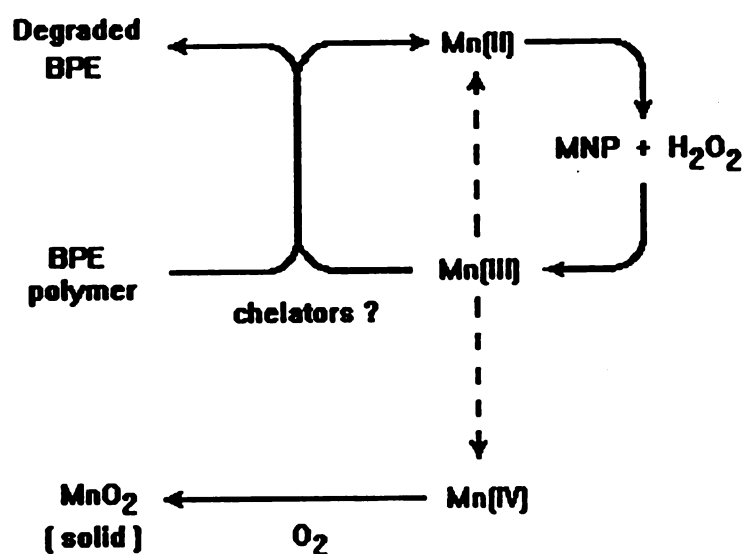
Figure 6.12 Proposed reaction scheme for the degradation of BPE and the deposition of manganese by manganese peroxidases (MNP) of *P. chrysosporium*.

CHAPTER 7

Conclusions and Recommendations

7.1 Conclusions

1. An integrated model based on the life-cycle of *P. chrysosporium* accurately predicts a wide range of culture characteristics including culture dry weight, substrate utilization rates and potential oxygen limitations in mycelial pellets, during primary growth and during secondary metabolism, when LIPs and MNPs as well as many industrially significant products are produced. The model suggests a relationship between the level of polysaccharides produced and the dissolved oxygen concentration within the mycelial pellets.

2. Analysis of the mass transfer limitations in nitrogen limited, peroxidase producing mycelial pellet cultures of *P. chrysosporium* indicates that intra-particle oxygen mass transfer can be rate limiting during secondary metabolism. Cultures which have oxygen effectiveness factors significantly less than one (E<0.4) produce little or no MNP or LIP. Thus, the effect of oxygen appears to have a physiological as opposed to a genetic basis.

3. Extracellular peroxidases play a key role in the decolorization of Kraft bleach plant effluents (BPE) by *P. chrysosporium*. MNPs play a predominant role, and LIPs a relatively minor role, in the process of Kraft bleach plant effluent decolorization.

118

7.2 Recommendations

1. Since oxygen limitations within mycelial pellets appear to limit the production of the extracellular peroxidases, methods for producing small pellets or thin mycelial films which are not oxygen limited should be studied.

2. The decolorization of BPE using whole cultures of *P. chrysosporium* requires a long period of incubation before the decolorization activity begins. The large volume of effluents generated by the paper industry would require enormous fermentation treatment volumes. Also, the production of the peroxidases is very sensitive to agitation, oxygen tension, nutrient composition and the presence of extracellular proteases. One alternative approach for BPE treatment would be to develop an immobilized enzyme decolorization system using MNPs so that enzyme production and BPE treatment could be decoupled. Immobilized enzymes would have a potentially longer life-span requiring less total enzyme production. A recommendation is that future work focus on the further development of an *in vitro* decolorization system. This system would involve enzymes and cofactors such as H_2O_2 and manganese.

3. Industrial BPE streams are relatively dilute. To reduce the fermentation system volume it may be beneficial to concentrate the BPE stream using ultrafiltration, precipitation or adsorption. The relative toxicity of the low and high molecular weight fraction must be considered.

BIBLIOGRAPHY

Aiba, S., A.E. Humphrey, N.F. Millis. 1973. Biochemical Engineering, 2nd ed., p.29. Academic Press Inc., New York.

An-Lac Nguyen and J.H.T. Luong. 1986. Diffusion in κ-Carrageenan gel beads. Biotechnol.Bioeng. 28:1262-1267.

Archibald, M. G. Paice, and L. Jurasek. 1990. Decolorization of kraft bleachery effluent chromophores by *Coriolus (Trametes) versicolor*. Enz. Microb. Technol. 12:846-853.

Barlev, S.S., T.K.Kirk. 1981. Effects of molecular oxygen on lignin degradation by *Phanerochaete chrysosporium*. Biochem.Biophys.Res.Comms. 99:373-378.

Bonnarme, P., and T. W. Jeffries. 1990. Mn(II) regulation of lignin peroxidases and manganese-dependent peroxidases from lignin-degrading white-rot fungi. Appl. Environ. Microbiol. 56:210-217.

Bonnarme, P., and T. W. Jeffries. 1990. Selective production of extracellular peroxidases from *Phanerochaete chrysosporium* in an airlift bioreactor. J.Ferm.Bioeng.70:158-163.

Boominathan, K., S. B. Dass, T. A. Randall, R. L. Kelley, and C. A. Reddy. 1990. Lignin peroxidase-negative mutant of the white-rot basidiomycete, *Phanerochaete chrysosporium*. J. Bacteriol. 172:260-265.

Boominathan, K., and C. A. Reddy. 1991. Lignin degradation by fungi: biotechnological applications, p. 763-822. In D. K. Arora, K. G. Mukerji, and R. P. Elander (eds.), Handbook of Applied Mycology, vol. 4. Biotechnology, Marcel Dekker Inc., New York.

Brown, A. B., J. K. Glenn, and H. H. Gold. 1990. Manganese regulates expression of manganese peroxidase by *Phanerochaete chrysosporium*. J. Bacteriol. 172:3125-3130.

Bumpus J.A., S.D.Aust. 1987. Biodegradation of DDT by the white-rot fungus *Phanerochaete chrysosporium*. Appl.Environ.Microbiol.53:2001-2008

Bumpus J.A., M.Tien, D.Wright, S.D.Aust. 1985. Oxidation of persistent pollutants by a white-rot fungus. Science 228:1434-1436.

Burkholder, P.R., E.W. Sinnott. 1945. Morphogenesis of fungal colonies in submerged shaken cultures. Amer.J.Bot. 32:424-431.

Campbell, A. G., Jr. 1983. A bench scale evaluation of a process for decolorization of bleach plant effluent using the white-rot fungus *Phanerochaete chrysosporium*. Ph.D. dissertation, North Carolina State University, Raleigh, NC.

Carnahan, B., H.A.Luther, J.O.Wilkes. 1969. Applied Numerical Methods p.462. John Wiley and Sons, Inc. New York.

Chang, H.M., T.W.Joyce, A.G.Campbell, E.D.Gerrard, V.B.Huynh, T.K.Kirk. 1983. Fungal decolorization of bleach plant effluents. pp.257-268 in Recent advances in lignin biodegradation research, H.M.Chang, T.K.Kirk eds., Uni publishers, Tokyo.

Chang, H.M., T.W.Joyce, T.K.Kirk. 1987. Process of treating effluent from a pulp or papermaking operation. U.S.Patent No. 4,655,926.

Crank J. 1975. The Mathematics of Diffusion, 2nd ed. Clarendon Press, New York.

Cresand, T.J., B.E.Dale, S.L.Hanson, R.J.Gillies. 1988. A stirred bath technique for diffusivity measurements in cell matrices. Biotech.Bioeng. 32:1029-1036.

Dass, S. B., and C. A. Reddy. 1990. Characterization of extracellular peroxidases produced by acetate-buffered cultures of the lignin-degrading basidiomycete *Phanerochaete chrysosporium*. FEMS Microbiol. Lett. 69:221-224.

deBoer, H.A., Y.Z.Zhang, C.Collins, C.A.Reddy. 1987. Ananlysis of nucleotide sequences of two ligninase cDNAs from a white-rot filamentous fungi, *Phanerochaete chrysosporium*. Gene 60:93-102

Dosoretz, C.G., A.H.-C.Chen, H.E.Grethlein. 1990a. Effect of oxygenation conditions on submerged cultures of *Phanerochaete chrysosporium*. Appl.Microbiol.Biotechnol. 34:131-137.

Dosoretz, C.G., S. B. Dass, C. A. Reddy, and H. E. Grethlein. 1990b. Protease-mediated degradation of lignin peroxidase in liquid cultures of *Phanerochaete chrysosporium*. Appl. Environ. Microbiol. 56:3429-3434.

Dosoretz, C.G., H.E.Grethlein. 1991. Physiological aspects of the regulation of extracellular enzymes of *Phanerochaete chrysosporium*. Appl.Biochem.Biotechnol.28:253-265.

Eaton, D.C. 1984. Mineralization of polychlorinated biphenyls by *Phanerochaete chrysosporium*. Enzyme Microb.Technol. 7:194-196.

Eaton, D.C., H.-M. Chang, T.W. Joyce, T.W. Jeffries, and T.K. Kirk. 1983. Method obtains fungal reduction of the color of extraction stage kraft bleach effluents. Tappi J. 65:89-92.

Eaton, D.C., H.-M. Chang, T.K. Kirk. 1980. Fungal decolorization of kraft bleach plant effluents. Tappi J. 63:103-106.

Eriksson, K.E., T.K.Kirk. 1985. Biopulping, biobleaching and treatment of kraft bleaching effluents with white-rot fungi. in: Comprehensive Biotechnology. Volume 4. pp.271-294.

Eriksson, K.E., M.C. Kolar. 1985. Microbial degradation of chlorolignins. Environ.Sci.Technol. 19:1086-1089.

Faison, B.D., T.K.Kirk. 1985. Factors involved in the regulation of ligninase activity in *Phanerochaete chrysosporium* Appl.Environ.Microbiol.49:299-304.

Farrell, R.L., K.E.Murtagh, M.Tien, M.D.Mozuch, T.K.Kirk. 1989. Physical and enzymatic properties of lignin peroxidase isozymes from *Phanerochaete chrysosporium*. Enzyme Microb.Technol.11:322-328

Fink, D.J., T.Y.Na, J.S.Schultz. 1973. Effectiveness factor calculations for immobilized enzyme catalysts. Biotech.Bioeng.15:879-888.

Forney, L. 1978. Studies on the degradation of Kraft lignin by bacteria. M.S. thesis, Michigan State University.

Ghiorse, W.C. 1984. Biology of iron- and manganese-depositing bacteria. Ann.Rev.Microbiol. 38:515-550.

Gold, M.H. 1991. The peroxidases of the lignin degrading white-rot basidiomycete *Phanerochaete chrysosporium*. Department of Microbiology and Public Health seminar. Michigan State University, December 8 , 1991

Gold, M.H., M.Kuwahara, A.A.Chiu, J.K.Glenn. 1984. Purification and characterization of an extracellular H_2O_2-requiring diarylpropane oxygenase from the white-rot basidiomycete *P. chrysosporium*. Arch.Biochem.Biophys.234:353-362.

Gold, M. H., H. Wariishi, and K. Valli. 1989. Extracellular peroxidases involved in lignin degradation by the white rot basidiomycete *Phanerochaete chrysosporium*, p. 127-136. In J. R. Whitaker and P. E. Sonnet (ed.), Biocatalysis in agricultural biotechnology. Amer. Chem. Soc., Washington, DC.

Gold, M.H., H.Wariishi, K.Valli, M.B.Mayfield, V.J.Nipper, D.Pribnow. 1990. Manganese peroxidase from *Phanerochaete chrysosporium* biochemical and genetic characterization. Proc.of the 4th Int.Conf on Biotech.in the Pulp and Pap.Ind., Raleigh.

Gupta, M.P., P.K. Bhattacharya. 1985. Studies on removal from bleach plant effluent of a kraft pulp mill. J.Chem.Tech.Biotechnol.35B:23-32.

Hammel, K.E., B.Kalyanaraman, T.K.Kirk. 1986. Oxidation of polycyclic aromatic hydrocarbons and dibenzo[p]-dioxins by *Phanerochaete chrysosporium*. J.Biol.Chem.261:16948-16952.

Huynh, V.-B., H. M. Chang, T. W. Joyce, and T. K. Kirk. 1985. Dechlorination of chloro-organics by a white-rot fungus. Tappi J. 68:98-102.

Jager, A., S. Croan, and T. K. Kirk. 1985. Production of ligninases and degradation of lignin in agitated submerged cultures of *Phanerochaete chrysosporium*. Appl. Environ. Microbiol. 50:1274-1278.

Jefferies, T.W., S.Choi, T.K. Kirk. 1981. Nutritional regulation of lignin degradation by *Phanerochaete chrysosporium*. Appl.Environ.Microbiol. 42:290-96.

Jones, S. 1990. Growth kinetics and lignin peroxidase production by *Phanerochaete chrysosporium* in a rotating biological contactor. M.S.Thesis, Michigan State University.

Jordan, J., E.Ackerman, R.L.Berger. 1956. Polaragraphic diffusion coefficients of oxygen defined by activity gradients in viscous media. J.Am.Chem.Soc.78:2979-2983.

Kelley, R. L., and C. A. Reddy. 1986. Identification of glucose oxidase activity as the primary source of hydrogen peroxide production in ligninolytic cultures of *Phanerochaete chrysosporium*. Arch. Microbiol. 144:248-253.

Kim, K. J., and C. A. Reddy. 1990. Unpublished data.

Kirk, T.K., E.Schutz, W.J.Conners, L.L.Lorenz and J.G.Zeikus. 1978. Influence of culture parameters on lignin metabolism by *Phanerochaete chrysosporium*. Arch.Microbiol.117:277-285.

Kirk, T.K., S.Croan, M.Tien, K.E.Murtagh, R.L.Farrell. 1985. Production of multiple ligninases by *Phanerochaete chrysosporium*: effect of selected growth conditions and use of a mutant strain. Enzyme Microb.Technol. 8:27-32.

Kirk, T.K., R.L. Farrell. 1987. Enzymatic "Combustion": the microbial degradation of lignin. Ann.Rev.Microbiol.41:465-505.

Kirkpatrick N., J.M.Palmer. 1987. Semi-continuous ligninase production using foam-immobilised *Phanerochaete chrysosporium*. Appl.Microbiol.Biotechnol.27:129-133.

Kobayashi,T., H.Suzuki. 1972. Studies on the decomposition of raffinose by α-galactosidase of mold. J.Ferment.Technol.50:625-632.

Kobayashi,T., G.VanDeem, M.Moo-Young. 1973. Oxygen transfer into mycelial pellets. Biotech.Bioeng.15:27-45.

Kuwahara, M., J. K. Glenn, M. A. Morgan, and M. H. Gold. 1984. Separation and characterization of two extracellular H_2O_2-dependent oxidases from ligninolytic cultures of *Phanerochaete chrysosporium*. FEBS Lett. 169:247-250.

Lackner, R., E.Srebotnik, K.Messner. (Aug.15) 1991. Oxidative degradation of high molecular weight chlorolignin by manganese peroxidase of *Phanerochaete chrysosporium*. Biochem.Biophys.Res.Comm.178:1092-1098.

Lamar, R. T., M. J. Larsen, and T. K. Kirk. 1990. Sensitivity to and degradation of pentachlorophenol by *Phanerochaete* spp. Appl. Environ. Microbiol. 56:3519-3526.

Leisola, M., C. Brown, M. Laurila, D.Ulmer, A.Fiechter. 1982. Polysaccharide synthesis by *Phanerochaete chrysosporium* during degradation of kraft lignin. European J. Appl. Microbiol. Biotechnol. 15:180-184.

Liebeskind, M., H.Hocker, C.Wandrey, A.G.Jager. 1990. Strategies for improved lignin peroxidase production in agitated pellet cultures of *Phanerochaete chrysosporium* and the use of a novel inducer. FEMS Microbiol.letts.71:325-330.

Lin, Jian-Er, H.Y. Wang. 1990. Degradation kinetics of pentachlorophenol by *Phanerochaete chrysosporium*. Biotechnol.Bioeng.35:1125-1134

Linko, S. 1988. Production and characterization of extracellular lignin peroxidase from immobilized *Phanerochaete chrysosporium* in a 10-liter bioreactor.
Enzyme Microb.Technol. 10:410-417

Litchfield, J.H. 1977. Morel mushroom mycelium as a food flavoring material. Biotechnol.Bioeng. 9:289-304

Livernoche, D., L. Jurasek, M. Desrochers, and J. Dorica. 1983. Removal of color from Kraft mill wastewaters with cultures of white-rot fungi and with immobilized mycelium of Coriolus versicolor. Biotechnol. Bioeng. 25:2055-2065.

Lundquist, K., T. K. Kirk, and W. J. Connors. 1977. Fungal degradation of kraft lignin and lignin sulfonates prepared from synthetic 14C-lignins.
Arch. Microbiol. 112:291-296.

Maxwell, J.C. 1973. A Treatise on Electricity and Magnetism vol.1 . Clarendon Press, New York.

Messner, K., G. Ertler, and S. Jaklin-Faucher, P.Boskovsky, U.Regensberger, A.Blaha. 1989. Treatment of bleach plant effluents by the MYCOPOR system. in "Biotechnology in pulp and paper manufacture". pgs.245-251. T.K.Kirk and H.-M.Chang eds. Butterworth Heinemann, Boston.

Metz, B., N.W.F.Kosen. 1977. The growth of molds in the form of pellets- A literature review. Biotechnol.Bioeng.19:781-799.

Michel Jr., F.C. 1988. The development of a stirred tank reactor system for the production of lignin peroxidase by *Phanerochaete chrysosporium*. M.S. Thesis, Michigan State University.

Michel Jr., F.C., E.A.Grulke, C.A.Reddy. 1990. Development of a stirred tank reactor system for the production of lignin peroxidases (ligninases) by *Phanerochaete chrysosporium* BKM-F-1767. J.Indust.Microbiol.5:103-112.

Michel Jr., F.C., S.B.Dass, E.A.Grulke, C.A.Reddy. 1991. Role of manganese peroxidases (MNP) and lignin peroxidases (LIP) of *Phanerochaete chrysosporium* in the decolorization of kraft bleach plant effluent. Appl.Environ.Microbiol. 57:2368-2375.

Michel Jr., F.C., E.A.Grulke, C.A.Reddy. 1992a. Use of oxygen microelectrodes to determine the intrinsic respiration kinetics of mycelial pellets of *Phanerochaete chrysosporium*. Appl.Environ.Microbiol. (submitted).

Michel Jr., F.C., E.A.Grulke, C.A.Reddy. 1992b. Kinetic model for growth, substrate utilization and respiration by peroxidase producing mycelial pellet cultures of *Phanerochaete chrysosporium* J.of AiCHE (submitted).

Mileski, G.J., J.A.Bumpus, M.A.Jurek. S.D.Aust. 1988. Biodegradation of pentachlorophenol by the white-rot fungus *Phanerochaete chrysosporium*. Appl.Environ.Microbiol.54:2885-2889.

Miller, G.L. 1959. Use of dinitrosalicylic acid reagent for determination of reducing sugar. Anal.Chem. 31:426-428.

Moo-Young, M., T.Kobayashi. 1972. Effectiveness Factors for immobilized enzyme reactions. Can.J.Chem.Eng.50:162-166.

Morrin, M., O.P.Ward. 1989. Relationships between fungal growth, morphology and fumaric acid production by *Rhizopus arrhizus*. Mycological.Res. 95:?.

Naidu, P.S., C.A.Reddy. 1990. Nucleotide sequence of a new lignin peroxidase gene GLG3 from the white-rot fungus, *Phanerochaete chrysosporium*. Nucleic Acids Res.18:7173.

National Council of the Paper Industry for Air and Stream Improvement (NCASI). 1971. Tech. Bull. No. 253.

Paice, M. G., and L. Jurasek. 1984. Peroxidase-catalyzed color removal from bleach plant effluent. Biotechnol. Bioeng. 26:477-480.

Paszczynski, A., V.B.Huynh, R.Crawford. 1985. Enzymatic activities of an extracellular, manganese dependent peroxidase from *Phanerochaete chrysosporium*. FEMS Microbiol.Lett. 29:37-41.

Perez, J., and T. W. Jeffries. 1990. Mineralization of ^{14}C-ring-labeled synthetic lignin correlates with the production of lignin peroxidase, not of manganese peroxidase or laccase. Appl. Environ. Microbiol. 56:1806-1812.

Perry R.H., D.W.Green, J.O.Maloney. 1984. Perry's chemical engineers' handbook (6th ed.). McGraw-Hill, New York.

Phillips, D.H. 1966. Oxygen transfer into mycelial pellets. Biotech.Bioeng. 8:457-460.

Pirt, S.J. 1966. A theory of the mode of growth of fungi in the form of pellets in submerged culture. Proc.Roy.Soc. B166;369-373.

Prouty, A.L. 1990. Bench-scale development and evaluation of a fungal bioreactor for color removal from bleach effluents. Appl.Biotechnol.Bioeng.(submitted)

Reddy, C.A. 1984. Physiology and biochemistry of lignin degradation. in "Current Perspectives on Microbial Ecology"; eds. M.Klug and C.A.Reddy., American Society of Microbiology, Washington D.C.

Reid, I.D., K.A.Seifert. 1982. Effect of an atmosphere of oxygen on growth, respiration, and lignin degradation by white-rot fungi. Can.J.Bot.60:252-260.

Revsbech, N.P., D.M.Ward. 1983. Oxygen Microelectrode that is insensitive to medium chemical composition: use in an acid microbial mat dominated by *Cyanidium caldarium*. Appl.Environ.Microbiol.45:755-759.

Roy-Arcand,L., F.S.Archibald. 1991. Direct dechlorination of chlorophenolic compounds by laccases from *Trametes* (Coriolus) *versicolor*. Enzyme Microb.Technol.13:194-203

Royer, G., M.Desrochers, L.Jurasek, D.Rouleau, R.C.Mayer. 1985. Batch and continuous decolorisation of bleached kraft effluents by a white-rot fungus (*Coriolus versicolor*). J.Chem.Tech.Biotechnol. 35B:14-22

Schugerl, K., R.Wittler, T.Lorenz. 1983. The use of molds in pellet form. Trends in Biotechnol. 1(4):120-123.

Sodeck, G.J., J.Modl, J.Kominek, W.Salzbrun. 1981. Production of citric acid by the submerged fermentation process. Proc.Biochem. 16:9-11.

Springer, A. 1985. Industrial environmental control, pulp and paper industry, John Wiley & Sons, NY.

Sun, Y.B., T.W.Joyce, H-M.Chang. 1989. Dechlorination and decolorization of high molecular weight chlorolignin from bleach plant effluents by an oxidation process. Tappi J. Sept.1989, 209-213.

Sundman, G., T. K. Kirk, and H.-M. Chang. 1981. Fungal decolorization of kraft bleach plant effluent. Tappi J. 64:145-148.

Swaney, J.M. 1983. Rapid infiltration effluent colour removal system becomes operational at Skookumchuck. Preprints of the 69th Annual Meeting of the Canadian Pulp and Paper Association, technical section. Febuary 1&2, 1983, Montreal, Quebec.

Tien, M., T.K. Kirk. 1984. Lignin degrading enzyme from *Phanerochaete chrysosporium*: purification,characterization and catalytic properties of a unique H_2O_2 requiring oxygenase. Proc. Natl. Acad. Sci. USA81:2280-2284.

Tien, M., C.D.Tu. 1987. Cloning and sequencing of a cDNA for a ligninase from *Phanerochaete chrysosporium*. Nature 326:520-523.

Tonon, F., C.P.deCastro, E.Odier. 1990. Nitrogen and carbon regulation of lignin peroxidases and enzymes of nitrogen metabolism in *Phanerochaete chrysosporium*. Exper.Mycol. 14:243-254.

Trinci, A.P.J. 1970. Kinetics of the growth of mycelial pellets of *Aspergillus nidulans*. Arch.Mikrobiol.73:353-367.

Valli, K., and M. H. Gold. 1991. Degradation of 2,4-dichlorophenol by the lignin-degrading fungus *Phanerochaete chrysosporium*. J. Bacteriol. 173:345-352.

van Suijdam, J.C., H.Hols, N.W.F.Kosen. 1982. Unstructured model for growth of mycelial pellets in submerged cultures. Biotechnol.Bioeng. 24:177-191.

Whitaker, A., P.A.Long. 1973. Fungal Pelleting. Proc.Biochem.66:27-31.

Wilkinson, G.N. 1961. Statistical estimations in enzyme kinetics. Biochem J. 80:324-332.

Willershausen, H., A.Jager, H.Graf. 1987. Ligninase production of *Phanerochaete chrysosporium* by immobilization in bioreactors. J.Biotechnol. 6:239-243

Wittler, R., H. Baumgartl, D.W.Lubbers, K.Schugerl. 1986. Investigations of oxygen transfer into *Penicillium chrysogenum* pellets by microprobe measurements. Biotechnol.Bioeng. 28:1024-1036.

Yano T., T.Kodama, K.Yamada. 1961. Fundamental studies of fermentation VIII: Oxygen transfer into mycelial pellets. Agr.Biol.Chem.25:580.

Yin, C. F., T. W. Joyce, and H.-M. Chang. 1989. Kinetics of bleach plant effluent decolorization by *Phanerochaete chrysosporium*. J. Biotechnol. 10:67-76.

Yoshida T., H.Taguchi, S.Teramoto. 1968. Studies on submerged culture of Basidiomycetes (IV) Distributions of respiration and other metabolic activities in pellets of Shitake (*Lentinus edodes*). J.Ferment.Technol. 46:119-129.

Zhang, Y.Z., C.A.Reddy, A.Rasooly. 1991. Cloning of several lignin peroxidase (LIP) encoding genes. Gene 97:191-198.

APPENDICES

(see list of tables for index)

Appendix 1

Extracellular peroxidase activity in air flushed and oxygen flushed agitated cultures of *P. chrysosporium* as reported by Dosoretz *et al.*, 1990a.

Data for Figure 2.2

Time (h)	LIP activity (U/l)		MNP activity (U/l)	
	air	O_2	air	O_2
0	0.00	0.00	0.00	0.00
24	0.00	0.00	0.00	0.00
48	0.00	0.00	0.00	0.00
72	0.00	0.00	0.00	2.37
96	0.00	70.00	0.21	3.67
120	0.00	145.00	1.47	3.27
168	0.00	165.00	1.30	1.64
192	0.00	149.00	1.07	1.47
216	0.00	135.00	0.90	1.35
240	0.00	101.00	0.00	0.62
264	0.00	72.00	0.00	0.00
288	0.00			
312	0.00			

Appendix 2

Solubility of Synthetic BPE as a function of pH.

Data for Figure 4.1

Synthetic BPE	
pH	Color Units
3	1511
3.56	2022
4	2204
4.5	2749
5	3749
5.88	6669

Industrial BPE	
pH	Color Units
2.23	7079
2.95	11092
3.39	13887
3.85	13592[b]
4.53	14832[b]
5.10	14874[b]
5.85	14810[b]

[b] maximum possible soluble color 15000 C.U. (data not used).

Appendix 3

Effect of pH on the activity of lignin peroxidases and manganese peroxidases.

Data for Figure 4.2

pH	LIP activity	MNP activity	
	veratryl alcohol oxidation	Phenol Red assay	Remazol Blue assay
2.05	0.544	0.050	0.014
2.57	1.000	0.150	0.037
3.05	0.913	0.202	0.060
3.57	0.522	0.360	0.114
4.05	0.217	0.948	0.928
4.53	0.109	0.915	0.622
5.08	0.043	0.487	0.538
5.56	0.021	0.402	0.083
7.13	0.001	0.272	0.011

Appendix 4

Time course of nutrient nitrogen (ammonium), biomass (culture dry weight), glucose, soluble carbohydrate, extracellular protein, acetate and extracellular LIP and MNP activity in agitated control cultures of *P. chrysosporium* BKM-F-1767.

Data for Figure 5.1

Time (d)	Ammonium (mg/l)	Dry Weight (g/l)	Glucose (g/l)	pH
0.00	39.10	0.11	10.64	4.50
0.33	25.40	0.13	9.77	4.43
0.79	2.74	0.64	8.85	4.48
1.00	0.00	0.90	8.54	4.45
2.00		1.07	8.38	4.52
3.00		1.13	7.16	4.98
3.92		1.39	5.91	4.68
5.00		1.36	4.23	5.18
6.00		1.49	3.52	4.84
6.92		1.57	2.38	4.53
8.00		1.87	0.34	4.52
8.96		1.98	0.11	4.61
10.04		1.91	0.08	4.84
10.96		1.51	0.07	5.06
11.92		1.33		5.17
12.96		1.14		

Time (days)	MNP[a] (U/l)	S.D.	LIP[a] (U/l)	S.D.
1.8	0	0	0	0
2.7	774	681	0	0
3.7	1215	421	0	0
4.6	1423	743	15	20
5.6	1182	716	35	49
6.7	982	199	230	15
7.5	700	175	243	3
8.6	699	72	240	1
10.0	273	64	120	
10.7	10	0	69	
11.5			0	

[a] values are means for triplicate cultures on one occasion

Appendix 4 (cont.)

Time (d)	Glucose (g/m³)	Carbo-hydrates (g/m³)	pH	Acetate (mM)	Biomass (g/m³)
0.00	12290	12130	4.45	21.55	60
0.92	11800	11410	5.14	7.86	890
1.08	11850	10660	5.80	2.50	1100
2.04	10200	10160	3.59	0.71	1450
2.92	9970	9570	5.18	0.34	1580
3.88	8770	8280	5.37	1.10	1780
4.92	6840	6750	5.38	0.15	1690
6.00	4990	5250	5.30		1800
7.17	3400	4170	5.31		1920
7.33	2380	3070	5.43		1790
8.29	1290	1860	5.36		2060
8.92	560	760	5.27	0	2300
9.92	350	180	5.51		1950
11.08	200	40	5.55		1760

Time (d)	Protein (g/m³)	LIP (U/l)	MNP (U/l)
0.00	88.7		
0.92	25.9		
1.08	22.5		0
2.04	8.3		0
2.92	12.0	0	450
3.88	21.9	12	866
4.92	26.5	145	811
6.00	24.3	163	582
7.17	24.8	185	433
7.33	23.8	189	415
8.29	24.3	177	388
8.92	17.5	99	234
9.92	16.7	62	44
11.08	13.0	28	0

Appendix 5

Manganese concentration in soluble and insoluble fractions of cultures of *P. chrysosporium* with three initial soluble manganese concentrations as measured using atomic absorption spectrophotmetry. (S.D. = 1.4 ppm)

Time (days)	Mn soluble fraction (ppm)	Mn insoluble fraction (ppm)	total Mn (sum) (ppm)

0 ppm MnSO$_4$ added at inoculation.

Time (days)	Mn soluble fraction (ppm)	Mn insoluble fraction (ppm)	total Mn (sum) (ppm)
0	0.05	0.01	0.06
2	0.05	0.02	0.07
4	0.02	0.00	0.02
6	0.02	0.02	0.04
8	0.04	0.01	0.04

12 ppm MnSO$_4$ added at inoculation.

Time (days)	Mn soluble fraction (ppm)	Mn insoluble fraction (ppm)	total Mn (sum) (ppm)
0	13.16	0.09	13.25
1	13.30	0.25	13.54
2	11.03	0.52	11.55
3	11.95	0.75	12.70
4	11.19	1.05	12.24
5	7.63	4.57	12.20
6	3.53	8.79	12.32
7	4.36	6.31	10.67
8	3.52	7.04	10.56
9	2.06	8.91	10.97

40 ppm MnSO$_4$ added at inoculation.

Time (days)	Mn soluble fraction (ppm)	Mn insoluble fraction (ppm)	total Mn (sum) (ppm)
0	43.21	0.86	44.07
1	36.23	2.26	38.48
2	40.68	1.46	42.14
3	36.70	2.27	38.97
4	42.37	1.94	44.30
5	5.82	30.64	36.45
6	5.03	34.98	40.01
7	3.45	36.66	40.11
8	3.31	37.74	41.05
9	4.68	29.73	34.41

Appendix 6

Decolorization of BPE as a function of the day of BPE addition.
BPE was added to approximately 3,000 C.U. on days 2 through 8 and the 465 nm
absorbance (pH 7.6) was measured.

Data for Figure 6.3

Color Units (C.U.)

Hour	Day 2	Day 3	Day 4	Day 5	Day 6	Day 7	Day 8	uninoc.
24								2878
42	2491							2972
69	1579	2552						2972
90	1170	1575	2915					3048
113	871	999	1325	2681				3010
137	621	674	867	1030	2650			2991
160	465	522	662	723	1151	2692		2934
188	492	401	416	651	507	935	2851	3029
207	280	291	314.	412	386	541	1223	

Appendix 7

Decolorization, culture dry weight and carbon dioxide evolution by cultures of *P. chrysosporium* amended with synthetic and industrial Kraft bleach plant effluents (BPE).

Data for Figure 6.2

Time (days)	Industrial BPE Color (C.U.)	% residual	Synthetic BPE Color (C.U.)	% residual
4.00	2885 ± 398	100	3622 ± 85	100
4.10	2548 ± 187	42	2076 ± 114	38
4.88	1209 ± 18	28	1373 ± 36	26
5.71	819 ± 51	21	927 ± 102	19
7.25	614	18	699	17

Day	Biomass (g/l) No BPE	Industrial BPE	Synthetic BPE	CO_2 evolved (mM/dy) No BPE	Industrial BPE	Synthetic BPE
3				34.5	34.5	34.5
4	1.26	1.26	1.26	43.2	43.2	43.2
5	1.35	1.55	1.66	54.3	43.9	47.9
6	1.31	1.48	1.53	56.1	50.2	40.1
7	1.40	1.55	1.6	41.1	36.1	23.9

Appendix 8

Effect of nutrient nitrogen (39 and 390 g/m3) and manganese (0, 12 and 40 ppm) on the decolorization of BPE, the depletion of glucose and the production of extracellular peroxidases.

(Data for Figure 6.6 and 6.8)

Lignin Peroxidase Activity (U/l)

Time (days)	0.00	3.08	4.63	5.58	6.67
12 ppm Mn	0	0	15 ±20	35 ±49	230 ±14
0 ppm Mn	0	0	118 ±13	129 ±18	63 ±27
40 ppm Mn	0	0	0	0	9 ±9

Time (days)	6.67	7.50	8.58	9.96	10.67
12 ppm Mn	230 ±14	243 ±3	240 ±1	120 ±1	69
0 ppm Mn	63 ±27	41 ±9	22 ±6	20 ±14	11 ±3
40 ppm Mn	9 ±9	101 ±21	215 ± 2	91 ±23	67 ±19

Manganese Peroxidase Activity (U/l)

Time (days)	0.9	2.67	3.69	4.63	5.58
12 ppm Mn	0	1780 ±260	1370 ±40	2430	1990 ±30
0 ppm Mn	0	0	170 ±10	70 ±20	180 ±50
40 ppm Mn	0	730 ±800	1170 ±150	1370 ±20	1950 ±60

Time (days)	6.67	7.50	8.58	9.96	10.67
12 ppm Mn	1170 ±10	760 ±60	630 ±1	320 ±1	10 ±1
0 ppm Mn	430 ±80	280 ±80	500 ±90	230 ±80	220 ±10
40 ppm Mn	1380 ±20	1460 ±140	1400 ±30	100 ±40	70 ±110

Appendix 8

(cont.)

Color (C.U.)

Time (day)	3.83	4.04	4.50	5.00	5.58	5.92
Nitrogen Suff.	3329	2335	2210	2062		1954
12 ppm Mn	3618	2704	1954	1642	1431	1295
0 ppm Mn	3488	2937	2573	2545	2409	2579
40 ppm Mn	3738	2602	1812	1528	1437	1392

Time (dy)	6.67	7.50	8.79	9.96	16.50
Nitrogen Suff.	2039	1539	1812	1750	1982
12 ppm Mn	1233	943	880	795	250
0 ppm Mn	2374	1937	2187	2159	1522
40 ppm Mn	1159	1062	846	704	528

Glucose (g/l)

Time (days)	0	0.94	1.71	2.67	3.69	4.63
Nitrogen Suff.	10	7.9 +0.3	5.8 +0.1	2.2 +1.1	0.78 +0.1	0.24 +0.1
Low Nitrogen	10	8.5 +0.1	7.9 +0.1	6.5 +0.5	5.8 +0.1	5.6 +0.1

Time (days)	5.58	6.67	7.50	8.58	9.96	10.67
Nitrogen Suff.	1.1 +0.1	0.5 +0.1	0.6+0.1	0.7 +0.1	0.5 +0.1	0.5 +0.1
Low Nitrogen	4.7 +0.2	3.0 +0.2	2.3 +0.3	1.4	0.8	0.6

Appendix 9

Residual color (percent) in wild-type and mutant strain cultures of *P. chrysosporium* (3,000 color units added).

Data for Figure 6.11

Time after BPE addition (Days)	*per* mutant	*lip* mutant	ME-446	BKM-F-1767
0	100	100	100	100
1	101	63	50	41
2	92	52	38	31
5	90	43	26	21

Appendix 10

Time course of the natural log of culture dry weight divided by average initial culture dry weight (Ln [X/Xo,avg]) during lag and primary growth phases.

Data for Figure 5.3

Time	Ln [X/Xo,avg]	
		Line fit
(s)	Data	(μmax= 3.9 s^{-1})
0	-0.00467	-1.13848
0	-0.24106	-1.13848
0	-0.02237	-1.13848
0	0.118947	-1.13848
0	0.108557	-1.13848
28800	0.118947	-0.01056
28800	-0.01348	-0.01056
28800	-0.05873	-0.01056
28800	-0.02237	-0.01056
34128	0.249567	0.198105
34992	0.242056	0.231942
48600	0.692856	0.764884
55800	0.784587	1.046864
68688	1.72232	1.551608
68340	1.399019	1.540329
68170	1.708023	1.531305
75600	1.401172	1.822308
86400	2.066737	2.245278
86400	2.165689	2.211441
86400	2.169885	2.279116

Appendix 11

Pellet characteristcis in nitrogen limited agitated culture of *P. chrysosporium*

Data for Figure 5.4

Time (h)	Pellet[a] Radius (mm)	Time (h)	Pellet Number m^{-3}
22	0.795 ± 0.13	22	7674
26	0.786 ± 0.14	26	6953
49	0.813 ± 0.13	49	7980
49	0.783 ± 0.13	49	5552
70	0.796 ± 0.14	70	6830
118	0.783 ± 0.15	70	7316
144	0.877 ± 0.14	118	9635
172	0.847 ± 0.10	144	7716
176	0.935 ± 0.20	172	7472
199	0.913 ± 0.14	176	6329
199	0.808 ± 0.11	199	7694
214	0.897 ± 0.17	199	4982
214	1.010 ± 0.26	214	7597
238	0.955 ± 0.20	214	6305
266	1.039 ± 0.15	238	8317
		263	8780
		Mean=	7320 ± 1129

[a] values are averages ± one standard deviation for a group of twenty pellets.

Appendix 12

Oxygen concentration profiles in mycelial pellets of *P. chrysosporium*.
Experimental data for pellets grown in nitrogen-limited medium and removed at the time indicated. Values at the top of each column represent the diameters of the individual mycelial pellets. Values were determined using an oxygen microelectrode.

DAY 1

Depth (mm)	2.15 mm O_2 (g/m^3)	1.85 mm O_2 (g/m^3)	1.65 mm O_2 (g/m^3)
0.00	6.61	6.84	6.80
0.05	5.17	5.99	6.06
0.10	3.42	4.35	4.28
0.15	2.33	2.88	2.95
0.20	1.48	1.63	2.02
0.25	0.86	0.70	1.09
0.30	0.31	0.16	0.54
0.35	0.08	0.00	0.16

Depth (mm)	1.85 mm O_2 (g/m^3)
0.00	6.84
0.06	5.83
0.08	5.05
0.10	4.59
0.13	3.65
0.18	2.57
0.23	1.56

DAY 2

Depth (mm)	2.35 mm O_2 (g/m^3)	2.30 mm O_2 (g/m^3)	1.55 mm O_2 (g/m^3)	1.15 mm O_2 (g/m^3)	2.10 mm O_2 (g/m^3)	1.65 mm O_2 (g/m^3)	2.00 mm O_2 (g/m^3)
0.00	6.34	6.92	6.73	6.54	6.73	6.73	6.73
0.05	5.38	5.38	5.96	5.38	5.77	4.81	5.38
0.10	4.23	4.23	5.19	3.27	3.84	3.08	4.04
0.15	3.27	3.27	4.23	1.54	1.92	1.73	2.31
0.20	2.31	2.31	3.65	0.77	0.77	0.77	1.35
0.25	1.54	1.35	2.88	0.19	0.38	0.38	0.58
0.30		0.58	2.50	0.00	0.00	0.00	0.00
0.40		0.19	1.73				
0.45		0.00	0.00				

Appendix 12 (cont.)

DAY 4

Depth (mm)	1.85 mm O_2 (g/m^3)	1.85 mm O_2 (g/m^3)	2.20 mm O_2 (g/m^3)	2.20 mm O_2 (g/m^3)
0.00	6.69	6.40	6.72	6.44
0.05	5.84	5.46	5.59	5.02
0.10	4.28	3.86	4.17	3.69
0.15	2.78	2.45	2.93	2.56
0.20	1.62	1.41	1.98	1.69
0.25	0.75	0.59	1.12	0.95
0.30	0.19	0.19	0.56	0.47
0.35	0.02	0.00	0.20	0.19
0.40	0.00		0.05	0.00
0.45			0.00	

DAY 5

Depth (mm)	1.65 mm O_2 (g/m^3)	2.35 mm O_2 (g/m^3)	1.85 mm O_2 (g/m^3)	2.35 mm O_2 (g/m^3)
0.00	6.92	6.92	6.23	6.46
0.05		5.67	4.84	5.44
0.10	5.44	4.06	3.51	4.43
0.15	4.80	2.86	2.31	3.51
0.20	3.60	1.98	1.38	2.77
0.25	2.49	1.15	0.55	1.75
0.30	1.61	0.60	-0.09	1.01
0.35	0.92	0.05	0.00	0.28
0.40	0.74			-0.09

DAY 12

Depth (mm)	2.65 mm O_2 (g/m^3)	2.65 mm O_2 (g/m^3)
0.00	6.00	6.40
0.05	5.80	6.20
0.10	5.60	5.80
0.15	5.40	5.60
0.20	5.30	5.45
0.25	4.90	5.40
0.30	4.60	5.30
0.35	4.40	5.00
0.40	4.20	4.90

Appendix 13

Carbon dioxide evolution and Oxygen depletion in mycelial pellet cultures of P. chrysosporium.

Data for Figure 5.6

CO_2 evolved

Time (days)	Data (g)	Model (g)
1	0.0914	0.0229
2	0.1076	0.1043
3	0.1238	0.1137
4	0.1361	0.1218
5	0.1456	0.1283
6	0.1264	0.1329
7	0.1365	0.1351
8	0.1336	0.1325
9	0.1092	0.1139
10	0.0585	0.0531
11	0.0266	0.0369
12	0.0245	0.0297
13		0.0239

Data for Figure 5.1c

Time (Days)	CO_2 evolved (g/m^3 media /dy)	O_2 depleted (g/m^3 media /dy)
0.92	1207	
2.04	1420	
2.92	1633	
3.88	1796	1418
4.92	1922	1525
6.00	1668	1155
7.17	1802	1054
8.29	1763	1093
8.92	1441	1267
9.92	772	553
10.96	352	382
12.00	323	103

Appendix 14

Respirometer Data for agitated cultures of *P. chrysosporium*.

(C_l = oxygen concentration in media, g/m^3)

(v = oxygen uptake rate by whole culture, $g\ O_2/\ m^3$ media/ s)

Data for Figure 5.8

time = 19 hours		43 hours		69 hours		91 hours	
C_l (g/m^3)	v ($g/m^3/s$)	C_l (g/m^3)	v ($g/m3/s$)	C_l (g/m^3)	v ($g/m^3/s$)	C_l (g/m^3)	v ($g/m^3/s$)
14.50	0.0183	13.10	0.0142	6.26	0.0126	29.33	0.0146
13.18	0.0172	10.55	0.0137	5.36	0.0114	26.70	0.0133
12.03	0.0155	8.16	0.0126	4.61	0.0097	24.56	0.0119
10.96	0.0137	6.02	0.0105	3.96	0.0086	22.41	0.0128
10.05	0.0132	4.37	0.0086	3.38	0.0080	19.94	0.0142
9.06	0.0126	2.92	0.0069	2.80	0.0065	17.30	0.0151
8.24	0.0114	1.90	0.0047	2.44	0.0052	14.50	0.0142
7.42	0.0103	1.24	0.0037	2.06	0.0043	12.20	0.0137
6.76	0.0103			1.81	0.0029	9.56	0.0146
5.93	0.0103			1.65	0.0023	6.92	0.0137
5.27	0.0086			25.91	0.0137	4.61	0.0119
4.70	0.0080			23.45	0.0141	2.64	0.0092
4.12	0.0080			20.83	0.0150	1.32	0.0073
3.54	0.0074			18.04	0.0150		
3.05	0.0063			15.41	0.0146		
2.64	0.0057			12.79	0.0146		
2.22	0.0052			10.17	0.0146		
1.90	0.0040			7.54	0.0128		
1.65	0.0034			5.58	0.0109		
1.40	0.0034			3.61	0.0091		
				2.30	0.0061		
				1.41	0.0049		

Wilkinson's Method

$Vmax_{app}$	$Vmax_{app}$	$Vmax_{app}$	$Vmax_{app}$
0.075 + 0.027	0.035 + 0.003	0.021 + 0.001	0.018 + 0.001

Km_{app}	Km_{app}	Km_{app}	Km_{app}
23.3 + 10.0	15.2 + 2.3	6.3 + 0.5	3.9 + 0.6

Appendix 14 (cont.)

time = 116 hours		143 hours		164 hours		212 hours	
C_l (g/m^3)	v (g/m3/s)	C_l (g/m^3)	v (g/m3/s)	C_l (g/m^3)	v (g/m^3/s)	C_l (g/m^3)	v (g/m^3/s)
29.33	0.0146	19.12	0.0146	19.45	0.0128	8.90	0.0174
26.70	0.0133	16.48	0.0151	17.14	0.0133	5.77	0.0149
24.56	0.0119	13.68	0.0156	14.67	0.0137	3.54	0.0103
22.41	0.0128	10.88	0.0156	12.20	0.0137	2.06	0.0064
19.94	0.0142	8.08	0.0151	9.72	0.0151	1.24	0.0046
17.30	0.0151	5.44	0.0137	6.76	0.0156	12.85	0.0275
14.50	0.0142	3.13	0.0110	4.12	0.0119	7.91	0.0238
12.20	0.0137	1.48	0.0073	2.47	0.0087	4.28	0.0169
9.56	0.0146	0.49	0.0055	0.99	0.0082	1.81	0.0110
6.92	0.0137					0.33	0.0082
4.61	0.0119						
2.64	0.0092						
1.32	0.0073						

Wilkinson's Method

Vmax$_{app}$	Vmax$_{app}$	Vmax$_{app}$	Vmax$_{app}$
0.015 + 0.001	0.017 + 0.001	0.014 + 0.001	0.044 + 0.011

Km$_{app}$	Km$_{app}$	Km$_{app}$	Km$_{app}$
1.4 + 0.2	1.4 + 0.3	1.0 + 0.4	8.1 + 4.0

234 hours		260 hours		284 hours		332 hours	
C_l (g/m³)	v (g/m3/s)	C_l (g/m³)	v (g/m³/s)	C_l (g/m³)	v (g/m³/s)	C_l (g/m³)	v (g/m3/2)
14.17	0.0064	20.44	0.0073	28.68	0.0087	21.75	0.0069
11.87	0.0066	17.80	0.0064	25.54	0.0085	19.28	0.0069
9.39	0.0066	15.82	0.0053	22.58	0.0080	16.81	0.0062
7.09	0.0066	14.01	0.0053	19.78	0.0080	14.83	0.0053
4.61	0.0066	12.03	0.0057	16.81	0.0082	13.02	0.0050
2.31	0.0064	9.89	0.0062	13.84	0.0078	11.21	0.0050
18.46	0.0101	7.58	0.0066	11.21	0.0073	9.39	0.0050
14.83	0.0096	5.11	0.0069	8.57	0.0069	7.58	0.0050
11.54	0.0092	2.64	0.0060	6.26	0.0066	5.77	0.0050
8.24	0.0087	0.82	0.0050	3.79	0.0064	3.96	0.0048
5.27	0.0082	28.35	0.0096	1.65	0.0060	2.31	0.0046
2.31	0.0066	24.88	0.0089	14.01	0.0073	0.66	0.0046
0.49	0.0050	21.92	0.0080	11.37	0.0071	17.14	0.0050
		19.12	0.0073	8.90	0.0066	15.33	0.0048
		16.64	0.0071	6.59	0.0066	13.68	0.0048
		14.01	0.0071	4.12	0.0066	11.87	0.0050
		11.54	0.0066	1.81	0.0053	10.05	0.0050
		9.23	0.0066	0.33	0.0041	8.24	0.0050
		6.76	0.0066			6.43	0.0048
		4.45	0.0064			4.78	0.0048
		2.14	0.0055			2.97	0.0048
		0.49	0.0046			1.32	0.0046

Wilkinson's Method

Vmax$_{app}$	Vmax$_{app}$	Vmax$_{app}$	Vmax$_{app}$
0.009 + 0.001	0.007 + 0.002	0.008 + 0.001	0.007 + 0.000

Km$_{app}$	Km$_{app}$	Km$_{app}$	Km$_{app}$
1.1 + 0.7	0.3 + 0.1	1.0 + 0.2	0.1 + 0.1

Appendix 14 (cont.)

time = 72 hours		96 hours		120 hours	
C_l g/m^3	v $g/m^3/s$	C_l g/m^3	v $g/m^3/s$	C_l g/m^3	v $g/m^3/s$
16.20	0.01918	7.34	0.01111	25.79	0.01463
14.82	0.01854	5.33	0.01032	23.15	0.01463
13.53	0.01598	3.62	0.00847	20.52	0.01488
12.52	0.01343	2.29	0.00635	17.80	0.01614
11.60	0.01279	1.33	0.00450	14.71	0.01665
10.68	0.01279	0.67	0.00291	11.80	0.01564
9.76	0.01215	0.29	0.00159	9.08	0.01463
8.93	0.01151	0.10	0.00106	6.54	0.01236
8.10	0.01151	6.57	0.01085	4.63	0.00984
7.27	0.01087	4.62	0.00995	3.00	0.00757
6.54	0.01023	2.99	0.00786	10.08	0.01816
5.80	0.00959	1.79	0.00566	6.81	0.01488
5.16	0.00927	0.95	0.00386	4.72	0.01059
4.47	0.00831	0.40	0.00238	3.00	0.00832
3.96	0.00799	0.10	0.00169	7.26	0.01261
3.31	0.00831	14.19	0.01641	4.99	0.01135
2.76	0.00703	11.24	0.01614	3.18	0.00878
2.30	0.00639	8.38	0.01588	1.83	0.00605
1.84	0.00575	5.53	0.01402	1.00	0.00391
1.47	0.00511	3.33	0.01045	0.43	0.00214
1.10	0.00448	1.76	0.00725	0.23	0.00073
0.83	0.00384	0.72	0.00437	0.16	0.00035
0.55	0.00320	0.19	0.00296	1.73	0.00580
0.37	0.00192	10.38	0.01588	0.91	0.00353
0.28	0.00160	7.53	0.01429	0.45	0.00189
11.14	0.00972	5.24	0.01191	0.23	0.00126
9.39	0.01023	3.24	0.00979	1.91	0.00530
7.46	0.01023	1.71	0.00701	1.09	0.00353
5.71	0.00895	0.71	0.00423	0.64	0.00189
4.24	0.00742	0.19	0.00291	0.41	0.00126
3.04	0.00639				
1.93	0.00511				
1.20	0.00358				
0.64	0.00243				
0.32	0.00128				

Wilkinson's Method			
$V_{max\,app}$	0.022 + 0.008	0.022 + 0.001	0.019 + 0.001
Km_{app}	8.0 + 1.2	4.3 + 0.6	3.7 + 0.5

Appendix 14 (cont.)

144 hours		168 hours		192 hours	
C_l g/m^3	v $g/m^3/s$	C_l g/m^3	v $g/m^3/s$	C_l g/m^3	v $g/m^3/s$
25.80	0.01635	7.25	0.01555	12.18	0.02055
24.63	0.01700	4.45	0.01308	10.70	0.02149
23.35	0.01635	2.55	0.00919	9.08	0.02009
22.27	0.01700	1.15	0.00601	7.80	0.01822
20.91	0.01471	0.38	0.00424	6.46	0.01775
20.15	0.01700	24.82	0.00177	5.25	0.01588
18.46	0.02158	24.69	0.00265	4.17	0.01401
17.05	0.01929	24.43	0.00619	3.23	0.01215
15.68	0.01897	23.80	0.01149	2.42	0.00981
14.31	0.01929	22.78	0.01502	1.82	0.00794
12.90	0.01691	21.63	0.01591	1.28	0.00701
5.79	0.01588	20.49	0.01856	0.81	0.00514
4.90	0.01144	18.96	0.02298	0.54	0.00346
4.14	0.01046	17.18	0.02474	0.31	0.00318
3.39	0.00981	15.40	0.02519	27.58	0.01495
2.73	0.00948	13.55	0.02563	26.50	0.01635
2.02	0.00817	11.71	0.02563	25.22	0.01775
1.55	0.00621	9.86	0.02474	23.95	0.01728
1.13	0.00490	8.14	0.02298	22.74	0.01962
0.85	0.00392	6.55	0.02121	21.12	0.02149
0.57	0.00392	5.09	0.01944	19.64	0.02055
6.45	0.01635	3.75	0.01679	18.16	0.02149
5.27	0.01570	2.67	0.01370	16.55	0.02242
4.19	0.01419	1.78	0.01060	14.93	0.02242
3.23	0.01243	1.15	0.00751	13.32	0.02336
2.40	0.01053	0.70	0.00557	11.57	0.02336
1.71	0.00844	0.34	0.00353	9.96	0.02242
1.19	0.00661	0.19	0.00212	8.34	0.02055
0.76	0.00562	18.45	0.02563	7.00	0.01868
0.38	0.00536	16.61	0.02519	5.65	0.01775
9.51	0.01831	14.83	0.02519	4.44	0.01495
8.19	0.01962	12.98	0.02519	3.50	0.01308
6.69	0.01962	11.20	0.02519	2.56	0.01121
5.37	0.01766	9.35	0.02430	1.88	0.00888
4.14	0.01635	7.70	0.02165	1.28	0.00747

Wilkinson's Method			
$Vmax_{app}$	0.021 + 0.001	0.032 + 0.001	0.029 + 0.001
Km_{app}	2.0 + 0.3	3.5 + 0.3	4.2 + 0.3

Appendix 14

Calculated values of Vmax in units of $\left[\dfrac{g\,O_2}{m^3\,s}\right]$ from units of $\left[\dfrac{g\,O_2}{m^3\,media\ s}\right]$.

Day	Vmax app g/m^3 media/s	Km app g/m^3	Vmax g/m^3/s	X (g/m^3)
1	0.075	23.00	*	
2	0.035	15.00	*	
3	0.022	8.00	0.97	1250
3	0.021	6.31	0.84	1375
4	0.022	4.30	0.88	1375
4	0.018	3.87	0.66	1500
5	0.019	3.69	0.70	1500
5	0.015	1.35	0.51	1625
6	0.021	2.07	0.71	1625
6	0.017	1.36	0.52	1750
7	0.032	3.52	1.00	1750
7	0.014	0.91	0.41	1875
8	0.029	4.23	0.85	1875
9	0.044	8.10	1.21	2000
10	0.009	1.08	*	*
11	0.007	0.33	*	*
12	0.008	0.97	*	*
14	0.007	0.07	*	*

mean Vmax	0.77 ± 0.23

* data not used. Only data for secondary metabolism was considered.

Appendix 15

Model test cases.

Experimental data for Figure 5.9

Condition 1

Time (h)	Glucose (g/m^3)	Dry Weight (g/m^3)
0	5689	90
7.92	4954	108
18.9984	4033	464
24	3268	998.8
48	2837	1052
72	2008	1236
93.84	918	1416
120	78.6	1370
144	13.1	1215
150	25	1239
165.84	15	1125
192		1080
214.8		818
240		666
285.84		602

Condition 2

Time (h)	Glucose (g/m^3)	Dry Weight (g/m^3)
0	10600	114
8	9770	129
19	8840	641
24	8540	904
48	8380	1071
72	7160	1133
94	5910	1388
120	4230	1359
144	3520	1493
150	2960	
165	2370	1571
192	339	1865
215	114	1984
240	80	1910
263	60	1512
311		1140

Appendix 15 (cont.)

Condition 2

Time (h)	Ammonium (g/m^3)	Glucose (g/m^3)	Dry Weight (g/m^3)
0	33.3	10090	129
10	23.7		147
28	1.3	9790	705
38	0		874
53		8960	1223
67			1240
76		9276	
98		7109	1333
120		6227	1373
149			1440
168		4729	1513
192		3293	
222		1539	1736
245		547	
262		238.9	2017
285		54	
338			1521
432			1247

Condition 3

Time (h)		Glucose (g/m^3)	Dry Weight (g/m^3)
0		17520	112
8		14980	113
19		14470	632
24		13280	1003
48		14400	1107
72		12290	1220
94		10700	1475
120		10480	1632
144		7760	1477
150		7450	
166		6730	1584
192		5290	1823
215		4170	1952
240		2900	2129
263		1700	
286		660	2548
311		327	
336			1980

Appendix 15 (cont.)

Condition 4

Time (h)	Ammonium (g/m^3)	Glucose (g/m^3)	Dry Weight (g/m^3)
0	2.89	11090	118
9	2.05		114
28	2.26	10380	174
38			131.8
53		10100	275.3
67			90.5
76		10732	
98		9997	261.2
120		10900	400
168		9755	476.5
192		9400	
222		8970	
245		9050	
262		8950	
285		9090	742.3
310.		8830	
337		8102	
432		7900	906

Condition 5

Time (h)	Ammonium (g/m^3)	Glucose (g/m^3)	Dry Weight (g/m^3)
0	117	11000	127.7
10	102		145.9
28	10.6	8993	1180
38	2.49		2202
53	1	7260	2568
67	1.14		2660
76	0	6250	2805
98		5375	2952
120		3383	3430
149			3480
168		573	4006
192		74	
222		80	2879
262			2496
338			2094
432			1739

Appendix 16

Sample output from shake flask simulation computer program.

Model data for Figure 5.9, Condition 2

Model parameter values

Ynx	μmax	Vmax	Km	fr	fx	fpg	Kaut	η	ρ	De
0.048	0.000039	0.76	0.5	0.84	0.12	0.04	2.5E-06	7320000	65000	2.9E-09

T h	N g/m^3	G g/m^3	X g/m^3	$E_{m.m.}$	C_1 g/m^3	O_2total g	CO_2 g	R m	pG g/m^3
4	39	11000	100	1	32.75	0.20709	0.00194	0.000369	0
8	39	11000	100	1	32.53	0.20568	0.003878	0.000369	0
12	35.2	10911	174.55	0.989	32.22	0.20375	0.006537	0.000444	0
16	28.5	10755	304.1	0.98818	31.69	0.20039	0.011153	0.000534	0
20	16.9	10485	529.55	0.9873	30.77	0.19455	0.019179	0.000643	0
24	-3.2	10015	921.6	0.98619	32.98	0.2085	0.033109	0.000773	0
28	0	9859.1	940.29	0.98666	31.01	0.19608	0.017077	0.000778	6.2312
32	0	9700.5	959.32	0.98573	29.01	0.18344	0.034456	0.000784	12.573
36	0	9539.3	978.67	0.98402	26.98	0.17058	0.052138	0.000789	19.024
40	0	9376.8	998.17	0.95477	24.93	0.15763	0.06995	0.000794	25.523
44	0	9217.8	1017.3	0.9084	22.92	0.14495	0.087386	0.000799	31.884
48	0	9064.4	1035.6	0.98737	32.98	0.2085	0	0.000804	38.016
52	0	8890.1	1056.6	0.98646	30.78	0.1946	0.019108	0.000809	44.988
56	0	8712.9	1077.8	0.98353	28.54	0.18047	0.038543	0.000815	52.08
60	0	8534.8	1099.2	0.95094	26.3	0.16627	0.058065	0.00082	59.202
64	0	8361.1	1120	0.90195	24.11	0.15242	0.077107	0.000825	66.149
68	0	8194.6	1140	0.8449	22.01	0.13914	0.095364	0.00083	72.809
72	0	8036.6	1159	0.98729	32.98	0.2085	0	0.000835	79.129
76	0	7842.7	1182.3	0.98532	30.53	0.19304	0.021261	0.00084	86.887
80	0	7647.7	1205.7	0.95336	28.07	0.17749	0.042641	0.000846	94.687
84	0	7457.5	1228.5	0.9035	25.67	0.16233	0.06349	0.000851	102.29
88	0	7275.5	1250.3	0.84507	23.38	0.14781	0.08345	0.000856	109.58
92	0	7103.5	1271	0.78272	21.21	0.13409	0.10231	0.000861	116.45
96	0	6942.3	1290.3	0.98721	32.98	0.2085	0	0.000865	122.9
100	0	6729.4	1315.9	0.96161	30.29	0.19153	0.023338	0.000871	131.42
104	0	6521.1	1340.9	0.91287	27.67	0.17492	0.046179	0.000876	139.75
108	0	6321.5	1364.8	0.85413	25.15	0.159	0.068062	0.000881	147.73
112	0	6133	1387.4	0.79076	22.77	0.14397	0.088731	0.000886	155.27
116	0	5956.9	1408.5	0.72612	20.55	0.12993	0.10804	0.000891	162.32

Appendix 16 (cont.)

T (h)	N	G (g/m³)	X (g/m³)	$E_{m.m.}$	C_l (g/m³)	O_2total (g)	CO_2 (g)	R (m)	pG (g/m³)
116	0	5956.9	1408.5	0.72612	20.55	0.12993	0.10804	0.000891	162.32
120	0	5793.6	1428.2	0.97372	32.98	0.2085	0	0.000895	168.85
124	0	5565.9	1455.5	0.92881	30.11	0.19035	0.024955	0.000901	177.96
128	0	5347.2	1481.7	0.87121	27.35	0.17291	0.04894	0.000906	186.71
132	0	5140.3	1506.5	0.80762	24.74	0.15641	0.071626	0.000911	194.98
136	0	4947	1529.7	0.74201	22.30	0.14099	0.09282	0.000916	202.71
140	0	4768.2	1551.2	0.67697	20.05	0.12673	0.11243	0.00092	209.87
144	0	4603.6	1571	0.94861	32.98	0.2085	0	0.000924	216.45
148	0	4365	1599.6	0.8942	29.97	0.18948	0.026152	0.000929	225.99
152	0	4138.8	1626.7	0.83166	27.12	0.17144	0.050959	0.000935	235.04
156	0	3927.1	1652.1	0.76589	24.45	0.15456	0.07417	0.000939	243.51
160	0	3731.2	1675.6	0.7	21.98	0.13893	0.095657	0.000944	251.35
164	0	3551.3	1697.2	0.63599	19.71	0.12459	0.11538	0.000948	258.54
168	0	3387	1716.9	0.9204	32.98	0.2085	0	0.000952	265.11
172	0	3142.3	1746.3	0.86087	29.894	0.18899	0.026826	0.000957	274.9
176	0	2913	1773.8	0.79647	27.002	0.1707	0.05197	0.000962	284.07
180	0	2700.6	1799.3	0.73098	24.323	0.15377	0.075257	0.000966	292.57
184	0	2505.8	1822.7	0.66683	21.86	0.13823	0.096623	0.000971	300.36
188	0	2328.4	1844	0.60554	19.62	0.12408	0.11608	0.000974	307.46
192	0	2167.3	1863.3	0.89199	32.98	0.2085	0	0.000978	313.9
196	0	1925.9	1892.3	0.83163	29.93	0.18925	0.026473	0.000983	323.56
200	0	1703	1919	0.76933	27.12	0.17148	0.050904	0.000987	332.47
204	0	1499.7	1943.4	0.70797	24.56	0.15527	0.073197	0.000992	340.6
208	0	1316	1965.5	0.64938	22.24	0.14061	0.093347	0.000995	347.96
212	0	1151.1	1985.2	0.59465	20.16	0.12747	0.11142	0.000999	354.55
216	0	1003.9	2002.9	0.8657	32.98	0.2085	0	0.001002	360.44
220	0	794.1	2028.1	0.81309	30.33	0.19177	0.022998	0.001006	368.83
224	0	610.49	2050.1	0.76309	28.02	0.17713	0.043128	0.00101	376.17
228	0	454.13	2068.9	0.71802	26.05	0.16467	0.060269	0.001013	382.43
232	0	325.35	2084.3	0.67938	24.42	0.1544	0.074387	0.001015	387.58
236	0	223.58	2096.6	0.64795	23.14	0.14629	0.085544	0.001017	391.65

Appendix 16 (cont.)

T (h)	N	G (g/m^3)	X (g/m^3)	$E_{m.m.}$	C_l (g/m^3)	O_2total (g)	CO_2 (g)	R (m)	pG (g/m^3)
240	0	146.97	2105.7	0.84707	32.98	0.2085	0	0.001019	394.72
244	0	76.158	2114.2	0.8298	32.08	0.20286	0.007761	0.00102	397.55
248	0	0	2069.2	1	31.18	0.19712	0.015648	0.00102	375.02
252	0	0	2025.7	1	30.31	0.19159	0.023255	0.00102	353.29
256	0	0	1983.8	1	29.46	0.18625	0.030592	0.00102	332.34
260	0	0	1943.4	1	28.65	0.1811	0.037669	0.00102	312.13
264	0	0	1904.4	1	32.98	0.2085	0	0.00102	292.63
268	0	0	1866.8	1	32.22	0.20371	0.006583	0.00102	273.83
272	0	0	1830.5	1	31.49	0.1991	0.012931	0.00102	255.7
276	0	0	1795.6	1	30.79	0.19464	0.019055	0.00102	238.21
280	0	0	1761.8	1	30.11	0.19035	0.02496	0.00102	221.34
284	0	0	1729.3	1	29.45	0.1862	0.030657	0.00102	205.07
288	0	0	1697.9	1	32.98	0.2085	0	0.00102	189.38
292	0	0	1667.6	1	32.37	0.20465	0.005299	0.00102	174.25
296	0	0	1638.4	1	31.78	0.20093	0.010409	0.00102	159.65
300	0	0	1610.3	1	31.21	0.19735	0.015338	0.00102	145.57
304	0	0	1583.1	1	30.67	0.19389	0.020092	0.00102	131.99
308	0	0	1556.9	1	30.14	0.19055	0.024677	0.00102	118.9
312	0	0	1531.7	1	32.98	0.2085	0	0.00102	106.27
316	0	0	1507.3	1	32.48	0.2054	0.004265	0.00102	94.086
320	0	0	1483.8	1	32.02	0.20241	0.008379	0.00102	82.336
324	0	0	1461.2	1	31.56	0.19952	0.012346	0.00102	71.004
328	0	0	1439.3	1	31.12	0.19674	0.016173	0.00102	60.075
332	0	0	1418.2	1	30.69	0.19405	0.019864	0.00102	49.533
336	0	0	1397.9	1	32.98	0.2085	0	0.00102	39.366
340	0	0	1378.3	1	32.58	0.206	0.003433	0.00102	29.56
344	0	0	1359.4	1	32.20	0.20359	0.006744	0.00102	20.103
348	0	0	1341.1	1	31.84	0.20127	0.009938	0.00102	10.981

Appendix 17

Oxygen effectiveness factor as a function of mycelial pellet radius and liquid phase oxygen concentration

Data for Figure 5.12

Oxygen Concentration (g/m³)

R (m)	1.0	2.0	3.0	4.0	5.0	6.0	7.0	8.0	9.0	10.0	11.0
0.00005	0.990	0.997	0.999	0.999	1.000	1.000	1.000	1.000	1.000	1.000	1.000
0.0001	0.964	0.989	0.995	0.997	0.998	0.999	0.999	0.999	0.999	1.000	1.000
0.00015	0.931	0.978	0.989	0.994	0.996	0.997	0.998	0.998	0.999	0.999	0.999
0.0002	0.713	0.965	0.983	0.990	0.993	0.995	0.996	0.997	0.998	0.998	0.999
0.00025	0.536	0.841	0.975	0.985	0.990	0.993	0.995	0.996	0.997	0.997	0.998
0.0003	0.420	0.664	0.869	0.980	0.986	0.990	0.993	0.994	0.995	0.996	0.997
0.00035	0.341	0.531	0.711	0.862	0.968	0.988	0.991	0.993	0.994	0.995	0.996
0.0004	0.285	0.435	0.584	0.722	0.841	0.936	0.988	0.991	0.993	0.994	0.995
0.00045	0.244	0.364	0.487	0.605	0.715	0.814	0.897	0.961	0.991	0.993	0.994
0.0005	0.212	0.310	0.412	0.513	0.610	0.700	0.783	0.857	0.920	0.968	0.993
0.00055	0.188	0.268	0.354	0.440	0.524	0.605	0.681	0.752	0.817	0.876	0.926
0.0006	0.168	0.235	0.308	0.381	0.454	0.525	0.594	0.660	0.722	0.780	0.833
0.00065	0.152	0.209	0.271	0.334	0.398	0.460	0.522	0.581	0.638	0.692	0.744
0.0007	0.138	0.187	0.240	0.295	0.351	0.406	0.461	0.514	0.566	0.616	0.664
0.00075	0.127	0.169	0.215	0.263	0.312	0.361	0.410	0.458	0.505	0.550	0.595
0.0008	0.117	0.154	0.194	0.237	0.280	0.324	0.367	0.410	0.452	0.494	0.534
0.00085	0.109	0.141	0.176	0.214	0.253	0.291	0.330	0.369	0.407	0.445	0.482
0.0009	0.102	0.130	0.161	0.195	0.229	0.264	0.299	0.334	0.369	0.403	0.437
0.00095	0.095	0.120	0.148	0.178	0.209	0.241	0.272	0.304	0.336	0.367	0.398
0.001	0.089	0.112	0.137	0.164	0.192	0.220	0.249	0.278	0.306	0.335	0.364
0.00105	0.084	0.104	0.127	0.151	0.176	0.202	0.228	0.255	0.281	0.307	0.333
0.0011	0.080	0.098	0.118	0.140	0.163	0.187	0.211	0.235	0.259	0.283	0.307
0.00115	0.076	0.092	0.110	0.130	0.151	0.173	0.195	0.217	0.239	0.261	0.283
0.0012	0.072	0.086	0.103	0.122	0.141	0.161	0.181	0.201	0.222	0.242	0.263
0.00125	0.069	0.082	0.097	0.114	0.131	0.150	0.168	0.187	0.206	0.225	0.244
0.0013	0.066	0.078	0.091	0.107	0.123	0.140	0.157	0.175	0.192	0.210	0.227
0.00135	0.063	0.074	0.086	0.101	0.116	0.131	0.147	0.163	0.180	0.196	0.212
0.0014	0.060	0.070	0.082	0.095	0.109	0.123	0.138	0.153	0.168	0.184	0.199
0.00145	0.058	0.067	0.078	0.090	0.103	0.116	0.130	0.144	0.158	0.172	0.187
0.0015	0.056	0.064	0.074	0.085	0.097	0.110	0.122	0.136	0.149	0.162	0.176
0.00155	0.054	0.061	0.070	0.081	0.092	0.104	0.116	0.128	0.140	0.153	0.165
0.0016	0.052	0.059	0.067	0.077	0.087	0.098	0.110	0.121	0.133	0.144	0.156
0.00165	0.050	0.056	0.064	0.073	0.083	0.093	0.104	0.115	0.126	0.137	0.148
0.0017	0.048	0.054	0.062	0.070	0.079	0.089	0.099	0.109	0.119	0.129	0.140
0.00175	0.047	0.052	0.059	0.067	0.075	0.085	0.094	0.103	0.113	0.123	0.133
0.0018	0.045	0.050	0.057	0.064	0.072	0.081	0.089	0.098	0.108	0.117	0.126
0.00185	0.044	0.049	0.055	0.061	0.069	0.077	0.085	0.094	0.102	0.111	0.120
0.0019	0.043	0.047	0.053	0.059	0.066	0.074	0.082	0.090	0.098	0.106	0.114
0.00195	0.041	0.045	0.051	0.057	0.063	0.071	0.078	0.086	0.093	0.101	0.109
0.002	0.040	0.044	0.049	0.055	0.061	0.068	0.075	0.082	0.089	0.097	0.104
0.00205	0.039	0.043	0.047	0.053	0.059	0.065	0.072	0.079	0.086	0.093	0.100
0.0021	0.038	0.041	0.046	0.051	0.056	0.062	0.069	0.075	0.082	0.089	0.096
0.00215	0.037	0.040	0.044	0.049	0.054	0.060	0.066	0.072	0.079	0.085	0.092
0.0022	0.036	0.039	0.043	0.047	0.052	0.058	0.064	0.070	0.076	0.082	0.088
0.00225	0.035	0.038	0.041	0.046	0.051	0.056	0.061	0.067	0.073	0.079	0.084
0.0023	0.035	0.037	0.040	0.044	0.049	0.054	0.059	0.064	0.070	0.076	0.081
0.00235	0.034	0.036	0.039	0.043	0.047	0.052	0.057	0.062	0.067	0.073	0.078
0.0024	0.033	0.035	0.038	0.042	0.046	0.050	0.055	0.060	0.065	0.070	0.075
0.00245	0.032	0.034	0.037	0.040	0.044	0.049	0.053	0.058	0.063	0.068	0.073
0.0025	0.032	0.033	0.036	0.039	0.043	0.047	0.051	0.056	0.060	0.065	0.070

Appendix 17 (cont.)

Oxygen Concentration (g/m^3)

R (m)	12.0	13.0	14.0	15.0	16.0	17.0	18.0	19.0	20.0	21.0	22.0
0.00005	1.000	1.000	1.000	1.000	1.000	1.000	1.000	1.000	1.000	1.000	1.000
0.0001	1.000	1.000	1.000	1.000	1.000	1.000	1.000	1.000	1.000	1.000	1.000
0.00015	0.999	0.999	0.999	1.000	1.000	1.000	1.000	1.000	1.000	1.000	1.000
0.0002	0.999	0.999	0.999	0.999	0.999	0.999	0.999	1.000	1.000	1.000	1.000
0.00025	0.998	0.998	0.999	0.999	0.999	0.999	0.999	0.999	0.999	0.999	0.999
0.0003	0.997	0.998	0.998	0.998	0.998	0.999	0.999	0.999	0.999	0.999	0.999
0.00035	0.997	0.997	0.997	0.998	0.998	0.998	0.998	0.999	0.999	0.999	0.999
0.0004	0.996	0.996	0.997	0.997	0.997	0.998	0.998	0.998	0.998	0.998	0.999
0.00045	0.995	0.995	0.996	0.996	0.997	0.997	0.998	0.998	0.998	0.998	0.998
0.0005	0.994	0.995	0.995	0.996	0.996	0.997	0.997	0.997	0.998	0.998	0.998
0.00055	0.966	0.992	0.994	0.995	0.996	0.996	0.996	0.997	0.997	0.997	0.998
0.0006	0.881	0.923	0.959	0.985	0.995	0.996	0.996	0.996	0.997	0.997	0.997
0.00065	0.792	0.837	0.878	0.915	0.947	0.973	0.992	0.996	0.996	0.997	0.997
0.0007	0.710	0.754	0.796	0.835	0.871	0.904	0.933	0.959	0.979	0.994	0.996
0.00075	0.638	0.679	0.719	0.757	0.793	0.828	0.860	0.890	0.917	0.942	0.963
0.0008	0.574	0.613	0.650	0.686	0.721	0.755	0.787	0.818	0.847	0.874	0.900
0.00085	0.519	0.554	0.589	0.623	0.656	0.688	0.719	0.749	0.778	0.806	0.832
0.0009	0.471	0.503	0.536	0.567	0.598	0.628	0.658	0.686	0.714	0.741	0.767
0.00095	0.428	0.459	0.489	0.518	0.547	0.575	0.603	0.630	0.656	0.682	0.707
0.001	0.392	0.420	0.447	0.474	0.501	0.527	0.553	0.579	0.604	0.628	0.652
0.00105	0.359	0.385	0.410	0.436	0.460	0.485	0.509	0.533	0.556	0.580	0.602
0.0011	0.331	0.355	0.378	0.401	0.424	0.447	0.470	0.492	0.514	0.536	0.557
0.00115	0.306	0.327	0.349	0.371	0.392	0.414	0.435	0.456	0.476	0.496	0.517
0.0012	0.283	0.303	0.324	0.344	0.364	0.384	0.403	0.423	0.442	0.461	0.480
0.00125	0.263	0.282	0.301	0.319	0.338	0.357	0.375	0.393	0.411	0.429	0.447
0.0013	0.245	0.263	0.280	0.298	0.315	0.332	0.349	0.366	0.383	0.400	0.417
0.00135	0.229	0.245	0.262	0.278	0.294	0.310	0.326	0.342	0.358	0.374	0.390
0.0014	0.214	0.230	0.245	0.260	0.275	0.290	0.306	0.321	0.335	0.350	0.365
0.00145	0.201	0.215	0.230	0.244	0.258	0.272	0.287	0.301	0.315	0.329	0.343
0.0015	0.189	0.202	0.216	0.229	0.243	0.256	0.269	0.283	0.296	0.309	0.322
0.00155	0.178	0.191	0.203	0.216	0.228	0.241	0.254	0.266	0.279	0.291	0.303
0.0016	0.168	0.180	0.192	0.204	0.216	.0.227	0.239	0.251	0.263	0.275	0.286
0.00165	0.159	0.170	0.181	0.192	0.204	0.215	0.226	0.237	0.248	0.259	0.271
0.0017	0.150	0.161	0.172	0.182	0.193	0.203	0.214	0.225	0.235	0.246	0.256
0.00175	0.143	0.153	0.163	0.173	0.183	0.193	0.203	0.213	0.223	0.233	0.243
0.0018	0.136	0.145	0.154	0.164	0.173	0.183	0.192	0.202	0.211	0.221	0.230
0.00185	0.129	0.138	0.147	0.156	0.165	0.174	0.183	0.192	0.201	0.210	0.219
0.0019	0.123	0.131	0.140	0.148	0.157	0.166	0.174	0.183	0.191	0.200	0.208
0.00195	0.117	0.125	0.133	0.141	0.150	0.158	0.166	0.174	0.182	0.190	0.198
0.002	0.112	0.120	0.127	0.135	0.143	0.151	0.158	0.166	0.174	0.182	0.189
0.00205	0.107	0.114	0.122	0.129	0.136	0.144	0.151	0.159	0.166	0.173	0.181
0.0021	0.102	0.109	0.116	0.123	0.130	0.138	0.145	0.152	0.159	0.166	0.173
0.00215	0.098	0.105	0.111	0.118	0.125	0.132	0.138	0.145	0.152	0.159	0.165
0.0022	0.094	0.101	0.107	0.113	0.120	0.126	0.133	0.139	0.146	0.152	0.158
0.00225	0.090	0.096	0.103	0.109	0.115	0.121	0.127	0.133	0.140	0.146	0.152
0.0023	0.087	0.093	0.099	0.104	0.110	0.116	0.122	0.128	0.134	0.140	0.146
0.00235	0.084	0.089	0.095	0.100	0.106	0.112	0.117	0.123	0.129	0.134	0.140
0.0024	0.081	0.086	0.091	0.097	0.102	0.107	0.113	0.118	0.124	0.129	0.135
0.00245	0.078	0.083	0.088	0.093	0.098	0.103	0.109	0.114	0.119	0.124	0.129
0.0025	0.075	0.080	0.085	0.090	0.095	0.100	0.105	0.110	0.115	0.120	0.125

Appendix 17 (cont.)

Oxygen Concentration (g/m^3)

R (m)	23	24	25	26	27	28	29	30	31	32	33
0.00005	1.000	1.000	1.000	1.000	1.000	1.000	1.000	1.000	1.000	1.000	1.000
0.0001	1.000	1.000	1.000	1.000	1.000	1.000	1.000	1.000	1.000	1.000	1.000
0.00015	1.000	1.000	1.000	1.000	1.000	1.000	1.000	1.000	1.000	1.000	1.000
0.0002	1.000	1.000	1.000	1.000	1.000	1.000	1.000	1.000	1.000	1.000	1.000
0.00025	0.999	1.000	1.000	1.000	1.000	1.000	1.000	1.000	1.000.	1.000	1.000
0.0003	0.999	0.999	0.999	0.999	0.999	1.000	1.000	1.000	1.000	1.000	1.000
0.00035	0.999	0.999	0.999	0.999	0.999	0.999	0.999	0.999	0.999	0.999	1.000
0.0004	0.999	0.999	0.999	0.999	0.999	0.999	0.999	0.999	0.999	0.999	0.999
0.00045	0.998	0.999	0.999	0.999	0.999	0.999	0.999	0.999	0.999	0.999	0.999
0.0005	0.998	0.998	0.998	0.999	0.999	0.999	0.999	0.999	0.999	0.999	0.999
0.00055	0.998	0.998	0.998	0.998	0.998	0.998	0.999	0.999	0.999	0.999	0.999
0.0006	0.997	0.998	0.998	0.998	0.998	0.998	0.998	0.998	0.999	0.999	0.999
0.00065	0.997	0.997	0.997	0.998	0.998	0.998	0.998	0.998	0.998	0.998	0.998
0.0007	0.997	0.997	0.997	0.997	0.998	0.998	0.998	0.998	0.998	0.998	0.998
0.00075	0.981	0.993	0.997	0.997	0.997	0.997	0.998	0.998	0.998	0.998	0.998
0.0008	0.923	0.944	0.963	0.979	0.991	0.997	0.997	0.997	0.998	0.998	0.998
0.00085	0.857	0.881	0.903	0.924	0.943	0.96	0.974	0.986	0.995	0.998	0.998
0.0009	0.793	0.817	0.84	0.862	0.883	0.903	0.922	0.939	0.954	0.968	0.98
0.00095	0.732	0.756	0.779	0.801	0.822	0.843	0.863	0.882	0.9	0.917	0.932
0.001	0.676	0.699	0.721	0.743	0.764	0.785	0.805	0.824	0.843	0.861	0.878
0.00105	0.625	0.647	0.668	0.689	0.71	0.73	0.749	0.769	0.787	0.805	0.823
0.0011	0.578	0.599	0.62	0.64	0.659	0.679	0.698	0.716	0.735	0.752	0.77
0.00115	0.536	0.556	0.575	0.595	0.613	0.632	0.65	0.668	0.686	0.703	0.72
0.0012	0.499	0.517	0.535	0.554	0.571	0.589	0.606	0.623	0.64	0.657	0.673
0.00125	0.464	0.482	0.499	0.516	0.533	0.55	0.566	0.583	0.599	0.615	0.63
0.0013	0.433	0.45	0.466	0.482	0.498	0.514	0.53	0.545	0.561	0.576	0.591
0.00135	0.405	0.421	0.436	0.451	0.466	0.481	0.496	0.511	0.526	0.54	0.554
0.0014	0.38	0.394	0.409	0.423	0.437	0.452	0.466	0.48	0.493	0.507	0.521
0.00145	0.356	0.37	0.384	0.397	0.411	0.424	0.438	0.451	0.464	0.477	0.49
0.0015	0.335	0.348	0.361	0.374	0.387	0.399	0.412	0.425	0.437	0.449	0.462
0.00155	0.316	0.328	0.34	0.352	0.365	0.377	0.389	0.4	0.412	0.424	0.436
0.0016	0.298	0.31	0.321	0.333	0.344	0.356	0.367	0.378	0.389	0.401	0.412
0.00165	0.282	0.293	0.304	0.314	0.325	0.336	0.347	0.358	0.368	0.379	0.39
0.0017	0.267	0.277	0.287	0.298	0.308	0.318	0.329	0.339	0.349	0.359	0.369
0.00175	0.253	0.263	0.272	0.282	0.292	0.302	0.312	0.321	0.331	0.34	0.35
0.0018	0.24	0.249	0.259	0.268	0.277	0.287	0.296	0.305	0.314	0.323	0.332
0.00185	0.228	0.237	0.246	0.255	0.264	0.272	0.281	0.29	0.299	0.307	0.316
0.0019	0.217	0.225	0.234	0.242	0.251	0.259	0.268	0.276	0.284	0.293	0.301
0.00195	0.207	0.215	0.223	0.231	0.239	0.247	0.255	0.263	0.271	0.279	0.287
0.002	0.197	0.205	0.213	0.22	0.228	0.236	0.243	0.251	0.259	0.266	0.274
0.00205	0.188	0.196	0.203	0.21	0.218	0.225	0.232	0.24	0.247	0.254	0.261
0.0021	0.18	0.187	0.194	0.201	0.208	0.215	0.222	0.229	0.236	0.243	0.25
0.00215	0.172	0.179	0.186	0.192	0.199	0.206	0.213	0.219	0.226	0.233	0.239
0.0022	0.165	0.171	0.178	0.184	0.191	0.197	0.204	0.21	0.216	0.223	0.229
0.00225	0.158	0.164	0.17	0.177	0.183	0.189	0.195	0.201	0.207	0.214	0.22
0.0023	0.152	0.158	0.164	0.169	0.175	0.181	0.187	0.193	0.199	0.205	0.211
0.00235	0.146	0.151	0.157	0.163	0.168	0.174	0.18	0.185	0.191	0.197	0.202
0.0024	0.14	0.146	0.151	0.156	0.162	0.167	0.173	0.178	0.184	0.189	0.195
0.00245	0.135	0.14	0.145	0.15	0.156	0.161	0.166	0.171	0.177	0.182	0.187
0.0025	0.13	0.135	0.14	0.145	0.15	0.155	0.16	0.165	0.17	0.175	0.18

Appendix 18

Glucose consumption and CO_2 evolution in air-flushed cultures as reported by Dosoretz et al., 1990a.

Data for Figure 6.4

Time (h)	CO_2 (g)	Glucose (g/m^3)
0	0	10000
24	0.0267	9500
48	0.0313	8700
72	0.0340	8000
96	0.0354	7000
120	0.0408	6800
144	0.0394	6000
168	0.0399	5800
192	0.0405	4500
216	0.0381	
240	0.0326	
264	0.0326	

Appendix 19

Data for agitated cultures of *P. chrysosporium* grown with methanol* as the sole carbon and energy source.

Time (days)	Biomass (g/l)	Acetate (g/l)	Methanol (g/l)	pH
0	0.187	1.2	10	4.6
1	0.352	0.441	8.61	6.03
2	0.540	0.043	7.59	6.56
4	0.507	0.036	6.77	6.53
5	0.521	0.018	6.21	6.58
6	0.515	0	5.52	6.55
7	0.539		4.39	6.56
12	0.378		2.06	6.71
13	0.336		1.96	6.65

Time (days)	Protein (mg/l)	MnP (U/l)	LiP (U/l)
1	22.2	0	0
2	21.9	0	0
4	20.6	0	0
5	21.0	0	0
6	21.9	0	0
7	23.2	0	2
12	31.8	0	4
13	39.0	0	2

*Culture conditions were as described for condition 2 cultures, except that methanol (10 g/l) was substituted for glucose and nitrogen sufficient conditions were used (390 g/m^3 ammonium).

Appendix 20

Data for agitated cultures of *P. chrysosporium* grown with ethanol* as the sole carbon and energy source.

Time (days)	Protein (mg/l)	pH	MNP (U/l)	LIP (U/l)
0.00		4.50		
1.00	8.56	6.12		
2.00	8.07	6.32		
3.00	6.01	6.21		
4.00	4.36	5.93	0	0
5.33	3.83	5.21	0	0
6.08	2.35	5.37	40	0
8.00	5.80	5.51	530	0
10.04	4.94	5.50	360	0
13.92	3.21	5.70	230	0

Time (days)	CO_2 (g)	Ethanol (g/l)	Biomass (g/l)	NH_4 (ppm)
0.00	0	7.67	0.13	39
1.00	0.063	8.09	0.38	0
2.00	0.039	7.11	0.55	0
3.00	0.028	3.53	0.78	
4.00	0.036	2.68	0.81	
5.33	0.040	2.47	1.01	
6.08	0.049	2.03	1.08	
7.04	0.042			
8.00	0.052	1.60	1.33	
9.00	0.036			
10.04	0.039	1.33	1.52	
11	0.035			
13.92	0.040	0.40	1.55	

*Culture conditions were as described for Condition 2 cultures, except that ethanol (7.7 g/l) was substituted for glucose. Cultures were also grown with acetate (10 g/l) as the sole carbon source. These cultures failed to grow in stationary Fernbach flask cultures and therefore agitated cultures were not inoculated.

Appendix 21

Shake flask simulation program listing

This program was used to generate all model data (Figures 5.4, 5.6, 5.9, 6.3, 6.4, 6.5).

```
2 REM                         SHAKE FLASK SIMULATION
5 OPEN "c:\windows\moddat\datan79.xls" FOR OUTPUT AS #1
10 DIM G(500),X(500),N(500),R(500),O2(500),PG(500),CO2(500),O2TOT(500)
15 DIM S(100),SS(4),SO(4),V(100),GI(10),PN(5)
20 REM ** constant physical values **
25  VLIQ=.000085:VHS=.000165:TLAG=8:PNUM=7320*1000:PDENS=65000!
27  H=37.8:DELT=3600:DEO2=2.9E-09
30 REM ** model parameter values **
35  YNX=.048:A=.84:B=.12:C=1-A-B:F=.4:YCO2O2=44/32:YO2G=176/6/32
40  VM=.76:KM=.5:UMAX=.000039:KAUT=.0000025:KPG=.5:KS=400:DES=2.9E-09
45 GOSUB 4000
50 GOSUB 5000
65 REM ** initial conditions (all units are seconds, meters or grams) **
70 FOR II=1 TO 1
75  G(0)=11000:N(0)=39:O2(0)=39.2:X(0)=100:PG(0)=0:CO2(0)=0:O2TOT(0)=.2085
80  NI(1)=39:NI(2)=117:NI(3)=3:NO2=1
85  N(0)=NI(II)
90 REM ********************* Lag phase ***************************
100 FOR T=1 TO TLAG
105 G(T)=G(0):N(T)=N(0):O2(T)=O2(0):X(T)=X(0):PG(T)=P(0):CO2(T)=CO2(0)
110 R(T)=(3/4/3.14159/PNUM/PDENS*X(T))^(1/3)
111 VPELS=X(T)/PDENS*VLIQ
115 DO2DT=-(VM*O2(T-1)/(KM+O2(T-1)))*(VPELS/VLIQ)
117 O2TOT(T)=O2TOT(T-1)+VLIQ*DELT*DO2DT
118  O2(T)=O2TOT(T)/(VLIQ+H*VHS)
119  CO2(T)=CO2(T-1)-44/32*DO2DT*DELT*VLIQ
120 GOSUB 3000
130 NEXT T
150 REM ******************** primary growth phase *******************
160 X(T)=X(T-1)*EXP(UMAX*NO2*DELT)
170 N(T)=N(T-1)-YNX*UMAX*NO2*X(T)*DELT
180 VPELS=X(T)/PDENS*VLIQ
200 DO2DT=-NO2*(VM*O2(T-1)/(KM+O2(T-1)))*(VPELS/VLIQ)/(KS/G(T-1)+1)
220 DELGT=.92*(X(T-1)-X(T))+DO2DT*YO2G*DELT
223  PG(T)=PG(T-1)
225  G(T)=G(T-1)+DELGT
227 R(T)=(3/4/3.14159/PNUM/PDENS*X(T))^(1/3)
230 IF NOT ((INT(T/24)-(T/24))=0) THEN 250
235 O2TOT(T)=O2TOT(0):CO2(T)=CO2(0)
240 GOSUB 4000
245 GOTO 260
250 O2TOT(T)=O2TOT(T-1)+VLIQ*DELT*DO2DT
260  O2(T)=O2TOT(T)/(VLIQ+H*VHS)
270  CO2(T)=CO2(T-1)-44/32*DO2DT*DELT*VLIQ
285 GOSUB 3000
290 GOSUB 1000
295 T=T+1:IF (T>350) THEN 760
300 IF (N(T-1)>0) AND (G(T-1)>0) THEN 150
400 REM ******************* secondary growth phase *******************
401 IF NOT ((INT(T/24)-(T/24))=0) THEN 410
402 GOSUB 4000
405 O2TOT(T)=O2TOT(0):CO2(T)=CO2(0):GOTO 420
410 O2TOT(T)=O2TOT(T-1)-(VPELS*VM*O2(T-1)/(KM+O2(T-1)))*DELT*NO2/(KS/G(T-1)+1)
420  O2(T)=O2TOT(T)/(VLIQ+H*VHS)
425  CO2(T)=44/32*(O2TOT(0)-O2TOT(T))
430 DO2DT=-NO2*(VM*O2(T)/(KM+O2(T)))*(VPELS/VLIQ)/(KS/G(T-1)+1)
440 DELGT=DO2DT*DELT*.8958/A
443  G(T)=G(T-1)+DELGT
445  PG(T)=PG(T-1)-C*DELGT
450  X(T)=X(T-1)-B*DELGT
460 R(T)=(3/4/3.14159/PNUM/PDENS*X(T))^(1/3)
465 VPELS=X(T)/PDENS*VLIQ
480 GOSUB 1000
490 GOSUB 3000
495 T=T+1:IF (T>350) THEN 760
500 IF G(T-1)>80 THEN 400
```

```
510 XF=F*X(T-1)
600 REM *********************** death phase ****************************
610 DXDT=-KAUT*(X(T-1)-XF):DPGDT=-KPG*KAUT*(X(T-1)-XF)
612 X(T)=X(T-1)+DXDT*DELT
620 R(T)=R(T-1):NO2=1
625 PG(T)=PG(T-1)+DPGDT*DELT
630 IF NOT ((INT(T/24)-(T/24))=0) THEN 650
635 O2TOT(T)=O2TOT(0):CO2(T)=CO2(0)
640 GOSUB 4000
645 GOTO 660
650 O2TOT(T)=O2TOT(T-1)+DPGDT*(176/6/32)
660   O2(T)=O2TOT(T)/(VLIQ+H*VHS)
670   CO2(T)=44/32*(O2TOT(0)-O2TOT(T))
680 GOSUB 3000
695 T=T+1:IF (T>350) THEN 760
700 IF PG(T-1)>0 THEN 600
760 ERASE G,X,N,R,O2,PG,CO2,O2TOT
770 DIM G(500),X(500),N(500),R(500),O2(500),PG(500),CO2(500),O2TOT(500)
775 NO2=1
780 PRINT #1,
800 NEXT II
900 END
999   REM *****************************************************************
1000 REM * oxygen effectiveness factor subroutine * (O2(t),R(t);NO2)*
1500 THIELE=R(T)/3*(VM/KM/DES)^.5
1505 ALPHA=KM/O2(T)
1510 IF (THIELE>5) THEN 1530
1520 TANH3T=(EXP(THIELE)-EXP(-THIELE))/(EXP(THIELE)+EXP(-THIELE)):GOTO 1550
1530 TANH3T=1
1550 E1=1/THIELE*((1/TANH3T-(1/3/THIELE)))
1560 PHI=6*DES*O2(T)*VM/R(T)/R(T)
1570 IF (PHI<1) THEN 1600
1580 E0=1:GOTO 1700
1600 E0=1-(1-PHI)^(3/2)
1700 NO2=(E0+ALPHA*E1)/(1+ALPHA)
1710 GOTO 1490
2999 REM *********************************
3000 REM **** printing subroutine ******
3010 PRINT USING "###";T;
3015 PRINT USING " ###.#";N(T);O2(T);
3020 PRINT USING " ###.####";O2TOT(T);CO2(T);NO2;
3030 PRINT USING " #####.#";PG(T);G(T);X(T);
3040 PRINT USING " #.#######";R(T)
3070 IF NOT ((INT(T/4)-(T/4))=0) THEN 3200
3100 PRINT #1,USING " #.#####^^^^";T,N(T),G(T),X(T),NO2,O2(T),O2TOT(T),CO2(T),R(T),PG(T)
3200 RETURN
4000 REM ***** LEGEND SUBROUTINE *******
4002 PRINT " t    NH4    O2    O2total    CO2    nO2    PG    G    X    R"
4010 RETURN
5000 REM ******* initial output subroutine *************
5005 PRINT #1,:PRINT #1," YNX    UMAX    VM   KM    A    B    C    KAUT  pelnum  peldens  DeO2"
5010 PRINT #1,USING " #.####^^^^";YNX,UMAX,VM,KM,A,B,C,KAUT,PNUM,PDENS,DES
5015 PRINT #1,
5020 PRINT #1," T(h)  N(g/m3)  G(g/m3)  X(g/m3)  nO2  O2(g/m3)  O2TOT(g)  CO2(g)  R(m)  PG(g/m3)"
5030 RETURN
```

Appendix 22

Mycelial pellet oxygen concentration gradient simulation program

This program was used to model oxygen profile data obtained using the oxygen microelectrode (Figure 5.5).

```
1 REM                ********* Program       *************
2 REM    Solves the equations for diffusion and reaction of oxygen within a
3 REM    spherical pellet. Michaelis-Menten kinetics for oxygen is assumed. A
4 REM    shooting algorithm is used with Newton-Raphson convergence.
5 REM
7   DIM S(200):DIM SS(4):DIM SO(4):DIM V(200):DIM RI(200)
9 OPEN "c:\pelgrad.xls" FOR OUTPUT AS #1
10  DES=2.9E-09:VM=.76:KM=.5
12  SSURF=10
13  CLS
14  PRINT:PRINT:PRINT:PRINT "             ************* N vs R **************":PRINT
16  PRINT " vmax=";VM;"g/m3/s,    Km=";KM;"g/m3,     Des=";DES;"m2/s    ss=";SSURF;
"g/m3"
25   R=3/1000/2
26   DIVISIONS=INT(180)
27   DR=R/DIVISIONS
30   SO(1)=SSURF:SO(3)=1E-30
35   SO(2)=(SO(1)+SO(3))/2
40   FOR K=1 TO 3
50    S(0)=SO(K)
60    S(1)=SO(K)
100    FOR I=1 TO DIVISIONS
105     V(I)=VM*S(I)/(KM+S(I))
120    S(I+1)=(I/(I+1))*((2*S(I)+S(I-1)*(1/I-1))+V(I)*DR^2/DES)
200    NEXT I
220   SS(K)=S(DIVISIONS)
230  NEXT K
240  CONVERGENCE=ABS((SS(2)-SSURF)/SSURF)
250  IF CONVERGENCE<.001 THEN 600
300 IF SSURF>SS(2) THEN 340
310 SO(1)=SO(2)
320 GOTO 35
340 SO(3)=SO(2)
350 GOTO 35
600  VSUM=0:RI(0)=0
605  FOR J=1 TO DIVISIONS
607 RI(J)=J*DR
610   IF S(J)<0 THEN V(J)=0
640   PRINT " O2 (g/m3) =    ";
641   PRINT USING "###.#####";S(J);
642   PRINT "     r (m)= ";
643   PRINT USING "#.#####";RI(J)
645 PRINT #1,USING "  ##.####^^^^   ";S(J),RI(J)
660 VSUM=VSUM+V(J)*(RI(J)^3-RI(J-1)^3)
720  NEXT J
800  EFFACTOR=VSUM/(R^3*VM*SSURF/(KM+SSURF))
805  PRINT:PRINT "          r (m)      effectiveness factor     ss calc    sO ca
lc"
810  PRINT USING "      ##.#######";R*.1;EFFACTOR;
815  PRINT USING "  ###.#########";SS(2);SO(2)
1000 END
```